Biomicrofluidics

Microfluidics for the biological analysis of atmospheric ice-nucleating particles: Perspectives and challenges

Mark D. Tarn,*[a] Kirsty J. Shaw,[b] Polly B. Foster,[a,c] Jon S. West,[d] Ian D. Johnston,[e] Daniel K. McCluskey,[e] Sally A. Peyman[c,f] and Benjamin J. Murray*[a]

[a] *School of Earth and Environment, University of Leeds, Leeds, LS2 9JT, United Kingdom. Mark D. Tarn: m.d.tarn@leeds.ac.uk, +44 (0) 113 343 5605; Benjamin J. Murray: b.j.murray@leeds.ac.uk, +44 (0) 113 343 2887.*

[b] *Faculty of Science and Engineering, Manchester Metropolitan University, Manchester, M1 5GD, United Kingdom.*

[c] *School of Physics and Astronomy, University of Leeds, Leeds, LS2 9JT, United Kingdom.*

[d] *Protecting Crops and Environment Department, Rothamsted Research, Harpenden, AL5 2JQ, United Kingdom.*

[e] *School of Physics, Engineering & Computer Science, University of Hertfordshire, College Lane, Hatfield AL10 9AB, United Kingdom.*

[f] *Institute of Biological Chemistry, Biophysics and Bioengineering, Heriot-Watt University, Edinburgh, EH14 4AS, United Kingdom.*

ABSTRACT

Atmospheric ice-nucleating particles (INPs) make up a vanishingly small proportion of atmospheric aerosol, but are key to triggering the freezing of supercooled liquid water droplets, altering the lifetime and radiative properties of clouds and having a substantial impact on weather and climate. However, INPs are notoriously difficult to model due to a lack of information on their global sources, sinks, concentrations, and activity, necessitating the development of new instrumentation for quantifying and characterising INPs in a rapid and automated manner. Microfluidic technology has been increasingly adopted by ice nucleation research groups in recent years as a means of performing droplet freezing analysis of INPs, enabling the measurement of hundreds or thousands of droplets per experiment at temperatures down to the homogeneous freezing of water. The potential for microfluidics extends far beyond this, with an entire toolbox of bioanalytical separation and detection techniques developed over 30 years for medical applications that could easily be adapted to biological and biogenic INP analysis to revolutionise the field, for example in the identification and quantification of ice-nucleating bacteria and fungi. Combined with miniaturised sampling techniques, we can envisage the development and deployment of microfluidic sample-to-answer platforms for automated, user-friendly sampling and analysis of biological INPs in the field that would enable a greater understanding of their global and seasonal activity. Here, we review the various components that such a platform would incorporate to highlight the feasibility, and the challenges, of such an endeavour, from sampling and droplet freezing assays to separations and bioanalysis.

INTRODUCTION

"*Historically, the measurement of ice nucleating activity has been found to be stubbornly difficult. Ice nucleation is sensitive to a large number of complex variables, so that the requirement that the measurements reflect the reaction of the nuclei to the state of those variables in natural clouds, is indeed a demanding one.*"

This statement by Gabor Vali was written nearly 50 years ago in a report on *The 3rd International Workshop on the Measurement of Ice Nuclei* in 1975[1, 2] regarding our understanding at the time of what we now call ice-nucleating particles (INPs). INPs are a rare aerosol particle type that can trigger freezing in supercooled cloud water droplets and so drastically alter the radiative properties and lifetime of clouds,[3, 4] in turn influencing weather and climate.[5-7] While there have been many great strides and findings made in both fundamental and atmospheric ice nucleation research in the decades since, in some ways the same statement could just as easily be made today.

We now have a far greater overview of the types of particles that can nucleate ice in the atmosphere,[3] their influence on cloud systems,[8, 9] and a greater understanding of their sources and concentrations via a number of global field campaigns (see the Ice Nucleation DataBase, INDB, that collates data from 50 years of INP campaigns: https://www.bacchus-env.eu/in/).[10, 11]

Desert dusts[12-14] and sea spray aerosols (SSAs)[13, 15, 16] have long been known as two of the most important INPs in the atmosphere,[17-19] and so are typically used to represent INPs in global aerosol models.[13, 17-20] K-feldspar mineral dust tends to dominate the atmospheric INP population where present.[17, 21-23] SSAs comprised of biogenic and organic materials,[13, 15, 16, 24-28]

including bacteria, viruses, phytoplankton and diatom fragments,[24-27, 29-33] aerosolised by wave breaking and bubble-bursting processes,[24, 34] represent less active INPs that can nonetheless become important in remote marine environments.[18, 24, 28, 34]

However, data from a number of field campaigns have demonstrated that there are "missing sources" of high temperature INPs in the models,[35 20, 36] i.e. INPs that trigger freezing at warmer temperatures (closer to 0 °C) than mineral dusts, and which may be of terrestrial biological origin, e.g. fertile soils and associated microorganisms.[19, 20, 36-51] In particular, mineral dusts are believed to dominate the INP population at temperatures below ~−18 to −20 °C when present (outside of remote marine environments), while INPs of biological and biogenic (i.e. materials produced by organisms) origin are believed to be important at temperatures warmer than around −18 to −15 °C, often presenting as a "biological hump" in INP temperature spectra during field measurements.[12, 37, 39, 40, 52-54]

Bioaerosols are believed to dominate ice-nucleating activity at warmer temperatures, depending on whether they are in high enough concentrations to compete with other sources such as mineral dust,[55] and are a key uncertainty in predictability of INPs in models.[37] Indeed, ice-nucleating bacteria have been found in the atmosphere[26, 55-58] and in rainwater,[59-61] snow,[59, 60, 62-64] hail,[63, 65] sleet,[60] and cloud water.[44, 66] Likewise, fungal spore INPs and pollen-based INPs have also been found in atmospheric samples such as rainwater and cloud ice crystals,[56, 67-69] and both fungal spores[26, 55, 56, 70-73] and pollen (and their contents)[26, 57, 74-76] can be emitted into the atmosphere. Biological INPs can be found in (or associated with) terrestrial sources such as plants and trees (including pollen, bark, leaves, branches and stems),[77-81] decaying leaf litter,[48, 49, 82-84] fertile and agricultural soils,[42, 53, 58, 85-87] fungi,[88] crops,[80] fruit[89, 90] and vegetables,[91] moss,[92, 93] liverworts,[93] and lichen on trees, rocks and soils.[94-97]

While ice-nucleating biological material can comprise intact cells or grains, they can also be present as cell fragments, or can produce or contain ice-nucleating macromolecules (INMs).[98-100] Some species of bacteria and fungi produce ice-nucleating proteins,[101-105] while pollen contains subpollen particle (SPP) INMs believed to be polysaccharides,[74, 99, 100, 106, 107] which may also be a form of INMs in fungi.[103] Further, INMs can be transported into the atmosphere with, and when attached to, dust and soil particles.[13, 14, 98, 108, 109]

Many lichens have been identified as excellent sources of warm-temperature INPs,[94-97] and tree-borne lichens may be important in boreal forest regions particularly when the ground is otherwise snow-covered.[50, 94] Some viruses[110, 111] and archaea[112] are also ice nucleation active, though it is not clear that they are present in sufficient concentrations to compete with other INPs. Likewise, cold-tolerant tardigrades[113] and insects[114-116] can contain exogeneous (i.e. in the gut or body) or endogenous (i.e. in the haemolymph fluid and muscle) ice-nucleating agents,[117-121] alongside ice-binding proteins[122] (including antifreeze and glycoproteins),[123, 124] to survive in freezing conditions, but their impact on the atmosphere may be low, if at all, due to their relatively low abundance in the atmosphere.

A comprehensive list of known biogenic INPs is provided in Table 1 in the Appendix. The reader is also further directed to more focused reviews of biological ice-nucleating particles in the atmosphere,[3, 55, 125] including specialised reviews of ice-nucleating pollen[74] and bacteria.[13, 43, 58, 126] However, it must be noted that levels of ice-nucleating activity can vary within the same species. The best example of this is the most well-known ice-nucleating bacteria, *Pseudomonas syringae*,[127] which has a number of strains that are deemed "not ice active",[128-130] although the minimum temperature at which a species is dubbed "non-active" may be limited by the experimental technique rather than the sample having no activity.

There is a need to address the missing biological sources in aerosol and climate models,[20, 36, 125] as well as to characterise the ice-nucleating properties of SSAs, but thus far the tools to achieve this have been limited,[125] either in (i) specificity, (ii) sensitivity, or (iii) lack of broad use throughout the community due to complexity or cost. Hence, new instrumentation is required to achieve these requirements, as highlighted by several recent reviews on the status and future of atmospheric ice nucleation research.[51, 125, 131-133]

A common technique for assessing the presence of biological ice nucleating entities is the simple "heat test" for proteinaceous INPs,[13, 59, 134] in which an aqueous sample is heated to denature the ice-nucleating proteins and results in a lower ice nucleation activity. However, other non-proteinaceous materials (such as quartz) can also lose activity upon such a treatment, hence there are many caveats to consider when interpreting these test results.[134] Other treatments include hydrogen peroxide for organic INPs and filtration for INMs, among others,[125] but each relies on a comparative decrease in activity to investigate one broad class of INP materials. Multiple tests per sample would therefore be required to address each class, a very impractical strategy when conducting field campaigns.

Other methodologies such as genomic analysis of bacterial (via 16S rRNA sequencing)[42, 135] and fungal communities (via ITS region sequencing),[135, 136] or scanning electron microscopy with energy dispersive X-ray spectroscopy (SEM-EDS),[137, 138] can provide an overview of the aerosol populations in a sample, but not which aerosols are ice nucleation active.

One of the most powerful bacterial INP detection methods available is specific quantitative polymerase chain reaction (qPCR) that allows for the identification and quantification of the *ina* gene that encodes the ice-nucleating proteins of certain gram-negative bacteria.[42, 63] However, this requires expertise and instrumentation that is not commonplace in ice nucleation research groups, while additionally INPs containing the known *ina* genes may only comprise a small portion of the biological INP population.[42] For example, while bacterial ice nucleation is caused by *ina* encoded proteins on the outer cell membrane, fungal ice nucleation is enabled by aggregation of extracellular proteins encoded by different genes that are largely, as yet, unidentified.[139] Further, it was recently demonstrated that there are gram-positive bacteria,[61, 140, 141] such as *Lysinibacillus parviboronicapiens* whose ice-nucleating activity appears to be based on polyketides rather than proteins.[141] Even amongst known bacterial *ina* genes,

there are stark similarities but also some differences in genetic domains[142, 143] between the *inaZ*,[101] *inaC*,[144] *inaK*,[145] *inaV*[146] and *inaQ*[147] genes of *Pseudomonas syringae*, *inaA* of *Erwinia ananas*[148] and *Pantoea ananatis* (formerly *Erwinia uredovora*),[149] *inaW* of *Pseudomonas fluorescens*,[150] *inaU* of *Pantoea ananatis*,[151] *inaX* of *Xanthomonas campestris* pv. *translucens*,[152] *inaPb* of *Pseudomonas borealis*,[153] and *inaE* (*iceE*) of *Pantoea aggolerans* (formerly *Erwinia herbicola*).[154]

The tools are not currently available for achieving systematic identification and quantification of biological and biogenic INPs in a format that can be used broadly throughout the community. This particularly applies to field campaigns where sample volumes, sample throughput, and automation become important.

Microfluidic technology offers a means of revolutionising INP analysis by enabling use of powerful bioanalytical techniques developed and refined over three decades[155] for a broad range of samples and analytes.[156-159] These lab-on-a-chip devices typically comprise networks of micrometre-scale channels within which fluids can be controlled and manipulated, allowing for sample processing, treatment and analysis. The ability to integrate actuation mechanisms and detection systems, together with the ability to perform rapid chemical reactions on small sample volumes, allows for automated, small footprint, portable devices that have been developed for point-of-care diagnostics in the field of clinical testing.[160-163]

Microfluidic technology has been applied throughout several areas of environmental analysis,[164-166] including for continuous and automated monitoring in the field,[167-171] for example in water analysis.[172-176] It has also been applied to various aspects of bioaerosol sampling and analysis, and the reader is directed to more general reviews on various aspects of microfluidic sampling and analysis of bioaerosols, pathogens and particulate matter.[177-182] Microfluidics have further been utilised on unmanned aerial vehicles (UAVs), i.e. drones.[183, 184] UAVs have also shown great potential for atmospheric aerosol[185] and INP analyses in recent years,[186-190] alongside balloon-borne instrumentation.[191, 192]

Here, we discuss the potential of microfluidic and lab-on-a-chip technology to revolutionise the monitoring of biological INPs in the atmosphere, focusing on the core aspects of: (i) aerosol sampling, (ii) aerosol particle separation, (iii) determination of INP concentration, (iv) separation of INP populations, (v) injection of chemicals for bioanalytical testing, and (vi) identification and quantification of biological INPs. With the integration of all of these steps into one apparatus, we can envisage an all-in-one, automated, sample-to-answer platform (see Figure 1): a micro total analysis system (μTAS)[156] for the quantification and characterisation of INPs.

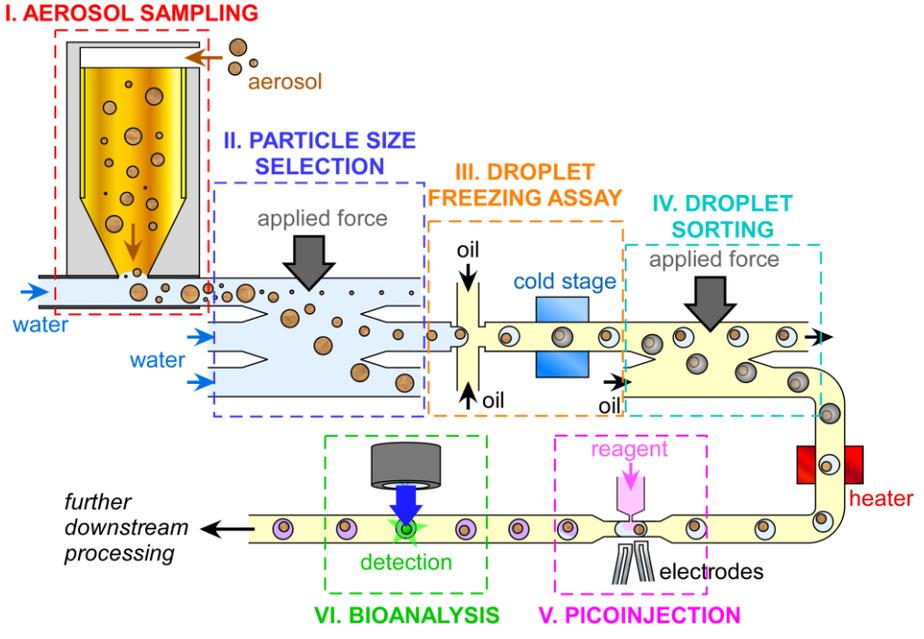

Figure 1: An idealised example of a sample-to-answer microfluidic platform for the sampling and analysis of biological ice-nucleating particles (INPs) incorporating all of the major processes, including: (i) aerosol samplng, (ii) particle size separation and selection, (iii) droplet freezing assay (DFA) for INP quantification, (iv) separation of frozen and unfrozen droplets, (v) picoinjection of biochemical reagents into droplets, and (vi) bioanalytical identification and quantification of biological species via methods such as immunoassays or DNA analysis.

We note that this article is not intended to be an extensive review of all of the relevant microfluidic literature pertaining to aerosol sampling and bioanalysis as such an endeavour would be overwhelming, rather it will provide an overview of viable microfluidic strategies regarding each of the key analytical steps defined above. Where possible we also provide citations to review

articles that provide a more detailed discussion of the theory, operation and application of specific techniques. Hereafter we cover the following topics associated with building a sample-to-answer microfluidic biological INP analysis platform (also see Figure 1), followed by a discussion of the challenges and considerations surrounding the development of such a system:

I. Miniaturised bioaerosol sampling
II. Particle size separation
III. Microfluidic ice-nucleating particle analysis
IV. Microfluidic droplet sorting
V. Droplet picoinjection
VI. Microfluidic bioaerosol analysis

I. MINIATURISED BIOAEROSOL SAMPLING

The first crucial step in bioaerosol analysis is the sampling method, which must provide excellent collection efficiency over a wide range of particle diameters, and for which there are many different methodologies,[133, 181, 193, 194] all of which could be used to collect aerosols for transfer into microfluidic analysis systems. Microfluidic analysis must also compromise the inherent small volume analysis with possible low concentrations of analytes, which could result in non-detection of the target without performing whole sample analysis. Nonetheless, a number of microfluidic strategies have been developed for efficient bioaerosol sampling, and these are covered more thoroughly in focused reviews[179, 180, 182, 195, 196] We also note that personal aerosol samplers, which have suffered similar drawbacks in the past, are now relatively low cost, small and efficient,[197, 198] and could be applied to microfluidic analyses in the future.

Here, we first cover the common sampling strategies that are used throughout the INP community, and then provide an overview of microfluidic bioaerosol sampling techniques that could be applied to INP analysis.

A. Traditional filter sampling

Aerosol filter sampling has been employed for INP analysis since the 1960s[199, 200] and is now a staple of atmospheric INP analysis. Here, air is drawn through a filter onto which aerosols are deposited, typically via an inlet head that controls the size of the particles being collected (e.g. total suspended particulates (TSP), or particulate matter smaller than 10, 2.5 or 1 µm (PM_{10}, $PM_{2.5}$, PM_1)), allowing recovery of the aerosol for offline analysis (Figure 2a). While many filter sampling instruments can be bulky, it is also possible to use small, lightweight setups for aerosol collection,[191, 192] which provides a powerful option for an integrated and miniaturised platform.

Sample filters collected for INP measurements would be immersed in a known volume of water and agitated by vortexing or shaking to release the collected aerosol particles into an aqueous suspension for offline analysis. This technique has been applied successfully in microfluidic droplet INP analysis, for example by Tarn et al.[201, 202] in the droplet emulsion-based "Microfluidic pL-NIPI" (Picolitre Nucleation by Immersed Particle Instrument) instrument and the continuous flow "LOC-NIPI" (Lab-on-a-Chip Nucleation by Immersed Particle Instrument),[203] and by Brubaker et al.[204] and Jahl et al.[205] in their microfluidic droplet array-based "store and create" platform.

However, due to ambient aerosol concentrations and sample volumes compared to the small volumes of a microfluidic droplet freezing device, the resultant INP spectra tend to cover the colder temperature regions, where higher concentrations of lower activity INPs are expected. This issue can be addressed by analysing more droplets, i.e. more or all of the sampled volume, in order to detect the rarer but more highly active INPs, which is a strategy more suited to continuous flow microfluidic systems where the user can define the number of droplets to be analysed.[203, 206, 207]

B. Microfabricated filter sampling

Microelectromechanical system (MEMS) devices have been developed towards enabling collection of aerosol onto microfabricated membrane filters (Figure 3a), though have largely not been used in such a manner. Rather, methods to "sweep" collected particles from a microfabricated filter or a solid substrate and across an air-liquid interface into a droplet following the aerosol collection step have been explored (Figure 3).

Desai et al.[208, 209] developed a glass and polydimethylsiloxane (PDMS)-based "active filter membrane" to provide an air-to-liquid particle capture scheme. Here, particles would be collected onto a microfabricated membrane filter grid then, in principle, dielectrophoretic (DEP) forces would be applied via electrodes to drive the collected aerosol particles across an oscillating air-liquid interface to "sweep" the particles into a liquid droplet, thus generating an aqueous suspension. However, the filter sampling aspect was not tested, with the focus of the work being on the transfer of particles across the interface via an external pressure source (rather than DEP) (Figure 3a), and collection efficiencies were low, but the principle showed promise.

Zhao and Cho[210-212] developed a silicon-based microfabricated filter that was integrated into an electrowetting-on-dielectric (EWOD) system,[213, 214] which comprises an array of patterned electrodes on which single droplets can be manipulated and moved by applying electric fields (Figure 3c). Here, particles collected onto the filter could be "swept" into droplets as they were moved across the electrode array. Although the filter sampling aspect was not performed here, the method was found to provide high collection efficiency.

This "droplet sweeping" method[215] may alleviate some of the issues with using traditional filter sampling with microfluidic INP analysis by entraining collected aerosol particles into a much smaller sampler volume, thus achieving a more concentrated suspension.

Liu et al.[216] fabricated a microfluidic module that contained a semi-porous PDMS filter membrane within it for the collection of bioaerosols and waterborne pathogens for DNA analysis. *Pseudomonas aeruginosa*, a known INP,[217] was aerosolised and drawn through the filter via a vacuum pump, then the collected bacteria was lysed to release target DNA that was detected via on-chip loop-mediated isothermal amplification.

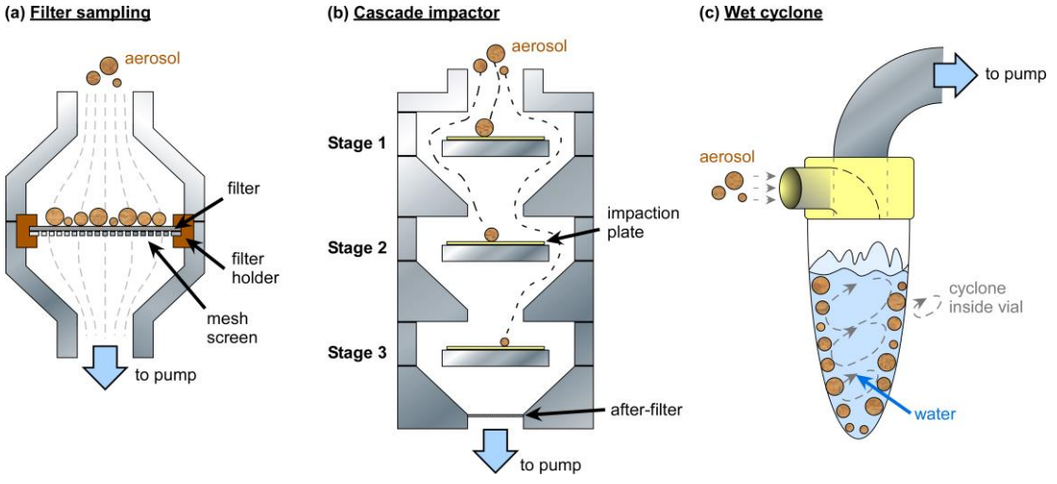

Figure 2: Traditional aerosol sampling techniques that have been employed for the microfluidic analysis of INPs. (a) Filter sampling, in which aerosols are pulled through a filter for the collection of particles, which are subsequently washed off the filter and into an aqueous suspension for analysis. Filter sampling is discussed further in Section I-A. (b) A cascade impactor, in which aerosols pass through a series of nozzles and aerosols of differing size impact upon different collection plates. A 3-stage impactor is shown. Plates (often small-pore filters) are then washed into aqueous suspension for analysis. Cascade impactors are discussed further in Section I-C. (c) A wet cyclone sampler that pulls aerosols directly into water circulating within a vial, allowing direct analysis of the aqueuoes suspension. Impingers are similar instruments in which air is bubbled into water, allowing transfer of the aerosols from the gas phase and into the aqueous phase (e.g. Greenburg-Smith bubble impingers). Wet cyclones are discussed further in Section I-E.

C. Cascade impactors

Impaction of aerosols is the method by which air is accelerated through an orifice then *over and around* a plate or substrate (rather than *through* a substrate as in filter sampling), with particles larger than a critical size (determined by the orifice and speed of air-flow) having enough momentum that they impact on the plate while smaller particles continue to follow the air stream.[218, 219] A single stage impactor can be used to cut-off particle collection above a particular size threshold. By having a series of orifices that provide greater jet speeds, resulting in smaller and smaller critical particle sizes, with an impaction plate between each orifice, particles of different size classes can be collected onto the plates for size-segregated analysis (Figure 2b). This methodology has proven useful in INP measurement campaigns for determining the size-resolved ice-nucleating activity of ambient samples.[47, 56, 191, 220-229]

Creamean et al.[47] have employed a 4-stage time-and-size-resolved Davis Rotating-drum Universal-size-cut Monitoring (DRUM) single-jet impactor[230] to collect aerosols in four size ranges for INP analysis. The DRUM impactor collects size-resolved aerosols onto Vaseline-coated Mylar tape attached to rotating drums, allowing sample to be deposited on the moving tape to enable time-resolved collection. Other impactors used in aerobiology include the Burkard or Hirst type spore trap, which uses a single impactor stage in addition to rotorods or rotating-arm traps used as impaction substrates.[194]

Reicher et al.[203, 220, 221] employed a commercial micro-orifice uniform deposit impactor (MOUDI)[231] cascade impactor to collect aerosols onto filters (used here as impaction substrates), for size-segregated INP analysis using their "WISDOM" (WeIzmann Supercooled Droplets Observation on a Microarray) droplet array microfluidic platform.

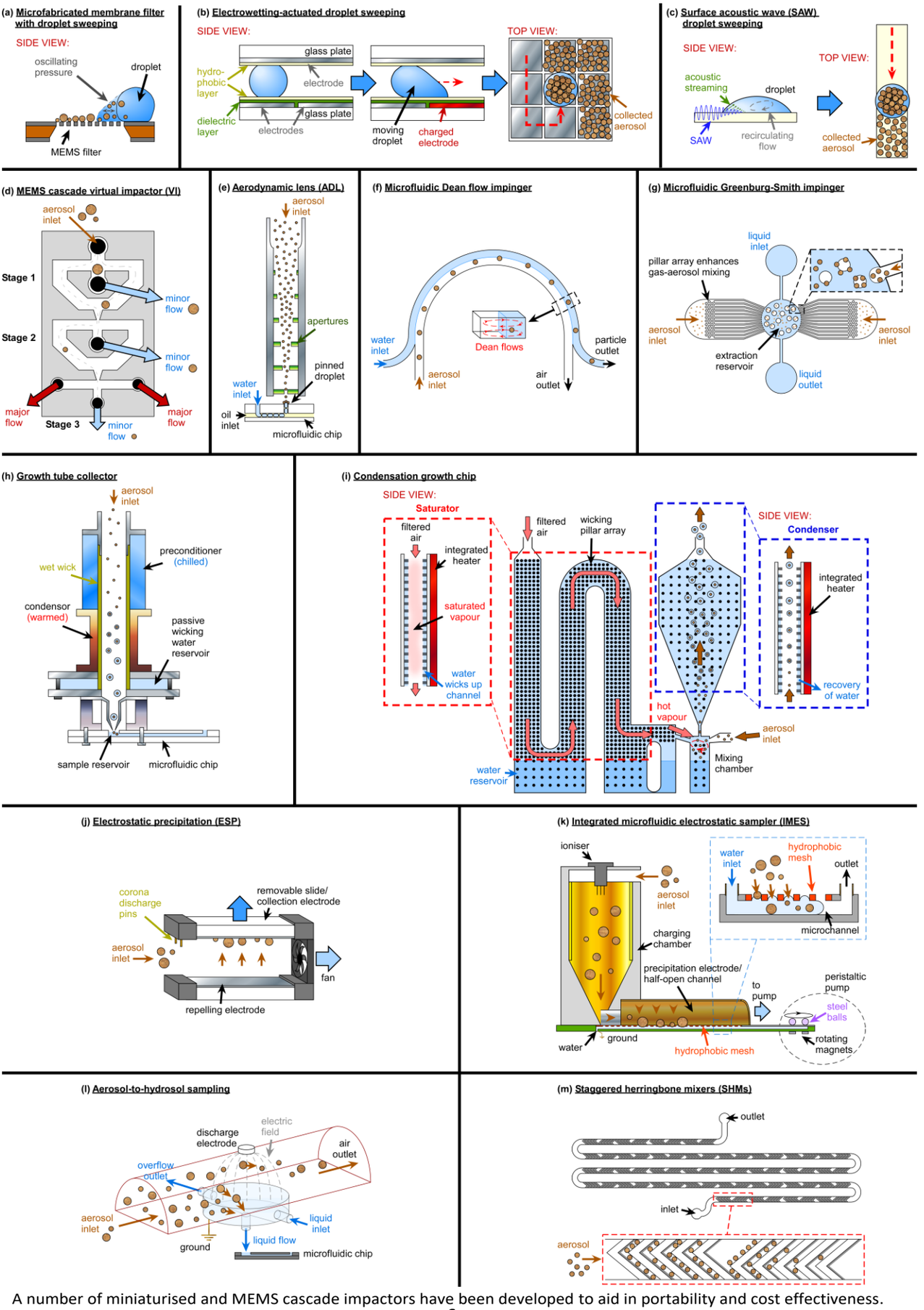

234 A number of miniaturised and MEMS cascade impactors have been developed to aid in portability and cost effectiveness.

Figure 3: Various miniaturised aerosol sampling techniques that have been developed to collect aerosol particles directly into aqueous suspensions in microfluidic platforms. (a)-(c) Examples of the "droplet sweeping" technique for the collection of aerosols into a droplet, upon prior sampling of the aerosols onto a microfabricated filter or a flat substrate. (a) A microfabricated membrane filter, with a droplet actuated by oscillating pressure to drive the air-liquid interface over the region of captured droplets.[208] (b) Principle of electrowetting-on-dielectric (EWOD), in which droplets can be moved across arrays of electrodes, to sweep up collected particles.[212] Adapted and used with permission of the Royal Society of Chemistry, from Zhao and Cho, *Lab on a Chip*, **6**, 137-144 (2006), permission conveyed through Copyright Clearance Center, Inc. (c) Surface acoustic waves (SAWs) applied via transducers to generate recirculating flows in a droplet to sweep up particles.[232] Adapted and used with permission of the Royal Society of Chemistry, from Tan et al., *Lab on a Chip*, **7**, 618-625 (2007), permission conveyed through Copyright Clearance Center, Inc. (d) Microelectromechanical systems (MEMS)-based virtual impactors (VIs).[233] Reprinted from Kim et al., *Applied Physics Letters*, **91**, 043512 (2007), with the permission of AIP Publishing. (e) An aerodynamic lens (ADL) that directs a narrow band of aerosol into a pinned droplet.[234] Adapted and used with permission from Damit et al., *Aerosol Science and Technology*, **51**, 488-500 (2017), reprinted by permission of the publisher (Taylor & Francis Ltd, http://www.tandfonline.com). (f) A curved microfluidic impinger that employs Dean forces to continuously transfer aerosols into water.[235] Reprinted (adapted) with permission from Choi et al., *ACS Sensors*, **2**, 513-521 (2017). Copyright 2017 American Chemical Society. (g) A microfluidic Greenburg-Smith impinger in which bubbles of aerosol are generated in liquid for their transfer into aqueous suspension.[236] Adapted and used with permission of the Royal Society of Chemistry, from Mirzaee et al., *Lab on a Chip*, **16**, 2254-2264 (2016), permission conveyed through Copyright Clearance Center, Inc. (h) A traditional condensation growth tube collector integrated with a microfluidic device.[237] Reprinted (adapted) with permission from Noblitt et al., *Analytical Chemistry*, **81**, 10029-10037 (2009). Copyright 2009 American Chemical Society. (i) A microfluidic condensational growth chip.[238] Adapted and used with permission of the Royal Society of Chemistry, from Kwon et al., *Lab on a Chip*, **19**, 1471-1483 (2019), permission conveyed through Copyright Clearance Center, Inc. (j) An electrostatic precipitator (ESP) with a removable collection slide that can be subjected to droplet sweeping particle collection, e.g. via EWOD.[239] (k) An integrated microfluidic electrostatic sampler (IMES).[240] Adapted and used from Ma et al., *Journal of Aerosol Science*, **95**, 84-94 (2016), with permission from Elsevier. (l) An aerosol-to-hydrosol sampler employing ESP.[241] Adapted and used from Park et al., *Analytica Chimica Acta*, **941**, 101-107 (2016), with permission from Elsevier. (m) Staggered herringbone mixer (SHM) micropatterned grooves in a microfluidic device that generate chaotic flows for the capture of aerosol in the grooves, allowing them to be later washed into aqueous suspension.[242] Reprinted (adapted) with permission from Jing et al., *Analytical Chemistry*, **85**, 10, 5255–5262 (2013), Copyright 2013 American Chemical Society.

Maldonado-Garcia et al.[243] designed a two-stage MEMS impactor in which the impactor plates were MEMS resonant microbalances capable of measuring the mass concentration of collected materials. Kang et al.[244] developed a three-stage microfabricated cascade impactor whose particle diameter cut-offs were found to be very similar to numerically predicted values.

Kwon et al.[245] fabricated a miniaturised, 3D printed cascade impactor system that incorporated sensing electrodes into the impactor plates. As aerosol entered the system a unipolar mini-discharger was used to electrically charge the particles, allowing their detection on the electrodes as the different size fractions were collected onto the impactor plates.

D. Virtual impactors

Virtual impactors (VIs) operate in a similar manner to cascade impactors, but rather than having aerosols impacting onto plates they instead enter a "virtual space" of slow moving air provided by a minor flow, allowing for collection of particles, while a major flow drives uncollected particles further through the system.[246] Large virtual impactors can sample high volumes of air, e.g. Burkard high-throughput jet samplers, since there are fewer restrictions on air flow than when using filters.[247] While multiple pumps are usually required in order to operate a virtual impactor, one for the major flow and one for the minor flows of each virtual impactor stage, Kim et al.[233, 248] micromachined a three-stage virtual impactor (Figure 3d) that featured a flow rate distributor. This avoided the need for multiple pumps by having the microfabricated distributor that control the flows to each part of the virtual impactor system, thus requiring only one pump to operate the entire three-stage impactor. The same group also developed a single-stage micro virtual impactor[249] that could be adapted to include cut-off diameters down to 15 nm by the application of electric fields via integrated electrodes to accelerate the smaller particles.[250, 251] The single virtual impactor was further integrated with a micro corona discharger that charged the separated particles and measured their number concentration based on the electrical current carried by the particles.[252]

Zhao et al.[253-255] 3D printed a single-stage miniaturised virtual impactor that incorporated a quartz crystal microbalance (QCM) to detect the mass loading of the collected aerosol, later replacing the QCM with a surface acoustic wave (SAW) sensor.[256] Kim et al.[257] demonstrated how, by integrating electrodes into a microfabricated single-stage virtual impactor, the particle size cut-off could be tuned from 35 nm to 70 nm by applying an electric field.

Further microfluidic virtual impactors have since been developed or proposed to enhance the separation and collection efficiency of airborne particles across multiple impactor stages.[258-264]

Liu et al.[265] developed a miniaturised virtual impactor for $PM_{2.5}$ separation combined with a thermophoretic precipitator, which uses the Soret effect to move particles in a temperature gradient towards the colder region,[266] to collect the particles for measurement of the mass loading on a SAW sensor.

E. Impingers and wet cyclone samplers

Impingers and wet cyclone samplers are forms of aerosol sampler that collects particles directly into a volume of water using a pump, eliminating the need to wash particles off collection substrates as in the above examples. Such devices have been employed for the collection of aerosol for INP analysis,[42, 203, 267-269] often allowing for higher sampling rates (e.g. hundreds of litres per minute) than commonly used filter samplers (e.g. ~10-33 L min^{-1}). A Greenburg-Smith bubble impinger, for example, involves bubbling sample air into a vial of water, allowing for aerosols in the bubbles to enter an aqueous suspension. Wet cyclone samplers rely on an airstream being directed tangentially into a tapering conical tube to create a vortex (e.g. the Coriolis Micro from Bertin Instruments).[270] The conical tube contains liquid which swirls in the airflow to wet the inside of the device, causing particles to be deposited on the wet walls of the tube by their inertia (Figure 2c).

A Coriolis Micro was used by Tarn et al.[203] to collect aerosol particles at 300 L min^{-1} for INP droplet freezing analysis in the continuous flow LOC-NIPI. The Coriolis Micro has also been applied to the collection of bioaerosols for the detection of *Escherichia coli* via microfluidic cytometry.[271] However, the technique suffers similar drawbacks for microfluidics analysis of rare particle types (e.g. INPs) as filter sampling in that the sample was drawn into a relatively large volume of water (~5 mL), though impingers can be used to concentrate samples due to evaporation of the working fluid during collection.

Several microfluidic impingers have been developed that enable the sampling of aerosol particles directly into water within a microchannel. Damit et al.[234] employed a commercially available aerodynamic lens (ADL),[272] which employs a series of orifices to focus aerosol particles within a specific size range into a narrow stream, to direct aerosol particles directly into pinned droplet of water in a detection channel of a microfluidic device for the detection of *E. coli* (Figure 3e).

Choi et al.[235] developed a continuous flow impinger based on a curved inertial microfluidics device (Figure 3f); while most microfluidic systems work within a regime of low Reynolds numbers (Re << 1), inertial microfluidic devices operate in the intermediate regime (Re ≈ 1-100) that yields unique flow and particle phenomena at, typically, high flow velocities (e.g. tens of metres per second).[273, 274] One such effect is the migration of particles to equilibrium positions within a microchannel as they flow,[275] with the position depending on particle size and shape.[276] In curved channels, secondary flows are generated based on the relative inertia of the fluid at different points in the bend, inducing Dean vortices to generate new equilibrium positions.[277] The device of Choi et al.[235] utilised these forces within a stratified flow of air and water to transfer into suspension as they flowed around the curved channel, allowing for the sampling of *Staphylococcus epidermidis* and its off-chip analysis by fluorescence microscopy. The Dean flow impinger was later updated to incorporate surface-enhanced Raman spectroscopy (SERS), with silver nanoparticles (AgNPs) pumped through the device to bind to the impinged aerosols, allowing their *in situ* detection as they passed through a Raman detection region.[278] This optofluidic SERS platform was used for the sampling and identification of several bacteria (*S. epidermidis*, *M. luteus*, *E. hirae*, *B. subtilis*, and *E. coli*), including the quantification and real-time monitoring of *S. epidermidis*.

Mirzaee[236] demonstrated a miniaturised version of a Greenburg-Smith bubble impinger (Figure 3g). Here, microfluidic channels were used to generate bubbles laden with aerosol into a central extraction reservoir, and demonstrated high sampling efficiency.

Thus, there are several means by which atmospheric INPs could potentially be drawn directly into microfluidic devices and deposited in liquid for ice nucleation and biological analysis.

F. Dry cyclone samplers

While dry cyclones have not been applied to INP sampling, to our knowledge, or for microfluidic purposes, adaptation of the methodology could enable both. Dry cyclone samplers were first developed in the 1950s and rely on a vortex of air being created inside a dry cylinder that transitions to a tapering conical tube, ending with a removable sample tube. Particles separate from the air flow into the dry collection tube as the air suddenly changes direction from the tightening vortex to flow vertically upwards through the centre of the vortex.[279] While collection efficiencies can be low for small particles, high sampling rates can be achieved, allowing for the collection and analysis of, for example, fungal spores by quantitative PCR analysis.[280] Dry cyclones typically result in a collection of dust, pollens and spores in a dry tube format, which is convenient for a wide range of downstream diagnostic and analytical applications and is highly amenable to the droplet sweeping aerosol-to-water collection method.

G. Condensation growth tube collectors

A growth tube aerosol collector-based system was developed by Noblitt et al.[237] to sample aerosol directly into a microfluidic device for electrophoretic separation and detection of inorganic ions. The system employed the growth tube from a conventional water-based condensation particle counter (WCPC), which sampled air through a wet-walled tube comprising cool and warm regions, such that aerosols passing through the tube would experience condensational growth to the supermicron size range (Figure 3h). The aerosols were then deposited into a buffer-filled microfluidic reservoir for analysis. The system collected aerosols at 1 L min^{-1} into 30 µL of buffer, and ran continuously for 28 h taking measurements. Given its basis on instrumentation found in commercial CPCs, it may be possible to adapt such technology for continuous sampling of INPs into microfluidic devices.

Kwon et al.[238] developed a MEMS-based condensation growth chip to grow nanoparticles (5-80 nm) to micrometre sized droplets. The chip comprised micropillar arrays throughout that allowed water to be wicked through the device from a reservoir, forming water-lined walls between which aerosols could pass (Figure 3i). By integrating MEMS heaters and temperature sensors,

regions of vapour saturation, aerosol introduction, and condensational growth were incorporated into the planar device, allowing downstream detection via a miniaturised optical particle counter (OPC).

H. Electrostatic precipitation

Electrostatic precipitation (ESP) is a sampling technique in which aerosols drawn through an inlet are charged by corona discharge needles and then deposited onto a hydrophobic surface (the ground electrode), allowing for collection and analysis of the particles. Such devices have been employed for INP analysis on conventional measurement platforms,[189, 281] and the technique is amenable to miniaturisation for microfluidic applications.[239]

Sandström et al.[282] developed a microfluidic air-liquid interface by fabricating a liquid ground electrode device, such that the particles charged by the corona needle were directly deposited into an electrolyte solution through a microfabricated silicon diaphragm. Pardon et al.[283] further developed this platform to incorporate the ESP concept into a miniaturised package for point-of-care (POC) sampling of aerosols that could be integrated with a silicon diaphragm-based microfluidic device.

Foat et al.[239] developed an EWOD platform integrated with a miniaturised ESP sampler, such that aerosol was precipitated onto the electrode array substrate. The substrate comprised a plate that could be removed from the sampler and inserted into an EWOD device (Figure 3j), allowing EWOD actuation of droplets to "sweep up" the collected particles[215] in a similar manner to the microfilter-EWOD device of Zhao et al. (Figure 3b).[210-212]

Ma et al.[240] utilised a half-open microchannel to collect precipitated aerosol through a mesh, allowing their transport to a collection reservoir in their "integrated microfluidic electrostatic sampler" (IMES) platform (Figure 3k). Shen et al.[284] combined an ESP system to deposit aerosol directly into liquid in a charged reservoir, with a peristaltic pump used to transfer the liquid continuously to a silicon nanowire field effect transistor for real-time airborne influenza monitoring.

Park et al.[241] used ESP-based aerosol-to-hydrosol (ATH) sampling to collect test bacteria (*Staphylococcus epidermidis*) into flowing liquid for on-chip analysis via an adenosine triphosphate (ATP) bioluminescence assay monitored using a photodetector (Figure 3l). Kim et al.[285] introduced a hydrosol-to-hydrosol (HTH) bacterial enrichment step in which magnetic particles were used to capture and concentrate the sampled bacteria and improve detection sensitivity via fluorescence microscopy, electrical detection, and qPCR DNA analysis.

I. Surface acoustic waves

It has been demonstrated above that EWOD can be used to transfer particles collected via microfabricated filters[210-212] or ESP substrates[215, 239] into droplets. SAWs are travelling waves that can be generated on piezoelectric substrates with integrated electrodes, and allow the movement of droplets using acoustic forces in a manner somewhat analogous to the electrically-induced movement of EWOD (Figure 3c). Tan et al.[232] demonstrated this capability by using SAW to "sweep up" bioaerosols deposited on a substrate into a droplet, and further showed that acoustically induced streaming and recirculation of droplets inside the droplets enhanced particle collection and efficiency. The device was not, however, integrated with an aerosol collection system, instead focusing on the post-sampling collection of particles into water, but demonstrates the potential of SAW for droplet sweeping of aerosols collected onto microfabricated filters or other substrates.

J. Staggered herringbone mixers

Staggered herringbone mixers (SHMs) are periodic but alternating microfluidic channel structures that induce chaotic mixing,[286] traditionally to rapidly mix solutions for chemical reactions since the laminar flow nature of microfluidic flow usually limits mixing to slow diffusional processes. However, by drawing air through SHM devices under vacuum, it has been demonstrated that airborne bacteria can be captured and concentrated (Figure 3m),[242] then eluted for on-chip immunoassay analysis[287] or on-chip DNA analysis by loop-mediated isothermal amplification (LAMP) of the ice-nucleating bacteria, *P. aeruginosa*.[288 289]

Bian et al.[290] demonstrated the enhancement of SHM-based aerosol collection by adding spiral microchannel-induced inertial forces and sawtooth wave-shaped walls to better accommodate aerosol particles for off-chip analysis by liquid chromatography-mass spectrometry (LC-MS) and colony forming unit assays.

II. PARTICLE SIZE SEPARATION

Once aerosol has been collected, and typically processed into a volume of liquid to prepare a particle suspension, it may be desirable to separate particle populations based on size for INP analysis. This may be to perform on-chip size-resolved INP assays as per Reicher et al., [220, 221] or to filter out larger bioaerosols (e.g. bacteria, pollen grains) in order to analyse only the INM content. Other mechanisms for separation could also be based on charge, hydrophobicity, or relative deformability or compressibility, for example to separate solid inorganic materials such as mineral dust for more pliable bioaerosols. Particle separations in continuous flow have proven to be a huge strength of microfluidics, often taking advantage of the laminar flow streams of fluid in such devices to transfer analytes of interest from one stream to another via a lateral force or barriers to facilitate separation (Figure 4), often for biomedical purposes.

As such, the scope for viable particle size separation techniques is far too large to cover in detail here, and the reader is directed to other dedicated reviews on the topic.[291-294] Suffice to say, a range of active[295] and passive[296] techniques can be readily applied to microfluidic separations, including inertial forces,[297, 298] pillars and barriers,[299] magnetism,[300] acoustic forces,[301] optical forces,[302] and dielectrophoretic (DEP) forces.[303] Here, we describe only specific examples of aerosol separations achieved in microfluidics, and note that microfluidic and MEMS devices for the separation and detection of aerosols have also been reviewed by Poenar.[304]

Cascade impactors and virtual impactors (VIs), described in Section 1C, also provide particle size-segregation as part of their collection process, and are not described again here.

A. Inertial microfluidics

As described earlier, inertial microfluidics can be used to manipulate particles at high flow rates such that they migrate to equilibrium positions (see Figure 3f),[273, 274] and by including multiple outlet channels within the microfluidic design it is therefore possible to separate and collect particles that have been stratified.

Schaap et al.[305, 306] demonstrated the use of both straight and curved inertial microfluidic devices to perform size-based separations of aerosol particles across sheath air streams, which compared well with simulations, while Hong et al.[307] demonstrated multi-stage separation via consecutive curved channels. Various numerical analyses and simulations have also been performed of the inertial migration of aerosol particles in microfluidic channels[305, 306, 308] and capillaries.[309-311]

Inertial microfluidics offers a rapid and passive means of achieving separations, although the high flow rates required to generate the requisite forces may not always be made easily compatible with upstream or downstream processes within an integrated platform.

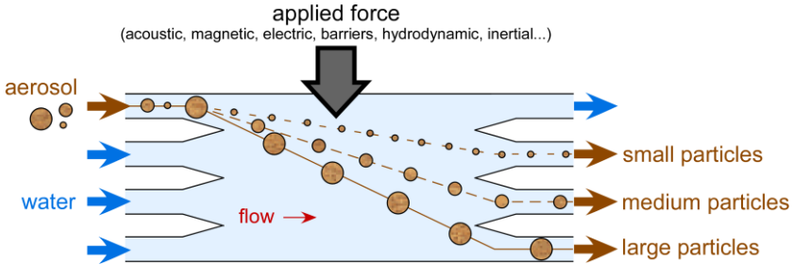

Figure 4: Principle of on-chip continuous flow size-based particle separations. Typically, a lateral force is applied to particles flowing across a microfluidic chamber, with different sized particles interacting with the force to differing extents. This allows some particles to migrate further in the lateral direction than others, enabling their collection via different outlet channels. Forces that can be utilised to induce the lateral flow include acoustic, magnetic, electric (e.g. dielectrophoretic), and hydrodynamic, or the use of pillars and barriers in the flow stream. Aerosol refers to particles suspended in air, but when introduced into water as shown here they become an aqueous particle suspension.

B. Deterministic lateral displacement

Deterministic lateral displacement (DLD) is a technique that employs a regular array of micropillars to separate particles in continuous flow.[299, 312, 313] Each row of the array is laterally shifted, generating distinct flow patterns between each pillar. As particles migrate with the flow stream, particles above a critical size are "bumped" laterally by the pillars while smaller particles continue in the direction of the flow, thus achieving separation. DLD is a powerful tool that has been applied to the separation of a range of biological, though the design of the pillar geometry for a critical size must be carefully determined, while complex biological matrices can foul and clog such platforms.

Yin et al.[314] fabricated a DLD platform comprising I-shaped pillars the separation of $PM_{2.5}$ aerosols followed by electrochemical detection with commercial screen-printed electrodes (SPEs). The separation of 1 and 10 µm polystyrene particles was achieved with nearly 100 % efficiency, though particles between these sizes or bioaerosols were not tested.

C. Electrical mobility analyser

While not strictly microfluidic, Kwon et al.[315] reported a micromachined nano-electrical mobility analyzer (NEMA) for separating and classifying nanoscale (<100 nm) aerosol based on aerodynamic and electrostatic forces. The NEMA was fabricated from silicon and featured integrated electrodes that applied an electric field across a microchannel, such that particles migrated laterally towards a ground electrode as they flowed through the channel. Larger particles with more inertia would be less affected by the electric field, thus exiting via a bypass outlet, while small particles would migrate towards and be captured at the ground electrode. By applying specific voltages, target particles could be manipulated into a collection outlet based on their size and charge for further processing. In many ways, the NEMA operated in a similar manner to the micro free-flow electrophoresis (FFE) continuous

flow separation technique,[316] but while the latter employs an electrolyte solution to separate target analytes the NEMA operated in air to process aerosol.

III. MICROFLUIDIC ICE-NUCLEATING PARTICLE ANALYSIS

A key measurement in atmospheric INP analysis is determination of the concentration of INPs in collected ambient samples. There are several techniques and instruments available for achieving this,[268, 317-319] but arguably the workhorse of INP analysis is the droplet freezing assay (DFA) or droplet freezing technique (DFT) developed by Vali in 1971.[320] In the standard technique, an array of aqueous droplets containing sample is deposited onto a hydrophobic substrate, then cooled to around −40 °C at a constant rate (usually 1 °C min^{-1}). The temperatures at which the droplets freeze are recorded, and these can be used to calculate the number of INPs within the collected volume of sample. This allows the determination of an "INP spectrum", a plot of INP concentration versus the temperature that those INPs are active at, i.e. the temperature at which they trigger freezing. INPs active at warmer temperatures (closer to 0 °C) tend to be rarer, while those active at colder temperatures tend to have much higher concentrations. DFAs can be used to determine INP concentrations from environmental samples or from lab-prepared samples and standards, and knowledge of key parameters such as sample mass or surface area allows normalisation of the DFA to allow comparison of ice-nucleating activities of samples in terms of the ice-active mass density, $n_m(T)$, or ice-active surface site density, $n_s(T)$. A number of variations and improvements have been made to DFAs over the years via the development of new instrumentation (overviews of modern instrumentation can be found in the literature,[317, 321-323] the most recent being in Miller et al.),[268] but the core principles of DFAs remain the same.

Purified water can be cooled to around −35 to −40 °C before freezing homogeneously,[322, 324, 325] and so in principle this should define the "background" or "baseline" of the DFA. However, DFAs typically employ droplets in the microlitre range, and droplets of purified water droplets tend to freeze below ~−20 to −25 °C, thus restricting INP measurements to warmer temperatures.[320, 326, 327] This can be caused by a number of factors, including increased chance of impurities in such relatively large droplet volumes or interferences from the hydrophobic substrates employed,[328] although with great care and preparation it is possible to reduce these effects.[329]

However, DFAs that employ picolitre droplets can readily achieve homogeneous freezing of water; reducing the size of the droplets means less chance of impurities on a droplet-by-droplet basis, and the droplets are typically immersed in an immiscible oil that eliminates interferences and impurities from solid substrates. In the past, such droplets have been generated via nebulisation[21, 330-332] or by emulsification with a vortex mixer,[327, 333] but these produce very polydisperse droplet populations and the former method in particular can be non-trivial.

Microfluidics offers the capability to generate monodisperse water-in-oil droplets of controlled size easily and with high throughput.[334-336] By pumping a liquid through a side channel (a T-junction)[337] (Figure 5a) or a nozzle (for flow focusing)[338] (Figure 5b), i.e. the discrete phase, into another flowing but immiscible liquid, i.e. the continuous phase, with a surfactant usually added to the immiscible phase to aid droplet stability, droplets of the discrete phase are "pinched off" due to the viscous forces. Droplet production rates of tens to thousands per second can be achieved relatively easily, while it is possible to produce >1M per second.[339] The integration of sensors and actuators into microfluidic platforms enables the manipulation, splitting, merging, trapping, separation, and counting of droplets for fields ranging from biochemical analysis to microparticle production via their use as reaction compartments.

The use of droplet microfluidics for ice nucleation builds on the back of centuries old discoveries.[340] While Daniel Gabriel Fahrenheit was the first to describe supercooling of rainwater in glass vials in 1724 (having observed the effect in 1721),[341] Swiss physicist Albert Mousson discovered in 1858[342-344] that water droplets smaller than 500 µm (<65 nL) could be supercooled on hydrophobic surfaces. UK geologist and metallurgist Henry Clifton Sorby was the first to discuss, in 1859,[345] the supercooling of water in capillary tubes, following a series of experiments in capillaries of 85, 36 and 25 µm diameter, some of which were performed with the prominent Irish physicist, John Tyndall. Sorby noted, however, that "Dr. Percy", likely in reference to UK metallurgist John Percy, had also observed the supercooling of water in capillary tubes. Dufour[346-348] found in 1861 that water droplets in oil and chloroform emulsions could be easily supercooled to as cold as −20 °C. Modern day microfluidic ice nucleation thus continue the legacies of these findings via the supercooling of small water droplets in emulsions within microchannels.

The advantages of droplet microfluidics have seen an explosion of their use in recent years in the ice nucleation community for DFAs since the first demonstration of microfluidic freezing in 2007.[349] The monodisperse picolitre droplets enable the homogeneous freezing regime to be accessed, thereby allowing INP spectra to be produced in the ~−20 to −35 °C region that standard microlitre DFAs cannot typically access.[322, 328] Further, the acquisition of high quality droplet freezing data comprising hundreds or thousands of uniformly sized droplets allows for improved statistics compared to standard techniques with limited (e.g. <50) droplet numbers. For example, it enables the use of the differential nucleus spectrum, rather than the commonly used cumulative spectrum, both derived from the number of frozen droplets versus unfrozen droplets at a given temperature, for quantitative comparisons of ice-nucleating ability and the activation of ice nucleating sites at specific temperatures. Differential spectra require the data to be binned into temperature intervals, hence experiments employing low droplet numbers suffer from a loss of fidelity upon binning. An in-depth discussion of the differential nucleus concentration is provided by Vali,[350] who employed microfluidic DFA data from Polen et al.[328] (using a microfluidic droplet array device discussed and validated by Brubaker et al.,[204]

described below) to illustrate its application and benefits. Fahy et al.[351] recently demonstrated a method, based on empirical bootstrapping, for interpolating DFA data and deriving differential spectra with high confidence bands for quantitative comparisons, again taking advantage of the large droplet freezing datasets achievable with microfluidic instruments.

Several microfluidic DFAs have been developed and were recently reviewed by Tarn et al.[322] in terms of their application to homogeneous freezing studies, and in a section in a review on microfluidic phase transfer studies by Roy et al.,[352] but all also could or have been applied to the analysis of atmospheric INPs. We briefly describe the main strategies here, an overview of microfluidic DFAs is provided in Table 2 in the Appendix. Most microfluidic DFAs employ water-in-oil emulsions, and a summary of suitable oils and surfactants for such emulsions and the lowest cooling temperatures achievable or tested are provided by Hauptmann et al.[353] A number of reviews are also available that discuss the various methods of microfluidic temperature control[354-356] and measurement.[354, 357] Outside of ice nucleation, the study of the nucleation and crystallisation processes in droplet microfluidics and their applications[358-363] has been performed for a number of species, including proteins,[364] acids[365] and inorganic crystallisation,[366] thanks to the high monodispersity achievable, the ability to control the microenvironment, and the high throughput that enables improved statistics.

A. Microfluidic droplet emulsions

The easiest and most accessible method of employing microfluidics for INP analysis is to pump an aqueous suspension of INPs or aerosol sample through a basic flow focusing or T-junction microchannel design to generate water-in-oil droplets and collect them off-chip in a vial as an emulsion (Figure 5). Droplets can then be pipetted from the vial onto a standard microscope cold stage where they can undergo an otherwise traditional DFA (Figure 5c). In a stable oil-surfactant system, the aqueous droplets will self-assemble into a hexagonal close packed array that, despite the proximity of the droplets, allows the droplets to freeze independently.

Riechers et al.[367] demonstrated the use of this method for the study of the homogeneous freezing of water using differential scanning calorimetry (DSC), in addition to cryomicroscope-based DFAs, to obtain high temperature accuracy, finding that temperature measurement is the most important parameter in the uncertainty of ice nucleation rates. At around the same time, Lignel et al. 2014[368] also performed DSC studies of microfluidically generated droplets as part of a test on emulsion stability towards studies in microgravity conditions.

Weng et al.[369] were the first to apply the technique to heterogeneous nucleation via INPs, focusing on cryopreservation studies. The authors tested Snomax®, a commercial form of the ice-nucleating bacteria, *P. syringae*, that has been sterilised and lyophilised, in water and heavy water (D_2O), as well as testing the effect of several cryoprotectants on freezing.

Tarn et al.[201] developed the "Microfluidic pL-NIPI" droplet emulsion technique to replace the previous pL-NIPI method that employed a nebuliser to generate droplets on a glass substrate. The original nebuliser technique yielded highly polydisperse populations with only minimal control over the droplet size, and employed a liquid nitrogen cooled cryomicroscope stage,[370, 371] while the Microfluidic version produced a highly monodisperse droplet population and employed a more user-friendly Peltier element-based thermoelectric cooler (TEC). The Microfluidic pL-NIPI was used to assess a range of atmospheric INPs, including filter samples collected from a rural site and during bonfire events,[202] and was also applied to Arctic sea surface microlayer (SML) and phytoplankton samples.[372]

These simple microfluidic devices require the use of otherwise standard cold stage equipment, which is an advantage of this technique, although it does require more steps than other microfluidic DFA techniques. The number of droplets typically analysed using this technique is on the order of hundreds to about one thousand, far higher than most standard DFAs. However, the stability of the droplet system tends to be lost once the droplets have been freeze-thawed, resulting in coalescence of the droplet population that prevents repeat freezing cycles from being performed. This method is also not so amenable to automation as other microfluidic methods, which would be an essential part of a sample-to-answer INP analysis platform.

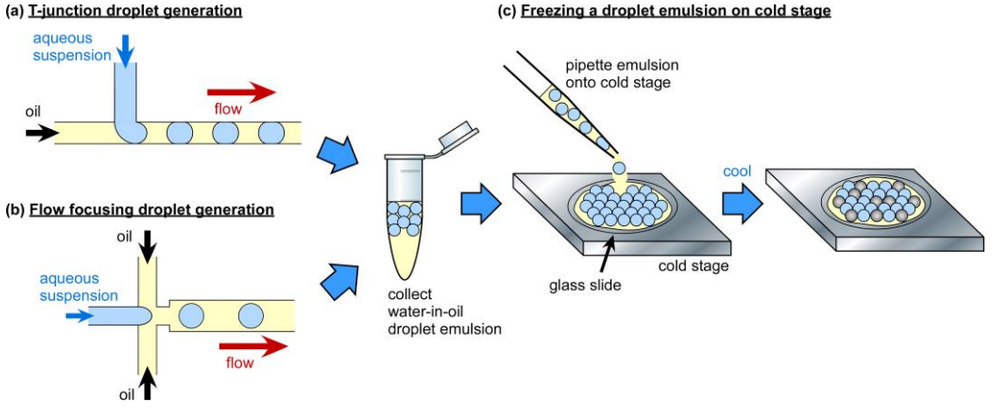

Figure 5: The use of microfluidically generated droplet emulsions for droplet freezing assays (DFAs). Waterin-oil droplets are typically generated in a (a) T-junction or (b) flow focusing channel configuration and collected off-chip in a vial. (c) The droplet emulsion can then be pipetted onto a glass slide on a cold stage and cooled until all of the droplets have frozen.[367] The temperatures at which the droplets freeze reveal information on the concentration and activity (e.g. ice active site density per mass or surface area) of the INPs. A transparent lid is usally placed atop the droplet suspension during freezing (not shown for clarity) to prevent evaporation.

B. Microfluidic droplet arrays

A more advanced form of the droplet emulsion technique involves the introduction of a chamber or channel structure following the droplet generation region that enables the trapping of droplets in an array (Figure 6). By situating the microfluidic chip directly onto a microscope cold stage, typically comprising a Peltier element-based thermoelectric cooler, the trapped droplet array can thus be cooled directly for DFA. This allows for a much greater degree of automation than the droplet emulsion DFA technique by eliminating several manual steps, though it does require somewhat more complex chip design and fabrication.

Edd et al.[373] developed the first instance of an on-chip array-based DFA using a "Dropspots" platform (Figure 6a),[374] which employs a series of parallel channels containing droplet-shaped wells. Droplets are generated and flow through the channels, then when the flow stops the droplets settle into the wells, allowing for a rapid and simple process of arraying. The authors performed nucleation and crystallisation experiments on water and aqueous solutions of glycerol.

The Dropspots technique was later developed into the INP analysis platform, WISDOM, by Reicher et al.,[220] initially demonstrating its capabilities on nucleation of minerals and the analysis of atmospheric samples collected using a MOUDI cascade impactor during dust storms in the Eastern Mediterranean.[203, 220, 221] WISDOM has since been applied to the study of various ice-nucleating materials such as sea ice diatoms,[32] soil and mineral dusts,[317] bacteria and proteins,[317, 375-379] and a variety of other samples and studies (see Table 2 for a complete list). A modified version of WISDOM, termed the "nanoliter Bielefeld Ice Nucleation ARraY (nanoBINARY)", was also recently applied to the study of ice nucleation by short- and long-chain poly(vinyl alcohol) (PVA).[380]

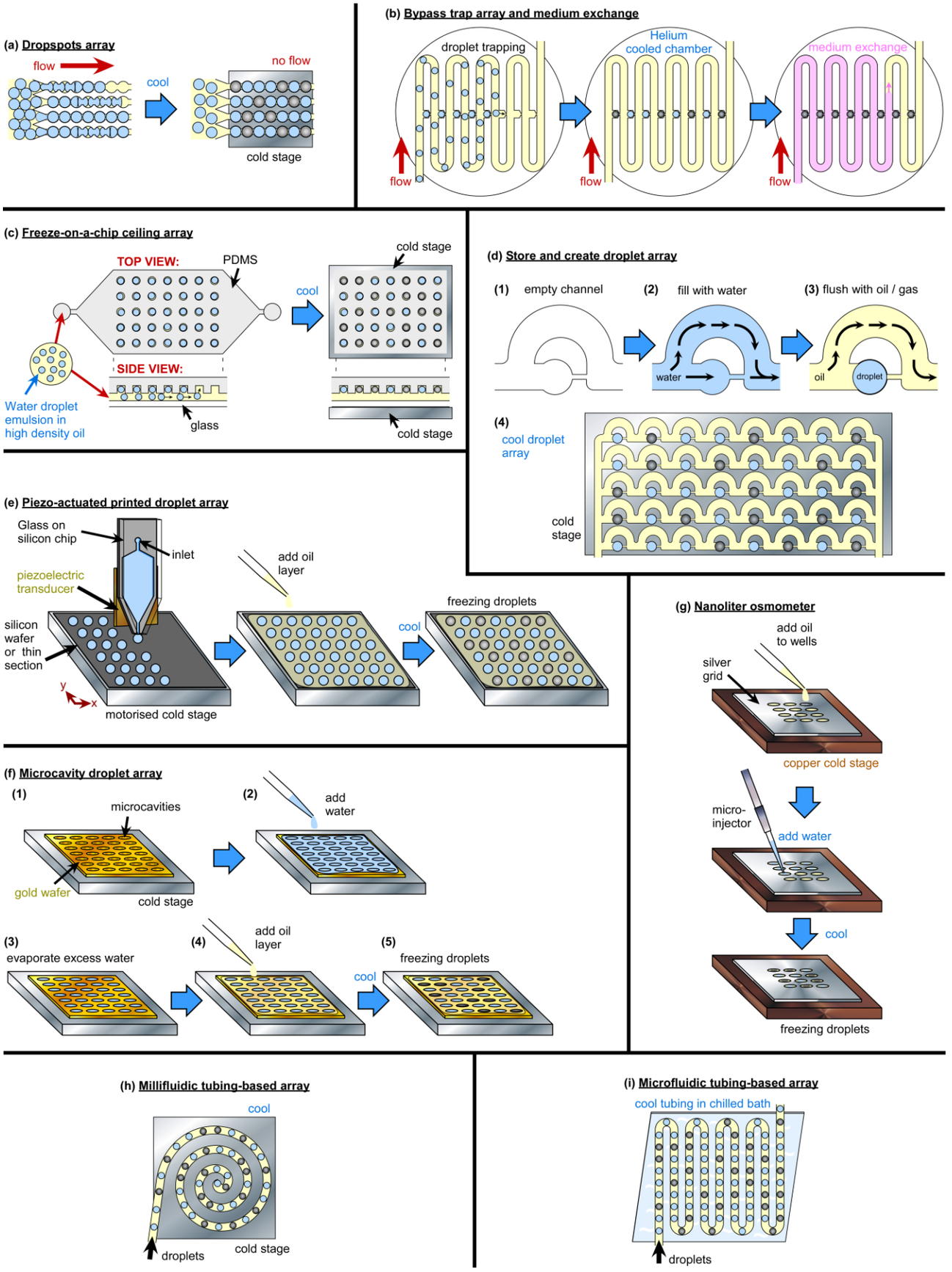

Figure 6: Microfluidic droplet array techniques for on-chip microfluidic DFAs, in which an array generated on a substrate is cooled on cold stage. (a) Dropspots array technique,[373, 374] utilised also in the WISDOM[220] and nanoBINARY[380] DFA methods. Adapted and used with permission of the Royal Society of Chemistry, from Schmitz et al., *Lab on a Chip*, **9**, 44-49 (2009), permission conveyed through Copyright Clearance Center, Inc. (b) A bypass trap array for the exchange of the medium around frozen droplets.[381] Adapted and used with permission of the Royal Society of Chemistry, from Sgro and Chiu, *Lab on a Chip*, **10**, 1873-1877 (2010), permission conveyed through Copyright Clearance Center, Inc. (c) "Freeze-on-a-chip" ceiling array that relies on a high density oil to trap aqueous droplets in ceiling wells.[382] Adapted and used from Weng et al., *Cryobiology*, **84**, 91-94 (2018), with permission from Elsevier. (d) "Store and create" droplet array, in which water is flushed through a channel then flushed with oil[204] (or backflushed with oil or gas)[383] to leave droplets in traps, eliminating the need for surfactants as in many other techniques.[204] Adapted and used with permission from Brubaker et al., *Aerosol Science & Technology*, **54**, 79-93 (2020), reprinted by permission of the publisher (Taylor & Francis Ltd, http://www.tandfonline.com). (e) Piezoeletric transducer actuated droplet printer used to automatically print a droplet array on a substrate on a motorised stage.[384] (f) Microcavity-based "Freezing on a Chip" platform in which microcavities in a gold or gold-coated substrate are used to generate droplets in an array for freezing.[321] (g) Nanoliter osmometer adapted for DFAs via the microinjection of droplets into oil-filled wells in a silver grid.[379] (h) Millifluidic spiral tubing-based array on a cold plate.[385] (i) Microfluidic serpentine tubing-based droplet array in a chilled bath.[386]

Sgro et al.[381] developed a droplet docking device in which droplets would be pulled into wells or "docks" and then frozen upon cooling, after which the immiscible environment around them was exchanged (Figure 6b), though a DFA was not performed on any samples.

Weng et al.[382] fabricated a "Freeze-on-a-chip" DFA device comprising a series of wells in the ceiling of a microfluidic chamber for cryobiology studies (Figure 6c). Water-in-oil emulsions were generated microfluidically their previously described device[369] and then injected into the Freeze-on-a-chip, with the high density of the fluorinated oil causing the droplets to rise to the top of the device and become trapped in the wells. Around 1,500 droplets could be trapped for DFAs of PVA as an antifreeze (glyco)protein mimic.

Brubaker et al.[204] developed a DFA based on the "store and create" droplet microfluidic technique of Boukellal et al.[387] that allows for the formation of droplets within wells in a parallelised microchannel structure (Figure 6d). Aqueous suspension is first pumped through the channels to fill the wells, then the channel flushed with an oil that removes the aqueous suspension but avoids the wells, resulting in the *in situ* surfactant-free generation of 6 nL water-in-oil droplets within the wells. The technique was applied to DFAs of NX illite, Snomax®, and filter-collected biomass-burning aerosol (BBA),[204] including the finding that atmospheric aging enhances the ice nucleation of BBA,[205] and as part of a study on interferences on purified water freezing in DFAs.[328] Since the droplets were relatively large, the authors refrained from labelling their purified water data as homogeneous freezing, but decreasing the droplet well size could easily achieve this in future. "Store and create" devices have also now been adopted by other research groups. Roy et al.[388] employed such a platform for the analysis of INPs and efflorescence in SSAs from bulk seawater and sea surface microlayer samples (SMLs), finding that the droplets that effloresced into aggregate and amorphous particles correlated with warmer droplet freezing temperatures during DFAs, while those effloresced into single and fractal crystals correlated with colder freezing temperatures. House et al.[389] studied the effects of cationic salts on the ice-nucleating ability of Snomax® as a seawater proxy and the final morphology of the particles, finding a decoupling of ice-nucleating activity and particle morphology. House et al.[390] later studied the effects of salinity and pH on montmorillonite bentonite clay, in addition to repeat freezing and efflorescence-deliquescence (E-D) cycling. The results showed that the ice-nucleating ability of montmorillonite decreased at low pH, possibly due to changes in particle aggregate sizes, while E-D cycling affected the freezing characteristics of the suspensions, which may be due to delamination of the clay particles. The group have also used "store-and-create" platforms for investigations into phase transitions such as crystallisation and liquid-liquid phase separations,[352] including in aerosols and SMLs.[391-393]

Tarn et al.[383] demonstrated a store-and-create array device that allowed for the generation of droplets onto polished minerals of thin sections to map the ice-nucleating activity across the mineral surface, in an update to the single droplet version of the technique used by Holden et al.[394] to study ice-active sites. The device used dried air or nitrogen gas to backflush the device (rather than flushing in the same direction as the original water fill, as per Brubaker et al.[204]) in a similar method to Kim et al.[366] for inorganic crystallisation, eliminating the need for oil, and allowing for operation by hand without the need for syringe pumps.

C. Printed droplet arrays

A different method of generating an array of picolitre droplets is to print them directly onto a substrate (Figure 6e). Peckhaus et al.[384] developed a system based on a commercially available piezoelectric microfluidic droplet generator (GeSiM, Germany) and a motorised cold stage, allowing up to 1,500 picolitre droplets to be printed automatically onto a silicon wafer that was then covered with a layer of oil. The printed array was used to analyse suspensions of ice-nucleating feldspars[384] and alumina,[395] as well as being used to array directly onto polished grain mounts and thin sections of minerals.[396, 397] The group used a similar approach to print larger droplets (21.6 nL) via a piezo-driven PipeJet Nano dispenser (BioFluidix GmbH) onto silicon wafers for DFAs of feldspar suspensions.[396 397]

D. Microcavity-based arrays

Droplet arrays have been demonstrated using microcavities or wells fabricated in a substrate into which droplets can be placed or generated. Häusler et al.[321] developed a "Freezing on a Chip" comprised of a gold-plated silicon or gold substrate into which an array of wells was etched (Figure 6f). 2 µL of an aqueous INP suspension were pipetted onto the chip to fill the wells, with the excess liquid between the wells evaporating, then the wells were covered in a layer of oil. The droplet size was determined by the size of the wells, and multiple chips of different well sizes were fabricated to accommodate different droplet volumes. The device was applied to DFAs of Snomax®, pollen and feldspar mineral.

Lee et al.[379] developed a DFA based on a commercially available nanoliter osmometer (µIce, Israel), originally developed for single droplet freezing studies by Braslavsky and Drori,[398] that comprises 12 oil-filled wells of 0.5 mm diameter into which ~10 nL aqueous droplets were added using a FemtoJet microinjector (Eppendorf, Germany) (Figure 6g). The device was applied to DFAs of ice-nucleating proteins from *P. borealis* bacteria to study their self-assembly, alongside DFAs performed using WISDOM.[376, 379]

E. Tubing-based arrays

Recently, microfluidic platforms have been developed that bridge the features of the droplet emulsion systems and the droplet array devices described above. Here, water-in-oil droplets are generated in a microfluidic channel and enter a very long section of spiralled or serpentine transparent tubing. However, rather than being collected in a vial for off-chip analysis, the flow is instead stopped such that the droplets in the tubing become stationary, forming a tubing-based droplet array that can be cooled perform a DFA. This methodology combines simple fabrication and setup with excellent temperature control over the droplet array, and could be automated relatively easily.

Atig et al.[385] fabricated a millifluidic capillary tubing-based T-junction droplet generator that fed into a spiral capillary immersed in an ethanol cold bath (Figure 6h). DFAs of montmorillonite clay, titanium dioxide, and highly ice nucleation active silver iodide were performed, though the droplets were on the scale of millimetres in diameter that yielded high background results for purified water DFAs.

Isenrich et al.[386] developed a microfluidic tubing array-based device, the Microfluidic Ice Nuclei Counter Zürich (MINCZ), in which microfluidically generated droplets were stored in capillary tubing held within a plastic holder with temperature probes and immersed in an ethanol cooling bath (Figure 6i). The platform was used to perform DFAs on purified water,[399] K-feldspar,[386] and aqueous sucrose solutions[400] with temperature accuracies of ±0.2 °C.

F. Continuous flow analysis

Continuous flow DFAs comprise a cold plate directly beneath a long microchannel, such that droplets freeze as they flow over the plate. This has the advantage that, unlike most other DFAs that are limited to tens to hundreds of droplets per experiment, thousands or tens of thousands of droplets can be assayed by allowing the platform to run for as long as desired. Continuous flow microfluidic systems are also very amenable to automation, and a raft of options are available for upstream or downstream processing including continuous flow separations,[291] reactions and sample treatment,[401, 402] and analysis.[403, 404]

However, maximising the potential for this technology can also lead to complexity and a potential for issues to arise. These include the need for accurate temperature measurements of the flowing droplets within the microchannel[355] without disturbing the droplets, which could potentially trigger freezing. Microchannel dimensions become very important: a small microchannel cross-section relative to the droplet size is desirable to limit the temperature differences through the cross-section and so improve heat transfer, but must be larger enough that the droplets do not become stuck when they freeze due to the ~9 % increase in volume (depending on temperature), or when spicules of ice extrude from a frozen droplet.[405]

While droplets can easily be generated at rates of hundreds to thousands per second, the flow rates required for this while still being able to freeze droplets would require very low cold stage temperatures and extremely high temperature gradients that would be far greater than the gradients the droplets would experience in updrafts in the atmosphere. Therefore, continuous flow DFAs would be limited to single digits to tens of droplets per second without incorporating measures to lower the temperature gradient, e.g. the use of serpentine channels. Despite these issues, continuous flow DFAs arguably offer the greatest potential for integrated lab-on-a-chip platforms with upstream and downstream processing.

Sgro et al.[349] demonstrated the first example of continuous flow droplet freezing, albeit for cryopreservation studies of cells rather than as a DFA, in 2007. Using a Peltier element-based thermoelectric cooler either above or below the microchannel, droplets containing single cells were frozen in flow and found to be viable provided cryoprotectants (in this case dimethyl sulfoxide, DMSO) were present.

Stan et al.[207] fabricated an elegant continuous DFA platform featuring a series of thermoelectric coolers that generated a temperature gradient along the length of the microchannel (Figure 7a). A series of microfabricated platinum resistance temperature (PRT) detectors were integrated into the bottom of the microchannel, such that temperature at which the droplets froze could be determined based on their position in the temperature gradient system. A platinum coating on the underside of the device served as a mirror to aid visualisation using reflected light microscopy. The apparatus allowed tens of thousands of droplets to be analysed at a rate of 75 droplets per second, with high temperature accuracy (±0.4 °C). DFAs of purified water and silver iodide were demonstrated, while the dendritic growth of ice in flowing droplets was studied with high-speed microscopy.

The instrument of Stan et al. was modified to determine whether electric fields influence the homogeneous nucleation of supercooled water by incorporating electrodes above and below the microchannel.[406] The authors found that applying electric fields up to 1.6×10^5 V m^{-1} had no effect on nucleation rates, though thermodynamic models suggested that fields >10^7 V m^{-1} could increase the rate of nucleation. Variations of the platform were also employed to demonstrate the effect of temperature on controlling droplet size and velocity,[407] and investigations of sheathless hydrodynamic positioning[408] and lift forces[409] on droplets and bubbles flowing through a microchannel.

Tarn et al.[203] developed the continuous flow LOC-NIPI platform that comprised a single cooling plate, similar to Sgro et al., [349] and performed DFAs by flowing droplets over the plate at a series of decreasing temperatures (Figure 7b), with hundreds or thousands of droplets analysed per temperature setpoint. Modelling of the flow and temperature was not required, and a temperature probe was located in a parallel reference channel to measure the temperature of the flowing oil as a proxy for droplet temperature measurements. The temperature gradient across the single cold plate varied with temperature, combined with the use of the temperature reference channel rather than direct measurements as in Stan et al.,[207] yielded conservative temperature uncertainties that ranged from ±0.4 °C at warmer temperatures to ±0.7 °C at the coldest temperatures.

The LOC-NIPI setup allowed for non-specialists in microfluidics to use the setup in the lab and in the field, being applied to DFAs of Snomax®, birch pollen, aerosol filter samples collected and analysed in the Eastern Mediterranean,[203] INP activity in river outflows,[410] and a study on homogeneous nucleation.[322] LOC-NIPI was designed to be built into an integrated analysis platform with upstream and downstream processing, the first step being an adaptation to sort ice crystals and water droplets in continuous flow,[411] described in the following section.

An issue with continuous flow DFAs is the sheer number of droplets that pass through the device and must be counted, an extremely laborious job if performed manually. Roy et al.[206] fabricated a continuous flow DFA platform based on that of Stan et al.[207] and developed a deep neural network (DNN) algorithm using AlexNet[412] to count droplet freezing events with 99 % accuracy, and applied it to the study of the effect of heat treatment on Snomax®. Using Fourier-transform infrared (FTIR) spectroscopy, the authors showed that heat treatment causes the β-helix secondary structure of Snomax's *inaZ* protein to convert to a β-sheet or strand-like structure, and that the extent of β-helix conversion correlated with a reduction in droplet freezing temperatures in the microfluidic device. The platform was limited to temperatures down to −20 °C due to the use of mineral oil, which becomes too viscous to pump through the microchannel, but this could easily be overcome by using similar oils to other continuous flow DFA systems.

A further potential issue with continuous flow DFAs is the typically very high cooling rate (100s-1000s °C min^{-1}), much faster than typical cooling rates experienced in cloud updrafts (e.g. 1-10 °C min^{-1}) that are more accurately represented in droplet emulsion or array-based DFAs, i.e. static rather than continuous systems. However, a comparison of LOC-NIPI data obtained for silver birch pollen (*B. pendula*) and Snomax® demonstrated that even at very high cooling rates of 2,400 °C min^{-1}, the data were comparable to other standard DFA techniques performed at 1 °C min^{-1}.[203]

While it has not been demonstrated yet, the microfluidic tubing array DFA platforms described in the previous section, such as MINCZ,[386] could easily be adapted to continuous flow analysis by having droplets flow through tubing immersed in a bath that is being cooled down while the droplets are observed.

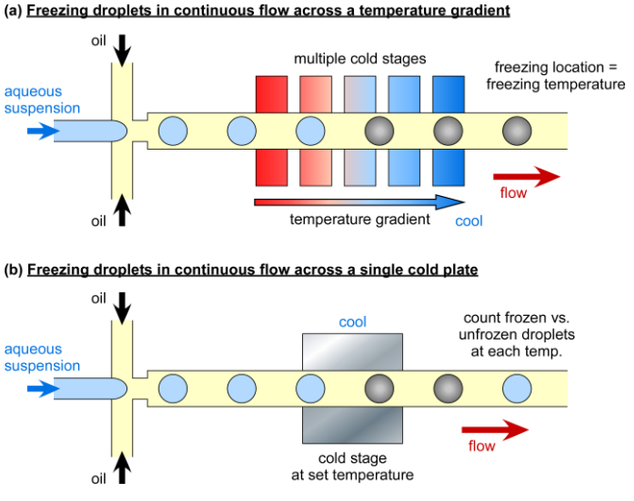

Figure 7: Continuous flow microfluidic DFAs, in which droplets are generated and then freeze as they pass over a cold stage, allowing the analysis of thousands of droplets. (a) Use of a multi-cold stage instrument to generate a defined temperature gradient.[207] The position at which a droplet freezes thus indicates the temperature at which it froze. (b) Use of a single cold plate, in which the relative number of frozen and unfrozen droplets are counted over a series of set temperatures of the stage, as used in the LOC-NIPI platform.[203] Adapted from Tarn et al., *Lab Chip*, **20**, 2889-2910 (2020), licenced under Creative Commons Attribution 3.0 Unported Licence.

IV. MICROFLUIDIC DROPLET SORTING

One of the most challenging aspects of atmospheric ice nucleation, as discussed earlier, is the identification of the dominant INP species in an atmospheric population. While there are bioanalytical techniques can be used to determine the presence of biological INPs, it may be necessary or beneficial to separate the dominant INPs, which trigger freezing in DFAs at warmer temperatures, from the "background" INP community that triggers freezing at colder temperatures, to determine what species are in the former (and in what concentrations) that are not in the latter. This can be achieved somewhat, for example, using laborious manual processes in which droplets that freeze at warmer temperatures in a DFA are repeatedly selected, divided and refrozen multiple times, then the final droplet evaporated and the residual analysed or photographed.[109]

Fahy et al.[413] recognised the potential for the density-based separation of frozen and unfrozen droplets ($\rho_{water} > \rho_{ice}$) after finding that ice crystals formed in an aqueous solution of 50% w/w propylene glycol floated to the top of the solution.[414] Kamijo and Derda[415] developed a cuvette-based "freeze-float" droplet selection system for 1 µL droplets suspended in layers of oils of differing densities, with single droplets finding equilibrium positions in the different layers depending on whether they were frozen or not, allowing for their collection (Figure 8a). The authors have since demonstrated a high-throughput version of the platform utilising multiwall plates and a robotic liquid handling system for automated pipetting of droplets.[416]

Porter et al.[411] demonstrated a density-based continuous flow microfluidic sorting system for frozen and unfrozen droplets by adding a separation chamber to the LOC-NIPI platform (Figure 8a). Droplets and ice crystals entered the separation chamber in a high density oil, such that both populations rose upwards (in the z-direction) in the oil against the force of gravity, with the less dense and therefore more buoyant ice crystals migrating further in the z-direction and thus being collected via a different outlet channel to the water droplets. A separation efficiency of 94 % was achieved, with scope for improvement by modifying the design.

The device of Porter et al.[411] is currently the only microfluidic platform to achieve an ice crystal-water droplet separation, but various continuous flow separation systems discussed in section II could also be applied here. Size-based separations could be feasible in principle, though the increase in volume by ~9 % of a droplet upon freezing may be too small to make this easily achievable. However, deformability-assisted sorting methods could be employed to separate the deformable water droplets from the solid ice crystals, and these methods have seen success in separations of biological cells.[417-419]

Such techniques can utilise microstructures, e.g. pillars or weirs, that the deformable species can flow under/over/around in a manner that solid particles cannot, or hydrodynamic forces (including inertial microfluidics) that leverage the hydrodynamic resistances of different species in fluids to force them into different laminar flow streams. Acoustophoretic forces,[420] applied via ultrasonic transducers, enable microfluidic separations based on size, density and compressibility to manipulate particles into equilibrium positions in a microchannel and could have potential applications here. Deformation cytometry techniques, often applied to single cell analysis of cell biomechanical properties, could also be applied here by exploiting the differences in mechanical stiffness to manipulate and separate droplets and crystals.[419]

A key point to consider here, however, is that the mechanism of separation does not induce the freezing of water droplets prior to the sorting outlets.

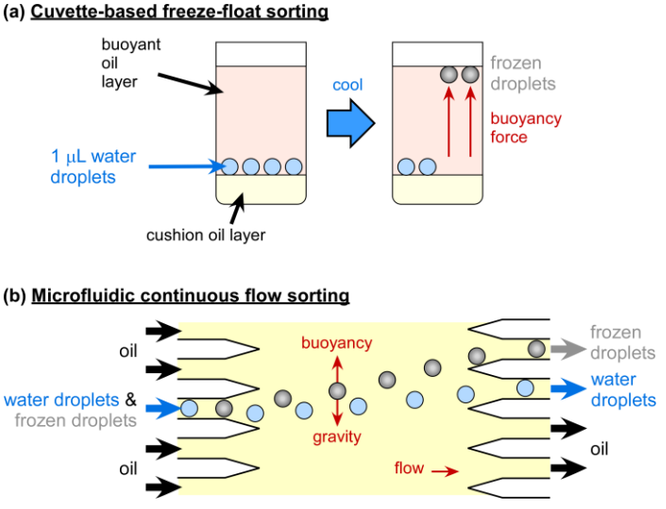

Figure 8: The sorting of frozen and unfrozen droplets for the later analysis and comparison of the two populations, based on the greater density of water to ice. (a) Freeze-float sorting in a cuvette in a non-microfluidic method, utilising oils of differing densities to generate cushion and buoyancy layers.[415] Reprinted (adapted) with permission from Kamijo and Derda, *Langmuir*, **35**, 359-364 (2019). Copyright (2019) American Chemical Society. (b) Microfluidic continuous flow sorting of frozen and unfrozen droplets based on their relative buoyancies under gravity, allowing the collection of the two populations via different outlets, as used in the LOC-NIPI platform.[411] Adapted from Porter et al., *Lab Chip*, **20**, 3876-3887 (2020); licensed under a Creative Commons Attribution 3.0 Unported Licence.

V. DROPLET PICOINJECTION

Following the DFA and potentially the droplet sorting steps, an ideal on-chip automated platform would incorporate various types of chemical and biological analysis, such as immunoassays, colourimetric or fluorimetric reactions, or DNA analysis. Many such measurements require the mixing of reagents with the sample in order to react with the analytes of interest, but since samples are compartmentalised in droplet microfluidics, the interfacial tension between the droplets and the immiscible oil can make this difficult to achieve.

One of the most common methods of injecting picolitre reagents into flowing microfluidic droplets utilises integrated electrodes to electrically induce a thin-film instability that momentarily rupture the water-oil interface, allowing reagent from a narrow side-channel under high pressure to be injected into the droplets (Figure 9). This technique was first demonstrated by Abate et al.,[421] and has since been applied to the injection of reagents for DNA amplification,[422, 423] single cell-lysis, [424] and microgel bead fabrication.[425, 426], and variations on the electro-injection method,[423, 427-429] The technique has also been applied to droplet merging to enable the merging and reaction of biochemical species in two different droplet populations.[430-432]

It many situations it may be desirable to not use electrodes within a device, hence electrode-free picoinjection methods have also been developed. O'Donovan et al.[433] developed a method in which dissolved electrolytes in the solution acted as the electrode, allowing picoinjection when an electric field was applied. Yuan et al.[434] demonstrated a truly electrode-free system in which picoinjection was achieved by finely controlling the pressures in the microfluidic device, with the picoinjection microchannel actuated by air pressure controlled via a regulator. Li et al.[435] by exploited the Venturi effect via a narrow hydrophilic microcapillary junction that injected reagents as droplets interacted with the capillary as they flowed past. Niu et al.[436] fabricated a pillar-based platform that slowed droplets and forced the succeeding droplet to merge with the slowed droplet under pressure.

Picoinjection is a powerful droplet manipulation method that is crucial for many subsequent downstream biochemical analyses, with several methods available depending on requirements.

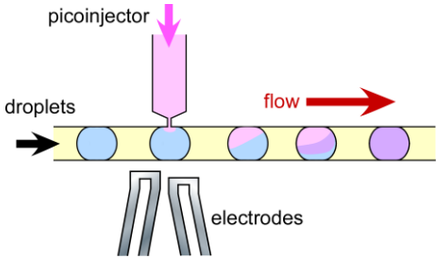

Figure 9: Picoinjection of biochemical reagents into droplet as they flow past a narrow channel picoinjector.[421] Reprinted (adapted) with permission from Abate et al., *Proc. Natl. Acad. Sci. U. S. A.*, **107**, 19163-19166 (2010). Copyright (2010) National Academy of Sciences. The interface between the aqueous droplet and the surrounding immiscible oil is momentarily perturbed, allowing injection. The perturbation is often achieved by applying an electric field via microelectrodes, though the use of controlled pressure or the Venturi effect can also be applied.[435] Picoinjection of reagents can allow downstream biochemical analysis to be performed, such as single cell analyses, immunoassays, or DNA analysis.

VI. MICROFLUIDIC BIOAEROSOL ANALYSIS

Microfluidic technology has a number of features that have made it particularly applicable to bioanalysis.[437, 438] The reduction in device size brings with it the ability to handle small amounts of potentially precious sample volumes, and reduces the amounts of expensive reagents consumed. The small volumes of microchannels reduce the diffusion distances between sample and reagent molecules which, combined with a myriad of potential mixing techniques, enables rapid reactions and assays. Large surface-to-volume ratios provided by microchannels allow for faster heating and cooling, and microfabrication technologies allow for the integration of miniaturised temperature control[355, 439] and detection[440] systems.

Droplet microfluidic (or digital microfluidic) systems employ monodisperse droplets that can be used as thousands of identical, highly efficient picolitre reaction vessels that can be manipulated and analysed on a droplet-by-droplet basis, allowing for powerful,

high throughput bioanalytical processing (e.g. single cell analysis, immunoassays, DNA analysis).[334] These features, combined with the potential for small footprint, portable devices, have made microfluidics an attractive technology for point-of-care medical devices,[441] for example. Likewise, microfluidic techniques have been applied to a variety of bioaerosol separation and analysis procedures, and reviews dedicated to this subject are available courtesy of Zhang et al.,[177] Ezzre et al.,[182] Lee et al.,[179] Wang et al.,[178] and Huffman et al.[181] Related to the topic of ice nucleation, Zhao et al.[442] reviewed the use of microfluidics for cryopreservation, including cell manipulation, cryoprotective agent exposure, programmed freezing/thawing, vitrification, and in situ assessment in cryopreservation, and some of those processes may be applicable to microfluidic INP analysis.[442]

Given the broad scope of microfluidic bioanalytical techniques, and with dedicated reviews available elsewhere for each topic, here we provide a brief overview of some of the major techniques that could be applied to an automated INP monitoring platform, many of which could be used in conjunction with the picoinjection technique described above.

A. Heat test for proteinaceous INPs

As described in the Introduction, the heat test is one of the most common techniques applied to the indirect determination of potential proteinaceous INP content.[13, 59, 134] This is based on the principle that heat (e.g. 95 °C for 30 min) will denature[443] an ice-nucleating protein and so reduce its ice-nucleating activity when comparing DFAs before and after the treatment. Heating to 95 °C in a microfluidic platform is easily achievable via a number of methods,[355, 439] though 30 min is a long timeframe for an envisaged automated analysis system. However, much as the confined nature of microfluidic devices make them amenable for deep supercooling for DFAs, they can likewise be used to achieve superheating of water (i.e. temperatures >100 °C without boiling) in the absence of nucleation sites in microchannels[444] and droplets.[445] Indeed, microfluidic superheating has been applied to the rapid breaking of spores[444] and decomposition of peptides[446] and proteins[447] in continuous flow and in a matter of seconds for their subsequent analysis.

While rapid heat test treatment is possible within a continuous flow microfluidic device, the test itself has a number of caveats in its interpretation. In particular, some minerals (such as quartz) also exhibit a loss of ice-nucleating activity upon heating, in addition to proteinaceous materials, while the mineral K-feldspar does not appreciably lose activity, Hence, if the ice-nucleating activity of a mineral population is dominated by K-feldspar then the heat test can be used to represent the presence of proteinaceous INPs, otherwise a loss of ice-nucleating activity could be due to either mineral content or proteinaceous materials. The heat test is also not suitable for all types of biological and biogenic INPs, for example those whose ice-nucleating activity is conferred by polysaccharides or other non-proteinaceous means. More direct analytical methods, such as many of those described below, are therefore more attractive for ensuring the identification and quantification of the presence of biological and biogenic INPs.

B. Chemical tests for INPs

Similar to heat tests, several simple chemical tests exist that can be routinely applied to INP analysis that provide indirect means of possible classification.[125] For example, treatment with hydrogen peroxide diminishes the activity of organic INPs, including biological INPs, via an oxidation reaction, while guanidinium chloride treatment denatures bacterial and fungal proteins. Lysozyme affects ice-nucleating bacteria via the hydrolysis of peptidoglycan in the cell walls, but may underestimate Gram-negative bacteria and also affects feldspar. Sometimes several of these tests are performed on the same samples, such as heat tests and peroxide treatments, to determine the fractions of different types of materials present in an INP population, e.g. the heat-labile proteinaceous fraction vs. the heat-resistant bio-organic fraction vs. the mineral fraction.

Each of these treatments could be readily applied to a microfluidic platform via, for example, picoinjection of the chemicals into INP-containing droplets, including in parallel, with DFAs performed before and after the treatment. However, like the heat test, there are more direct bioanalytical procedures that can be applied to the identification and quantification of biological INPs.

C. DNA analysis

Typically, an air particulate sample comprises hundreds or thousands of different biological particles, containing relatively few species in high abundance, a few tens of species with moderate abundance, and dozens or even hundreds of other species in very low abundance.[448] DNA analysis is a powerful tool that allows for identification and quantification of biological species in a sample, including INPs, with a number of strategies available depending on requirements. This generally follows several key steps: extraction of DNA, amplification of specific genes or sequences, and analysis of the amplified DNA.

DNA sequencing of a sample allows for species identification and the determination of community composition and relative abundance. 16S rRNA[449] and ITS[450] sequencing have been employed during INP analyses for bacteria[135] and fungal[451] populations, respectively. Commercially available instrumentation, such as nanopore sequencing,[452] has been readily demonstrated for in-field applications such as environmental DNA analysis.[453] One challenge is that a significant number of genetic sequences remain unknown, for example only around 1 % of the estimated 2.2M-3.8M species of fungi have actually been sequenced,[454] hence it can be difficult to assign a detected sequence to an unknown species.

While sequencing is not specific for INPs, and requires assignment of detected sequences to known species, other forms of DNA analysis enable the identification of known INP species. This is one of the more commonly applied biological measurements

for INPs by groups with the requisite expertise. There are various methods of nucleic acid analysis that can provide useful information depending on the particular application. A simple presence/absence analysis for specific biological species, for example *P. syringae*, can be achieved using traditional PCR techniques, in which amplification of the DNA is achieved by thermocycling of the extracted nucleic acids followed by gel electrophoretic analysis or fluorescence detection. The presence/absence also lends themselves well to the use of LAMP techniques. LAMP assays are highly sensitive, do not require precision thermal cycling instrumentation, and can be monitored using a variety of detection techniques including easy to interpret colour change reactions.

However, neither sequencing nor presence/absence assays would, by themselves, inform on the ice-nucleating ability of the species present. To achieve this, it is necessary to identify and potentially quantify the *ina* gene that encodes the ice-nucleating proteins. Identification of *ina* can be achieved via PCR, though the gene can be detected in culturable, viable but non-culturable (VBNC), moribund, and dead cells. Further, detection of the *ina* gene also does necessarily indicate an efficient INP since high nucleation efficiency of bacteria is typically conferred by the aggregation of proteins, which PCR cannot

A modified version of the PCR technique, known as quantitative PCR (qPCR)[455] provides information not only on the presence of the *ina* gene, but also to what extent. While allelic variation exists in the *ina* gene, it is possible to design qPCR primers that are able to amplify all known variants by targeting conservated sequences.[63] Variations of traditional qPCR include digital qPCR, which separates the sample into microscopic droplets that each contain PCR reagents, and microarrays that allow for the targeting of different sequences in each well of the array, enabling multiplexed identification and quantification of several species simultaneously.

Microfluidic devices for the analysis of nucleic acids have become popular in many fields, particularly for clinical diagnostics, due to short reaction times and rapid heating/cooling times afforded by miniaturised sample and reagent volumes.[456,457] While not yet fully explored for the analysis of INPs, there is great potential for these techniques to be adapted in this field for detection and characterisation of biological components. Compared to conventional nucleic acid analysis, microfluidics is particularly advantageous in enabling integration of the multiple steps required, commonly cell lysis, nucleic acid extraction, amplification and detection, as well as high sensitivity.

The field of microfluidic nucleic acid analysis is vast and the reader is directed to comprehensive reviews of the common individual elements, DNA extraction, LAMP[458] PCR and detection,[458] as well as integrated analysis[459] for further details. The use of a microfluidic LAMP assay for bioaerosols has already been demonstrated for the rapid detection of *P. aeruginosa*, an ice-nucleating bacteria studied in this instance as a multidrug resistant pathogen, collected via on-chip SHM-based sampling in a sample-to-answer platform.[216, 288, 289]

Microfluidic digital DNA analysis[460, 461] is particularly amenable to integration into an on-chip INP measurement platform given that droplets are required for the DFA step, and that reagents such as primers can be introduced into each droplet via picoinjection. This strategy brings with it the capability for single cell analysis.[462] Likewise, microfluidic DNA microarray analysis can also be exploited.[463] However, despite the huge potential offered by microfluidic approaches to examining nucleic acids for INP analysis, there remain some key challenges.

Firstly, a key issue for long-term monitoring is that of reagent storage, with the enzymes used for DNA amplification being particularly temperature sensitive, though, this could be addressed using lyophilisation of reagents, as has been demonstrated for both PCR[464] and LAMP[465] reagents.

Secondly, while sequencing is a very powerful method, it generates a large amount of data that must be processed using bioinformatics techniques, which can require considerable scientific expertise. While sequencing itself could be performed relatively quickly and easily on-chip, the amount and complexity of the data produced may be the main drawback to its use in long term atmospheric monitoring. However, more focused DNA analytical techniques would be far more amenable to long term automated monitoring in the field, for example the use of LAMP or qPCR for identification and/or quantification of the *ina* gene or specific species.

D. Cell culture and colony counting

The culturing of cells and subsequent counting of colony forming units (CFUs) has been performed on fungal and bacterial colonies from samples collected during INP measurement campaigns, including the testing of the ice-nucleating activity of the cultures.[56, 140] Culturing typically takes days to weeks, hence culturing and colony counting is not particularly amenable to sample-to-answer platforms.

However, the culturing of mammalian[466] and bacterial cells[467] in microfluidic devices is now routine, with fields such as organ-on-chip[468] and bacterial biofilm models[469] becoming increasingly popular. Microfluidic environments enable spatial and temporal control over the cells alongside continuous replenishment of culture media and *in situ* monitoring and analysis of the cells. Microfluidic single cell analysis is likewise routine[470, 471], with droplet-based methods being very powerful,[472] and amenable to a range of detection techniques described here (e.g. fluorescence staining, immunoassays, DNA analysis…). Hence there are a number of opportunities for cell culture or single cell analysis for the microfluidic study of biological INPs.

Traditional off-chip cell culturing and CFU assays have also been applied to the analysis of bioaerosols collected using microfluidic sampling techniques. The SHM-based microfluidic sampler of Jing et al.[242] was applied to the capture and CFU analysis

of *E. coli* and *M. smegmatis*. The spiral SHM collected of Bian et al.[290] was employed for *V. parahemolyticus*, *L. monocytogenes*, and *E. coli*, while the continuous Dean flow implinger of Choi et al.[235] was applied to the analysis of *S. epidermidis*.

E. Immunoassays

Immunoassays are a powerful bioanalytical tool that allow for high sensitivity and specificity in the detection of biological species via an antigen-antibody interaction.[473] Typically, the target analyte (antigen), such as a bacterial cell or protein, is captured by an antibody specific for that analyte, allowing it to be processed in a number of ways including its isolation from a sample matrix and detection via techniques such as fluorescence, colourimetric assays, or electrochemical sensors.

Immunoassays are traditionally performed in multi-well plates and typically require multiple laborious and manual processing steps, but are highly amenable to microfluidics thanks to the rapid reactions and high surface-to-volume ratios that are available. Immunoassays have become one of the most routinely employed bioanalytical techniques employed in microfluidic technology,[474-477] including for automated systems and point-of-care diagnostics,[160] most commonly via heterogeneous assays that occur on antibodies bound to surfaces such as channel walls or microparticles.[474] Magnetic particles find extensive use in microfluidic immunoassays thanks to the ability to manipulate them using internal or external magnets, allowing easy extraction of target analytes from samples and for sequential reactions to be easily performed.[478] The integration of electrochemical and optical sensors into microfluidic devices enables the detection of the extracted and labelled analytes.[440]

Microfluidic immunoassays have successfully been applied to bioaerosol analysis. Jing et al.[287] employed SHM-based bioaerosol capture of *M. tuberculosis* on-chip, followed by elution and introduction into a second microfluidic device for bacterial lysis and analysis via a microparticle-based immunoassay with fluorescence detection. Coudron et al.[479] developed an EWOD-based immunoassay platform for the automated analysis of *E. coli*, *B. atrophaeus*, and MS2 bacteriophage via magnetic particle-based extraction and chemiluminescence detection. While the platform was not applied to bioaerosol analysis, it was proposed to be used in conjunction with the ESP sampler and EWOD droplet system developed by Foat et al.[239]

While immunoassays have not been performed for INP analysis to our knowledge, the assay of known biological INPs is possible via commercially available antibodies for those targets, such as *P. syringae*.[480] However, since different strains of the same species can have varying or no ice-nucleating ability, the presence of the target analyte would not necessarily identify it as an INP. In this case, targeting known ice-nucleating proteins (e.g. *inaZ* recombinant protein) would provide a direct means of identifying and quantifying biological ice-nucleating activity. However, this depends on the availability of suitable antibodies, which are currently limited, or the capability to produce them.

F. Raman spectroscopy

Raman spectroscopy is a vibrational spectroscopy technique that allows for chemical identification and quantification via structural fingerprints. While by no means routinely applied to INP analysis, it has been used to characterise ice residuals following DFAs in terms of organic matter, nitrates, sulphates, carbonates, and clay minerals,[481-483] and measuring changes in ice-nucleating materials such as Snomax® following their chemical treatment.[484]

On-chip Raman spectroscopy and surface-enhanced Raman spectroscopy (SERS), which employs metallic surfaces to enhance the Raman signal,[485, 486] have been applied to analytes including proteins, DNA, RNA, and cells, and carbonates.[487] Raman spectroscopy can provide a chemical fingerprint unique to a Raman-active compound and, importantly, on-chip Raman could be applied to microfluidic determination of mineral vs. organic content in aerosol samples during INP analysis. Portable or integrated Raman probes and spectrometers have also been developed for microfluidic platforms that can be used for static or continuous flow measurements, and are therefore amenable to analysis in the field. [488-490]

Continuous on-chip sampling and *in situ* SERS analysis of bioaerosols has been demonstrated by Choi et al.[278] who employed their continuous Dean flow microfluidic impinger[235] to sample bacteria (*S. epidermidis*, *M. luteus*, *E. hirae*, *B. subtilis*, and *E. coli*). Silver nanoparticles (AgNPs) were introduced into the device in continuous flow, which bound onto the bacterial cells and allowed their identification as they passed through a detection region in the chip, with the quantification of *S. epidermidis* and its monitoring over time also achieved. This demonstrates the possibility for on-chip Raman to be applied to biological INP analysis in future platforms.

G. Fluorescence spectroscopy

Fluorescence spectroscopy and microscopy are highly sensitive detection tools that are based on the excitation of fluorophore molecules with certain wavelengths of light (excitation), exciting the molecules such that they emit light at a longer wavelength (emission). Direct detection of fluorescent primary biological aerosol particles (FBAPs), including bacteria, pollen, molds, and others, is possible using ultraviolet laser-induced fluorescence (UV-LIF), for example via online aerosol measurement instruments such as the Wideband Integrated Bioaerosol Sensor (WIBS).[491] Online UV-LIF measurements[38, 56, 492, 493] and fluorescence microscopy[56] have been employed during a number of INP measurement campaigns to compare FBAP concentrations to INP activity.

Fluorescence detection is a common analysis technique in microfluidics, often used in immunoassays and various DNA analyses following the labelling on the target analyte with a fluorophore,[494] and has been applied to several microfluidic bioaerosol analyses.

Kang et al.[495] developed a real-time detection system for bioaerosols using inertial impaction and mini-fluorescent microscopy based on a webcam. A curved channel provided an impaction zone within the microfluidic device, with the particle diameter cut-off determined by the channel dimensions and the flow rate. A camera module from a webcam was combined with filters and a blue light source to observe the FBAPs impacted on the channel wall.

The continuous Dean flow microfluidic impinger developed by Choi et al.[235] was employed for the collection of *S. epidermidis*, followed by its off-chip analysis by fluorescence microscopy. Choi et al.[496] also developed on-chip flow cytometer for the detection of bioaerosol particles via LIF detection with an integrated optical fibre connected to a photodetector. Samples of *E. coli*, *B. subtilis*, and *S. epidermidis* were collected using a conventional bubble impinger and pumped through the microfluidic chip where they were stained with SYTO82 fluorescent dye and detected as they flowed through the detection region.

H. Electrical detection

Electrical and electrochemical sensors can be employed for a number of measurements via a range of detection methods (e.g. impedance, voltammetry, amperometry), and are amenable to integration into microfluidic devices via microfabricated electrodes and SPEs,[497] while the functionalisation of electrodes with antibodies allows for use as sensors for immunoassays.[498, 499] The use of microelectrodes allows for small footprint analytical platforms, making electrochemical microfluidic detectors extremely attractive for point-of-care diagnostic devices.[500] While electrical detection has, to our knowledge, has not been applied to INP analysis, electrochemical detection of aerosols has been achieved when using microfabricated systems and microfluidic devices, and could be applied to biological INPs in the future.

Kwon et al.[245] incorporated sensing electrodes into the impactor plates of their 3D printed cascade impactor system, allowing for detection of electrically charged aerosol particles as they were collected on the plates. Yin et al.[314] tested the use of electrical impedance measurements of particles using commercial SPEs, with the intended application to their microfluidic continuous flow DLD platform comprising I-shaped pillars for the separation of $PM_{2.5}$ aerosols. Kim et al.[252] developed a microfabricated single-stage virtual impactor that separated aerosols, whereupon a micro corona discharge was used to charge the separated particles and allow their detection via electrometers based on the electrical current carried by the particles.

I. Pyroelectric thermal sensors

Pyroelectric materials are capable of generating a voltage when they experience heating or cooling. Cook et al.[501] recently demonstrated that polyvinylidene fluoride (PVDF), an inexpensive pyroelectric polymer that can be purchased in sheets and cut to shape, can be used to detect freezing events during INP DFAs based on the release of latent heat when a droplet freezes. A sheet of PVDF was placed atop a cold stage and covered in a thin layer of Vaseline, onto which a standard microlitre droplet array was pipetted. As the stage was cooled and the droplets froze, the latent heat released by the droplets yielded a spike in voltage in the pyroelectric detection system.

The incorporation of pyroelectric materials, particularly PVDF, into microfluidic devices has been demonstrated for the on-chip temperature monitoring via incorporation of a layer of the polymer in the device.[502-504] Given the wide range of polymer microfabrication methods available,[505-510] it is conceivable that devices could be manufactured directly out of PVDF if desired.

J. Infrared thermal imaging

Infrared thermal imaging is another technique that has been used to detect droplet freezing events during INP DFAs based on the release of latent heat, typically being applied to multiwell plates containing droplet volumes of tens to hundreds of microlitres and using a thermal camera.[511-516] While thermal imaging has not yet been applied to microfluidic INP analysis, it has been employed for monitoring a number of processes (e.g. temperature cycling) in microfluidic devices,[517-521] hence it is feasible that it could be employed for microfluidic DFAs or for monitoring temperature-dependent biochemical assays.

K. Differential scanning calorimetry

Differential scanning calorimetry (DSC) also measures the latent heat released upon the freezing of droplets and is capable of very high temperature accuracy. However, it is not capable of detecting individual droplet freezing events as in other methods, typically requiring water-in-oil emulsions for ice nucleation studies. DSC has been applied to a number of ice nucleation studies, including homogeneous freezing, bacterial INPs,[522] mineral dusts,[523, 524] pollen,[524] and water confined in silica capsules.[525]

DSC has been applied to microfluidically generated droplet emulsions. Reicher et al.[367] used DSC to demonstrate that absolute temperature is the most important uncertainty in homogeneous freezing measurements, while Lignel et al.[368] tested the stability of droplet emulsions towards experiments in microgravity.

While DSC is not particularly suited to biochemical analysis or for in-the-field monitoring, MEMS-based DSCs have been developed and could be employed for microfluidic ice nucleation studies.[526-530] The miniaturised dimensions of MEMs technology allow for smaller thermal masses and therefore faster scanning, together with low sample consumption.

Challenges and considerations

The scope for the application of microfluidic separation and analysis techniques to biological INP measurements is enormous, providing an opportunity to enable the identification and quantification of biogenic INPs as a matter of course for the atmospheric ice nucleation community. However, there are several challenges that must be acknowledged in the development of a sample-to-answer INP platform. Knowledge of these issues allows their consideration or avoidance when building a complex multi-step analysis system.

A. High density mineral dusts

While biological analysis is the focus here as a means to identify "missing sources" of INPs in models, there must also be a means of assessing the relative contributions of other important INP types such as mineral dusts. This could, for example, be achieved via chemical or spectroscopic (e.g. Raman) analysis, or informed assumptions about the environment that sampling is taking place in and the sources of the air masses that have sampled. Parallelised screening with chemical treatment and repeat DFAs could allow for categorisation or classification of the organic vs. inorganic components.

However, an issue with relatively large (several micron in diameter) mineral dust particles, which have a high density (~2.65 g cm^{-3}) is that they can sediment relatively quickly (e.g. 90 µm s^{-1} for a 10 µm diameter K-feldspar particle). This can potentially be problematic when using syringes and pumps to drive them through a microfluidic device.[201] Such an issue could be alleviated, however, via the use of perpetual sedimentation pumps,[531] in-syringe magnetic stirrer bars (including commercial products such as the Cetoni Nemix 50),[532] or the incorporation of magnetic stirrer bars into reservoirs used in pressure-based systems (e.g. pressure controllers from Dolomite, Elveflow or Fluigent).

B. Sampling and analysis of rare INPs and bioaerosols

INPs are an important but incredibly rare subset of aerosols, often comprising only 1 in 10^3-10^6 ambient particles in the troposphere.[4] The most active INPs (i.e. those that trigger freezing at warmer temperatures), such as biogenic species, are also the rarest but can have a great impact, while the less active particles can have much larger concentrations. Therefore, to capture the rarer but important warm-temperature INPs, it can be necessary to sample hundreds or even thousands of litres of air to obtain INP signals above an instrument's detection limit once the particles have been washed into or collected as an aqueous suspension.

The problem is further compounded by the volume of aqueous suspension that is processed in a microfluidic device. If 50 droplets of 1 µL volume are analysed in a conventional microlitre DFA, then nearly 100,000 droplets of 100 µm diameter (~524 pL) would need to be analysed in a microfluidic DFA in order to process the same volume of sample, thereby ensuring that the rarer particles detected in the former are also captured in the latter. It is for this reason that many microfluidic DFA results show INP concentrations in a colder temperature regime than standard microlitre assays. This is nonetheless useful to access temperature regimes that standard microlitre DFAs cannot, but by greatly increasing the droplet throughput and automation of microfluidic DFAs it is highly feasible that INP concentrations could be obtained across the entire relevant temperature spectrum (around −35 to 0 °C). This may be where continuous flow DFAs, which would also be more amenable to upstream and downstream processing techniques, come to the fore in order to easily analyse tens or hundreds of thousands of droplets.

Therefore, systems are typically sought that combine high throughput air sampling with small liquid collection volumes to greatly increase aerosol concentrations for analysis. This may be where direct sampling into a microfluidic device with a form of sample concentration would be of great benefit. A further issue for bioaerosol analysis in general can be the scarcity of the target analytes compared to background contaminants that can interfere with the detection of bioaerosols, resulting in false negatives or artificially low results.

C. DFA analysis

While microfluidic DFAs can enable the processing of thousands of droplets in DFAs, this could present an issue in automated platforms in terms of their analysis. Currently, microfluidic DFAs employ cameras to observe droplet freezing events, with videos analysed either manually or using an automated program on an experiment-by-experiment basis. In the case of continuous flow DFAs, high-speed cameras are required that generate a large amount of data and whose analyses are more difficult to automate. This could be alleviated by the use of machine learning-based analysis,[206] for example, while modification of droplet throughput could enable the use of cameras that do not need to operate at high-speed.

A far more suitable method for analysis in a sample-to-answer platform would be to remove the camera entirely and replace it with a single-point detection system that provides a readout of a detection signal over time. On-chip laser light scattering[533] may allow for frozen and unfrozen droplets to be distinguished using a single detection system. Alternatively, the use of a droplet sorting system to separate frozen and unfrozen droplets into separate outlets with 100 % efficiency would allow for simple light-based or electrochemical detectors to detect the number of droplets that pass through each channel. This would greatly simplify the output and analysis of DFAs, particularly when processing tens of thousands of droplets.

A recent consideration that affects many of the microfluidic DFA techniques discussed here is the use discontinuation of many of the per- and polyfluoroalkyl substances (PFAS) (e.g. Fluorinert™ FC-40, Novec™ 7500) that are used as the immiscible oil in droplet production. These oils provide excellent heat transfer properties, low pour points, and both hydrophobic and oleophobic properties that make them ideal for DFAs. However, they are highly persistent, allowing these "forever chemicals" to accumulate

in organisms and the environment, and have implications for human health and ecology,[534] hence they have started being phased out of production since they will likely start to become significantly regulated and restricted in the near future,[535, 536] though the impact on their use in microfluidics may be less immediate.[537] Therefore, other less harmful and persistent PFAS-free oils with suitable properties for the DFA of choice will need to be employed in future.

Thankfully, several microfluidic DFAs, particularly array-based DFAs, already use PFAS-free oil and surfactant systems (see Table 2), with some such as the "store and create",[204, 388] printed array,[384] or microcavity[321] methods not requiring surfactant (or even oil in some cases).[383, 396] The issue may impact the droplet emulsion (in terms of emulsion stability) and continuous flow DFAs (in terms of the oil viscosity at colder temperatures) the most, but there are a wide variety of oil-surfactant systems that may be suitable (see Hauptmann et al.[353] and Baret et al.,[538] for example) while PFAS-free oils with similar properties to PFASs will also likely be developed as a replacement. The discontinuation of PFASs affects not only DFAs but microfluidic droplet applications in general given their widespread use for forming highly stable droplets,[539, 540] which should facilitate the discovery of a suitable alternative in the shorter term given the common goal of the community.[537]

D. Reagent storage

As discussed earlier, one of the considerations for long term bioaerosol monitoring or analysis in-the-field is the stability of the reagents. Some reagents may have a short lifetime, particularly if not properly stored or when prepared as an aqueous solution. This remains a consideration in fields such as point-of-care clinical diagnostics, but for this reason there have been a myriad of solutions to microfluidic reagent storage and release developed over the years for bioanalytical purposes.[541] These include the use of lyophilised reagents in reservoirs or spotted into microfluidic channels that can be reconstituted as and when required. Liquid reagents can be held in blister packs prior to their mixing for a reaction, while the implementation of various micropump and microvalve techniques can allow for chemicals to be accessed and released at specific timeframes.

E. Integration of components and processes

This review has demonstrated that there are a myriad of microfluidic techniques available for each individual step of an envisaged sample-to-answer INP bioanalysis platform, with each offering a range of operational conditions and benefits or drawbacks. However, particularly for bioaerosol analysis, only a handful of examples thus far exist in which several of these steps have been integrated together.[216, 237, 238, 287-289]

Various operating parameters and compromises must be considered when integrating multiple components, since some may function in very different regimes to others. This may be in terms of flow rates, throughput, temperatures, and particle sizes. Sample carry-over and biofouling can also be issues in sample-to answer monitoring systems, hence rigorous cleaning processes may be required between samples, and the use of single-shot consumables.

While the potential for complex integrated systems is enormous and feasible, it may often be easier and faster to remove some functionality in order to produce an integrated platform that is less complex but more robust and reliable in performing a specific purpose. The thoughtful selection of compatible techniques for integration is important, and compromise is key.

Conclusions

Microfluidics has the potential to revolutionise biological INP analysis by providing a toolbox of bioanalytical separation and analysis techniques that have been developed over decades for point-of-care diagnostics and medical applications. These proven capabilities, combined with miniaturised aerosol sampling technologies and microfluidic droplet freezing assays (DFAs) that have been in development for over a decade and allow high droplet number DFAs down to homogeneous freezing, provide an opportunity to produce novel, small footprint, sample-to-answer platforms that could be deployed in the field for automated and even remote sensing of atmospheric.

This has the potential for the construction of a network of micro total analysis systems (μTAS) that would enable continuous measurement of atmospheric INPs at monitoring stations around the world, providing unprecedented data sets describing the spatial and temporal behaviour of INPs in terms of their concentrations and composition. Such an endeavour would greatly improve our understanding of atmospheric INPs and enable better representation in global models, in turn reducing the uncertainties in aerosol-cloud interactions and climate projections.

However, this is not without its challenges. While there are many possible methodologies available for performing each step of the sample-to-answer process, not all are compatible with each other, and even those that are will likely face fluid and mechanical engineering challenges related to integration of different procedures, e.g. flow rates, timings, reagent lifetimes and compatibilities. Nonetheless, the necessary tools are already in place to achieve this, and overcoming these challenges will pave the way for a revolutionary atmospheric INP analysis platform that will dramatically enhance our ability to predict and understand the impacts of a changing climate.

Author Contributions

Conceptualisation: M.D.T., K.J.S., B.J.M.; **Funding acquisition:** B.J.M., M.D.T.; **Writing (original draft preparation):** M.D.T., K.J.S., P.B.F., J.S.W., I.D.J., S.A.P.; **Writing (review & editing):** M.D.T., K.J.S, P.B.F, J.S.W., I.D.J., D.K.M, S.A.P., B.J.M.

SUPPLEMENTARY MATERIAL

Tables 1 and 2 from the Appendix are available as Supplementary Material in the form of downloadable CSV files. The CSV of Table 1 contains a comprehensive list of known biological INPs. The CSV of Table 2 provides details of microfluidic droplet freezing assays, including their operating parameters and the types of samples that have been processed.

CONFLICTS OF INTEREST

The authors have no conflicts to disclose.

ACKNOWLEDGEMENTS

This work was supported by the Natural Environment Research Council (NERC; grant no. NE/X013081/1 FluidIce and grant no. NE/T00648X/1 M-Phase) and the Engineering and Physical Sciences Research Council (EPSRC) Centre for Doctoral Training (CDT) in Aerosol Science (grant no. EP/S023593/1). The authors thank Grace C. E. Porter, Sebastien N. F. Sikora, and Jung-uk Shim for early discussions.

DATA AVAILABILITY

Data sharing is not applicable to this article as no new data were created or analysed in this study.

APPENDIX

Table 1: List of known biological ice-nucleating particles. Note that many (if not all) species also contain strains that may not be ice-nucleating or have varying ice-nucleating activity.

Organism	Notes	Refs.
Bacteria		
Bacillus sp.	Gram-positive soil bacteria	[61]
Brevibacterium sp.	Gram-positive soil-based actinobacteria	[61]
Cellulosimicrobium sp.	Gram-positive human pathogen	[61]
Cupriavidus pauculus	Waterborne human pathogen	[542]
Erwinia ananas	Contains *inaA* gene[148]	[148, 543]
Erwinia stewartii	Plant pathogen	[544]
Exiguobacterium sp.	Extremophile	[545]
Flavobacterium sp.	Soil and fresh water bacteria	[545]
Idiomarina sp.	Marine bacteria	[61]
Lysinibacillus sp.	Gram-positive bacteria. Freezing rain sample, source: Virginia, USA	[140]
Lysinibacillus parviboronicapiens	Gram-positive bacteria. Freezing rain sample, source: Virginia, USA	[140, 141]

Paenibacillus sp.	Gram-positive, endospore-forming bacteria	61
Pantoea sp.	Opportunistic human pathogen	61
Pantoea agglomerans (formerly *Erwinia herbicola*)	Contains *inaE* (*iceE*) gene[154]	63, 546-548
Pantoea ananatis (formerly *Erwinia uredovora*)	Plant pathogen, contains *inaA*[149] and *inaU*[151] genes	63, 549
Phormidium cf. *attenuatum*	Source: Antarctic soil, cyanobacterium	550
Phormidium scottii	Source: Antarctic soil, cyanobacterium	550
Planococcus sp.	Gram-positive bacteria	61
Prochlorococcus sp.	Marine bacterium	551
Pseudomonas sp.	Plant pathogen	56, 64, 66, 552
Pseudomonas aeruginosa	Plant and animal pathogen	217
Pseudomonas antarctica	Isolated from sand, source: Ross Island, Antarctica	553, 554
Pseudomonas auricularis [1]	Snow sample, source: Greece	63
Pseudomonas borealis	Contains *inaPb* gene[153]	375, 376, 555
Pseudomonas fluorescens	Contains *inaW* gene[150]	63, 547, 553, 556, 557
Pseudomonas poae [1]	Non-pathogenic	63
Pseudomonas putida	Soil bacterium	63, 558
Pseudomonas syringae	Plant pathogen, contains *inaZ*,[101] *inaC*,[144] *inaK*,[145] *inaV*,[146] and *inaQ*[147] genes	63, 66, 88, 127, 129, 547, 553, 557, 559-562
Pseudomonas syringae as Snomax®	Sterilised and lyophilised form of *P. syringae*[563]	35, 89, 99, 201, 203, 204, 206, 317, 321, 369, 561, 564-567
Pseudomonas syringae pv. *coronafaciens*	Plant pathogen	130
Pseudomonas syringae pv. *lachrymans*	Plant pathogen	130
Pseudomonas syringae pv. *pisi*	Plant pathogen	130
Pseudomonas viridiflava	Plant pathogen	63, 90, 553, 568-570
Pseudophormidium sp.	Source: Antarctic soil, cyanobacterium	550
Pseudoxanthomonas sp.	Plant pathogen	66, 571
Psychrobacter sp.	Human pathogen	61, 545
Sphingomonas sp.	Human pathogen	545
Stenotrophomonas sp.	Plant and animal pathogen, antibiotic resistant	140
Vibrio harveyi	Marine bacterium	572
Xanthomonas sp.	Plant pathogen	66, 561
Xanthomonas campestris	Plant pathogen	63, 66, 571

Xanthomonas campestris pv. *raphani*	Plant pathogen	[63]
Xanthomonas campestris pv. *translucens*	Plant pathogen, contains *inaX* gene[154]	[63, 556]
Fungi		
Aureobasidium sp.	Yeast	[573]
Cladosporium spores	Common mould, plant pathogen and allergen	[574]
Cryptococcus sp.	Cryptococcaceae (contains yeasts and filamentous forms)	[61]
Fusarium sp.	Plant and animal pathogen	[118, 119]
Fusarium acuminatum	Plant pathogen	[88, 103, 139, 575]
Fusarium armeniacum	Plant pathogen	[103]
Fusarium avenaceum	Plant pathogen	[88, 98, 103, 108, 128, 201, 575, 576]
Fusarium begoniae	Plant pathogen	[103]
Fusarium concentricum	Plant pathogen	[103]
Fusarium langsethiae	Cereal pathogen	[103]
Fusarium oxysporum	Plant pathogen	[577]
Fusarium sporotrichioides	Plant pathogen	[56]
Fusarium tricinictum	Plant pathogen	[103]
Isaria farinosa	Entomopathogenic (insect pathogen)	[56, 100, 103]
Metschikowia sp.	Yeast	[61]
Mortierella alpina	Soil fungi	[100, 103, 136]
Puccinia sp.	Rust fungi	[103, 578]
Puccinia allii	Rust fungi	[578]
Puccinia aristidae	Rust fungi	[578]
Puccinia graminis f. sp. *tritici*	Rust fungi	[578]
Puccinia lagenophorae	Rust fungi	[578]
Puccinia striiformis	Rust fungi	[578]
Puccinia triticina	Rust fungi	[578]
Sarocladium implicatum (formerly named *Acremonium implicatum*)	Wheat fungi	[56, 100, 103]
Pollen		
Abies balsamea	Balsam fir	[107]
Acer negundo	Manitoba maple	[579]
Acer pseudoplatanus	Sycamore maple	[107, 579]
Agrostis alba	Redtop grass	[580]
Agrostis gigantea	Redtop	[99]
Alnus glutinosa	Common European alder	[106, 107]
Alnus incana	Grey alder	[579, 580]
Amaranthus hybridus	Smooth pigweed	[107]
Ambrosia artemisiifolia	Ragweed	[99]
Ambrosia trifida	Giant ragweed	[581]
Araucaria araucana	Monkey puzzle tree	[107]

Artemisia absinthium	Wormwood	[99]
Arundo formosana	Taiwanese reed grass	[107]
Betula alba	White birch pollen	[582, 583]
Betula alleghaniensis	Swamp birch	[107]
Betula x *caerulea*	Hybrid birch	[107]
Betula ermanii	Erman's birch	[107]
Betula fontinalis occidentalis	Water birch	[584]
Betula pendula	Silver birch	[79, 98-100, 106, 107, 201, 203, 321, 579, 585-587]
Betula utilis subsp. *jacquemontii*	Himalayan birch	[107]
Camellia reticulata	Camellia species	[107]
Camellia saluenensis	Camellia species	[107]
Carpinus betulus	European hornbeam	[107, 586]
Carpinus cordata	Heartleaf hornbeam	[107]
Cedrus atlantica	Atlas cedar	[107]
Cedrus atlantica f. *glauca*	Blue atlas cedar	[107]
Cedrus deodara	Deodar cedar	[107]
Cestrum fasciculatum	Early jessamine/red cestrum	[107]
Clerodendrum speciosissimum	Java glorybower	[107]
Corylus avellana	Common hazel	[99, 107]
Crocus vernus	Spring crocus/giant crocus	[107]
Cupressus arizonica	Arizona cypress	[579]
Cupressus sempervirens	Mediterranean cypress	[107]
Cynosurus cristatus	Crested dog's-tail	[107]
Dactylis glomerata	Cat grass	[107, 582, 583]
Encephalartos equatorialis	Cycad species found in Uganda	[107]
Erica multiflora	Mediterranean heath	[107]
Fraxinus pennsylvanica	Red ash	[579]
Juniperus chinensis pfizeriana	Pfitzer juniper	[99]
Juniperus communis	Common juniper	[99, 321, 579]
Hedychium coronarium	White ginger lily	[107]
Helianthus annuus	Common sunflower	[107]
Hordeum vulgare	Barley	[107]
Hymenocallis littoralis	Beach spider lily	[107]
Juglans regia	English walnut	[107]
Lolium sp.	Ryegrass	[581]
Morus rubra	Red mulberry	[579]
Musa rubra	Wild banana	[107]
Narcissus papyraceus subsp. *polyanthos*	Paperwhite	[107]
Nymphaea 'Kew's Stowaway Blues'	Tropical day blooming water lily	[107]
Ostrya carpinifolia	Hop hornbeam	[107]
Picea abies	Norway spruce	[107]

Picea brachytyla	Sargent spruce	[107]
Pilgerodendron uviferum	Conifer	[107]
Pinus contorta var. *contorta*	Shore pine	[107]
Pinus coulteri	Coulter pine	[107]
Pinus halepensis	Aleppo pine	[107]
Pinus mugo	Dwarf mountain pine	[107]
Pinus ponderosa	Ponderosa pine	[107]
Pinus sylvestris	Scots pine	[99, 106, 582, 583]
Plantago lanceolata	Ribwort plantain	[107]
Platanus orientalis	Plane tree	[99]
Poa pratensis	Kentucky blue pollen	[580]
Populus nigra	Black poplar	[580]
Populus nigra v. *italica*	Lombardy poplar	[579]
Quercus rubra	Red oak	[579, 582, 583]
Quercus suber	Cork oak	[107]
Quercus velutina	Black oak	[579]
Quercus virginiana	Live oak	[581]
Salix caprea	Goat willow	[99]
Sambucus nigra	Common elder	[107]
Sequoiadendron giganteum	Giant sequoia	[107]
Spathiphyllum wallisii	Peace lily	[107]
Taxus baccata	Common yew	[99, 107]
Triticum aestivum	Common wheat	[107]
Thuja occidentalis	Northern whitecedar	[99]
Thuja orientalis	Chinese Arborvitae	[99]
Urtica dioica	Common (stinging) nettle	[99]
Zea mays	Corn	[99]
Moss		
Andrae rothui	In the form of leaf material	[93]
Anthoceros punctatus	In the form of leaf material	[93]
Atrichum undulatum	In the form of leaf material	[93]
Aulacomnium turgidum	In the form of leaf material	[93]
Dichodontium palustre	In the form of leaf material	[93]
Dicranella palustris	In the form of leaf material	[93]
Homalothecium sericeum	In the form of leaf material	[93]
Hypnum cupressiforme	In the form of leaf material	[93]
Orthotrichium anomalum	In the form of leaf material	[93]
Orthotrichum diaphanum	In the form of leaf material	[93]
Polytrichum commune	Moss spores;[92] leaf material[93]	[92, 93]
Polytrichum juniperinum	In the form of leaf material	[93]

Racomitrium lanuginosum	In the form of leaf material	[93]
Sphagnum cuspidatum	In the form of leaf material	[93]
Sphagnum palustre	In the form of leaf material	[93]
Syntrichia latifolia	In the form of leaf material	[93]
Tortula muralis	In the form of leaf material	[93]
Phytoplankton		
Apocalathium malmogiense	Dinoflagellate	[33]
Ascophyllum nodosum	Brown algae	[588]
Botrydiopsis cf. *eriensis*	Source: Antarctic soil, green algae	[550]
Bracteacoccus cf. *minor*	Source: Antarctic soil, green algae	[550]
Bumilleria sp.	Source: Antarctic soil, yellow-green algae	[550]
Chlamydomonas sp.	Source: Antarctic soil, green algae	[550]
Chlamydomonas cf. *nivalis* [2]	Snow algae, Alga of the Year 2019	[589]
Chlamydomonas reinhardtii	Unicellular green alga	[589]
Chlorella minutissima	Source: Antarctic soil, green algae	[550]
Chlorella vulgaris	Source: Antarctic soil, green algae	[550]
Chlorococcum sp.	Source: Antarctic soil, green algae	[550]
Chloromonas nivalis	Snow algae	[589]
Chlorophyta-Chlorophyceae	Green algae	[33]
Chlorophyta-Trebouxiophyceae	Green algae	[33]
Coccomyxa sp.	Source: Antarctic soil, green algae	[550]
Desmococcus olivaceus	Green algae	[33]
Dictyosphaerium chlorelloides	Source: Antarctic soil, green algae	[550]
Elliptochloris subsphaerica	Source: Antarctic soil, green algae	[550]
Emiliania huxleyi	Coccolithopore, Alga of the Year 2009	[572, 590]
Fernandinella alpine	Source: Antarctic soil, snow algae	[550]
Fragilariopsis cylindrus [2]	Sea ice diatom, Alga of the Year 2011[591]	[32]
Fucus serratus	Brown algae	[588]
Fucus spiralis	Brown algae	[588]
Fucus vesiculosus	Brown algae	[588]
Gonyostomum semen	Algae	[33]
Interfilum paradoxum	Source: Antarctic soil, green algae	[550]

Heterocapsa niei (formerly *Cachonmia niei*)	Dinoflagellate	[27, 592]
Klebsormidium flaccidium [2]	Source: Antarctic soil, green algae, Alga of the Year 2018	[550]
Laminaria digitata [2]	Brown algae, Alga of the Year winner 2007 (*Laminaria* sp.)	[588]
Laminaria saccharina [2]	Brown algae, Alga of the Year 2007 (*Laminaria* sp.)	[588]
Mastocarpus stellatus	Red algae	[588]
Melosira arctica [2]	Algae, Alga of the Year 2016	[593]
Microcystis sp. [1]	Cyanobacteria	[33]
Myrmecia irregularis	Source: Antarctic soil, green algae, associated with lichen	[550]
Nannochloris atomus	Green algae	[63, 572, 590]
Ochromonus Danica	Golden algae	[27]
Palmaria palmata	Red algae	[588]
Pelvetia canaliculata	Brown algae	[588]
Peridinium aciculiferum	Brown algae	[33]
Phaeocystis sp.	Algae	[542]
Phormidium cf. *attenuatum*	Source: Antarctic soil, cyanobacterium	[550]
Phormidium scottii	Source: Antarctic soil, cyanobacterium	[550]
Porphyridium aerugineum	Red algae	[27]
Polarella glacialis	Dinoflagellate	[33]
Prochlorococcus marinus	Cyanobacterium	[63]
Prasiola crispa	Source: Antarctic soil, green algae	[550]
Pseudococcomyxa simplex	Source: Antarctic soil, green algae	[550]
Pseudophormidium sp.	Source: Antarctic soil, cyanobacterium	[550]
Rhopalocystis cucumis	Source: Antarctic soil, green algae	[550]
Schizochlamydella minutissima	Source: Antarctic soil, golden algae	[550]
Scotiellopsis sp.	Source: Antarctic soil, green algae	[550]
Scotiellopsis terrestris	Source: Antarctic soil, unicellular green algae	[550]
Stichococcus bacillaris	Green algae	[33, 550]
Stramenopiles-Xanthophyceae	Yellow-green algae	[33]
Synechococcus elongatus	Cyanobacterium	[30]
Tetracystis vinatzeri	Green algae	[33]
Thalassiosira pseudonana	Diatom	[31, 34, 572, 594]
Thalassiosira weissflogii	Diatom	[30]

Trebouxia asymmetrica	Lichen symbiotic algae	[589]
Trebouxia decolorans	Green algae	[33]
Trebouxia erici	Lichen symbiotic algae	[589]
Trebouxia glomerata	Lichen symbiotic algae	[589]
Xanthonema debile	Source: Antarctic soil, yellow-green algae	[550]
Lichen		
Acarospora sp.	Source: New Mexico, USA; Colorado, USA	[95]
Alectoria sarmentosa	Source: Alaska	[97]
Aspicilia contorta	Source: UK	[96]
Bryocaulon divergens	Source: Alaska	[97]
Bryoria sp.	Sources: Alaska,[97] Hyytiälä, Finland[94]	[94, 97]
Bryoria fuscescens	Source: Alaska	[97]
Buellia frigida	Source: Antarctica	[96]
Caloplaca sp.	Source: UK	[96]
Candelariella vitellina	Source: UK	[96]
Cetrariella delisei	Source: Norway	[96]
Cladonia sp.	Source: UK	[96]
Cladonia chlorophaea	Source: UK	[96]
Cladonia coniocraea	Source: UK	[96]
Cladonia cristatella	Source: Alaska	[97]
Cladonia macilenta	Source: Alaska	[97]
Cladina portentosa	Source: Alaska	[97]
Cladonia pyxidata	Source: UK	[96]
Cladonia rangiferina	Source: Norway	[96]
Cladonia squamosa	Source: Alaska	[97]
Clauzadea immersa	Source: UK	[96]
Dactylina arctica	Source: Alaska	[97]
Evernia prunastri	Sources: UK,[96] Alaska,[97] Hyytiälä, Finland[94]	[94, 96, 97]
Farnoldia jurana	Source: UK	[96]
Flavocetraria nivalis	Sources: Norway,[96] Alaska[97]	[96, 97]
Hypogymnia enteromorpha	Source: Alaska	[97]
Hypogymnia physodes	Source: Hyytiälä, Finland	[94]
Imshaugia aleurites	Source: UK	[96]
Lasallia pustulata	Source: UK	[96]
Lecanora gangaleoides	Source: UK	[96]
Lepraria sp.	Source: UK	[96]
Leptogium sp.	Sources: UK,[96] New Mexico, USA[95]	[95, 96]
Letharia sp.	Source: California, USA	[95, 595]
Lobaria oregana	Source: Alaska	[97]
Lobaria pulmonaria	Source: Alaska	[97]
Nephroma arcticum	Source: Norway	[96]

Parmelia omphalodes	Source: UK	[96]
Parmelia saxatilis	Sources: UK, Faroes Islands	[96]
Parmelia sulcata	Source: Alaska	[97]
Parmotrema perlatum	Source: UK	[96]
Pelitgera sp.	Source: New Mexico , USA	[95]
Peltigera britannica	Source: Alaska	[97]
Peltigera neopolydactyla	Source: Alaska	[97]
Pertusaria hemisphaerica	Source: UK	[96]
Pertusaria hymenea	Source: UK	[96]
Physcia adscendens	Source: UK	[96]
Physcia tenella	Source: UK	[96]
Platismatia sp.	Source: New Mexico, USA	[95, 595]
Platismatia glauca	Source: Hyytiälä, Finland	[94]
Platismatia herrei	Source: Alaska	[97]
Platismatia norvegica	Source: Alaska	[97]
Porpidia sp.	Sources: Alaska,[97] UK[96]	[96, 97]
Protoblastenia incrustans	Source: UK	[96]
Psora decipiens	Source: New Mexico, USA	[95]
Ramalina subfarinacea	Source: UK	[96]
Rhizocarpon geographicum	Source: UK	[96]
Rhizoplaca chrysoleuca	Source: New Mexico, USA	[95, 595, 596]
Solorina crocea	Source: Norway	[96]
Sphaerophorus globosus	Source: Alaska	[97]
Stereocaulon sp.	Source: Alaska	[97]
Stereocaulon alpina	Source: Norway	[96]
Stereocaulon alpinum	Source: Alaska	[97]
Stereocaulon evolutum	Source: UK	[96]
Stereocaulon vesuvianum	Source: UK	[96]
Sticta fulignosa	Source: Alaska	[97]
Thamnolia tundrae	Source: Alaska	[97]
Thamnolia vermicularis	Source: Norway	[96]
Usnea sp.	Sources: UK,[96] New Mexico, USA[95, 595]	[95, 96, 595]
Usnea longissima	Source: Alaska	[97]
Usnea wirthii	Source: Alaska	[97]
Xanthoparmelia sp.	Source: New Mexico, USA	[95, 595]
Xanthoparmelia cumberlandia	Source: Alaska	[97]
Xanthoria calcicola	Source: UK	[96]
Xanthoria candelaria	Source: UK	[96]
Xanthora elegans	Source: New Mexico, USA	[95]
Xanthoria parietina	Source: UK	[96]
Liverworts		
Aneura pinguis	In the form of leaf material	[93]

Eucalypta streptocarpa	In the form of leaf material	[93]
Fissenden bryoides	In the form of leaf material	[93]
Frullania tamarisci	In the form of leaf material	[93]
Lepidozia reptans	In the form of leaf material	[93]
Lunularia cruciata	In the form of leaf material	[93]
Metzgeria temperata	In the form of leaf material	[93]
Plagiochila porelloides	In the form of leaf material	[93]
Viruses		
His1	Bacteriophage	[110]
HRPV6	Bacteriophage	[110]
Phi6	Bacteriophage	[110]
Phi8	Bacteriophage	[110]
Phi12	Bacteriophage	[110]
Phi13	Bacteriophage	[110]
Phi2954	Bacteriophage	[110]
PhiX174	Bacteriophage	[110]
PRD1	Bacteriophage	[110]
Tobacco mosaic	Plant virus	[111]
Archaea		
Halococcus morrhuae	Prokaryotic organism	[112]
Haloferax sulfurifontis	Prokaryotic organism	[112]
Tardigrades		
Adorybiotus coronifer		[113]
Milnesium tardigradum		[597]

[1] Noted as "possibly ice-nucleating" by the publication's authors.

[2] The Alga of the Year is selected by the Phycology Section of the German Botanical Society (German Society for Plant Sciences): https://www.dbg-phykologie.de/en/alga-of-the-year.

Table 2: Microfluidic droplet freezing assays (DFAs), their operating parameters, and samples that have been analysed. Note that some instruments have been used for applications outside of DFAs, and these are indicated in itallics. Where purified water has been used in multiple publications for background measurements, only the initial publication is provided unless a dedicated study on water was also undertaken. The number of droplets analysed does not account for the theoretical number of droplets that could be analysed, e.g. an instrument may hold 1,000 droplets but if only 100 were observed under a microscope then the value of 100 is provided here.

Publication & technique	DFA type	Chip material	Droplet generation method	Droplet size (µm)	Droplet volume (pL)	Droplets analysed per DFA	Oil	Surfactant	Temperature uncertainty (°C)	Cooling rate (°C min^{-1})	Cold stage	Experiments / Samples
Droplet emulsions												
Riechers 2013[367]	Droplet emulsion	PDMS on silicon	T-junction	53 ± 6 to 96 ± 11	78 ± 30 to 463 ± 178	>1,000	Methyl cyclohexane	2 % w/w Span 80	±0.3	1	Linkam MDBCS196 cryostage or TA-Instruments DSC-Q100 differential scanning calorimeter	Homogeneous freezing of purified water[367]
Lignel 2014[368]	Droplet emulsion	PDMS on glass	Flow focusing nozzle	60 to 80	113 to 268	>1,000	Paraffin oil	1.8 % w/w Span 80	N/A	0.5	Setaram Intrumentation microDSC 7 evo differential scanning calorimeter	Purified water[368]
Weng 2016[369]	Droplet emulsion	PDMS on glass	Flow focusing nozzle	35 ± 2	22 ± 5	200	3M™ Novec™ 7500 (HFE-7500) fluorocarbon	1.5 % w/w Pico-Surf™ 1 (Sphere Fluidics)	N/A	1	Linkam FDCS196 cryostage	Purified water[369] Heavy water (D_2O) [369] Snomax®[369] Ethylene glycol[369] Propylene glycol (PEG)[369] Trehalose[369]
Tarn 2018;[201] "Microfluidic pL-NIPI"	Droplet emulsion	PDMS on glass	Flow focusing nozzle	94 ± 3	435 ± 43	250 to 500	3M™ Novec™ 7500 (HFE-7500)	2 % w/w Pico-Surf™ 1 (Sphere Fluidics)	±0.5	1	TEC (aq. PPG cooled)	Purified water[201] Homogeneous freezing of water[201] Tap water[201] Snomax®[201]

							fluorocarbon					*B. pendula* (silver birch) pollen washing water[201] *F. avenaceum* fungi washing water[201] K-feldspar microcline BCS-376[201] UK rural (agricultural) aerosols[201] UK bonfire aerosols[201, 202] Arctic sea surface microlayers (SMLs)[372] *S. marinoi* phytoplankton[372]
Microfluidic droplet arrays												
Edd 2009;[373] "Dropspots"	Microfluidic droplet array (based on Dropspots)[374]	PDMS on glass	Flow focusing nozzle	37 ± 2	26 ± 5	~100	3M™ Fluorinert™ FC-40 fluorocarbon	PFPE-PEG block copolymer	N/A	0.6	Linkam FDCS196 cryostage	Purified water[373] Glycerol[373]
Sgro 2010[381]	Microfluidic droplet array	PDMS on glass	Flow focusing nozzle	~100	N/A	10s	Silicone oil (AR 20)	0.05 % w/v Span 80	N/A	N/A	Helium gas cooled using LN_2 and flowed through a chamber	Purified water[381] *Immiscible phase medium exchange*[381]
Weng 2018[382]	Microfluidic droplet array (employing droplets produced in Weng 2016 device)[369]	PDMS on glass	Flow focusing nozzle (from the Weng 2016 device)[369]	35 ± 2	22 ± 5	1,500	3M™ Novec™ 7500 (HFE-7500) fluorocarbon	N/A (droplets stabilised in 1.5 % w/w Pico-Surf™ 1 prior to introduction as an emulsion)[369]	N/A	1	Linkam FDCS196 cryostage	Purified water[382] Poly(vinyl alcohol) (PVA)[382] Poly(vinylpyrrolidone) (PVP)[382] Polyethylene glycol (PEG)[382]
Reicher 2018;[220] "WISDOM"	Microfluidic droplet array (based on Dropspots)[374]	PDMS on glass	Flow focusing nozzle	39 ± 3 or 96 ± 6	31 ± 8 or 463 ± 87	550 (for 39 µm droplets) or 120 (for 96 µm droplets)	Mineral oil	2 % w/w Span 80	±0.3	1	Linkam THMS600 cryostage	Purified water[220] Homogeneous freezing of water[220] K-feldspar microcline BCS-376[220, 317] NX illite[220, 598] Arizona test dust (ATD) [220] Snomax®[317] Glucose[220] NaCl[220]

												Ammonium sulphate[220] Size-resolved eastern Mediterranean aerosol (dust storms)[203, 220, 221] *F. cylindrus* diatoms[32] Argentinian soil dust[317] Tunisian soil dust[317] Microcrystalline cellulose (MCC)[323] Nanocrystalline cellulose (NCC)[323] Poly(vinyl alcohol) (PVA)[380] Birch pollen washing water[380] *E. coli* (ArcticExpress strain)[379] Phosphate buffered saline (PBS) [375, 379] Miller's LB broth medium[375, 379] Bacterial ice-nucleating proteins (from *P. syrinage* and *P. borealis*)[375-377, 379] Ice-binding proteins (from snow fleas)[378] Stochasticity and time dependence[598] Antifreeze proteins (type-III AFP, *Tm*AFP)[599] Secondary ice production[600]
Brubaker 2020;[204] "Store and create"	Microfluidic droplet array (based on store and create)[387]	PDMS	Store and create	300 µm ∅ × 95 µm deep, or 450 µm ∅ × 95 µm (pancake-shaped)	6 nL (for 300 µm ∅) or 14 nL (for 450 µm ∅)	40 (for 450 µm ∅) or 720 (for 300 µm ∅)	Squalene oil	None	±0.2	1	TEC cooled via a TECA AHP-1200CAS air chiller	Purified water[204] Interferences in purified water[328] NX illite[204] Snomax®[204] Biomass burning aerosol (BBA) [204] Aged BBA[205]
Tarn 2021;[383] "Store and create"	Microfluidic droplet array (based on store and create)[387] on mineral thin section (based on Holden 2019)[394]	PDMS on mineral thin section	Store and create	~110	~700	100s	None (dry air or nitrogen gas)	None	±0.4	1	TEC (aq. PPG cooled)	K-feldspar mineral thin section[383]

Roy 2021:[388] "Store and create"	Microfluidic droplet array (based on store and create)[387]	PDMS on glass	Store and create	450 µm ∅ × 150 µm deep (pancake-shaped)	21 nL	185	Silicone oil	None	±0.69	0.5	Linkam LTS420 cryostage	Purified water[388] Bulk seawater[388] Sea surface microlayers (SMLs)[388] Heat treated SMLs[388] Peroxide treated SMLs[388] Snomax®[389] Snomax® treated with cationic salts[389] Montmorillonite clay[390] Effects of pH, salinity, repeat freezing, and efflorescence-deliquescence (E-D) cycling on montmorillonite clay[390] Sodium chloride (freezing point depression)[390] *Crystallisation and liquid-liquid phase transitions[352] including in aerosols and SMLs*[388, 391-393]
Eickhoff 2023;[380] "nanoBINARY"	Microfluidic droplet array (based on Dropspots[374] and WISDOM[220])	PDMS on glass	Flow focusing	96 ± 4	463 ± 58	70	3M™ Novec™ 7500 (HFE-7500) fluorocarbon	2 % w/w PFPE-Tris	±0.3	1	Linkam BCS 196 cryostage	Purified water[380] Birch pollen washing water[380] Poly(vinyl alcohol) (PVA) [380] Ethanol[380] Propan-2-ol[380] 1,3-Butanediol[380]
Printed droplet arrays												
Peckhaus 2016;[384] GeSIM droplet generator	Printed droplet array	Glass on silicon on piezoelectric transducer	Piezoelectric actuation	107 ± 14 (spherical cap)	215 ± 70	160 to 1,500	Silicone oil (Rhodorsil 47V 1000)	None	±0.1	1, 5, 10	Linkam MDBCS196 cryostage	Purified water[384] K-feldspar microcline FS02* (BCS-376)[384] K-feldspar FS01[384] K-feldspar FS04[384] Na/Ca-feldspar FS05[384] Aluminium oxide (α-alumina)[395]
Kiselev 2021;[396] GeSIM droplet generator for mineral grain mounts and thin sections	Printed droplet array on mineral thin sections (based on Peckhaus 2016)[384]	Glass on silicon on piezoelectric transducer	Piezoelectric actuaction	N/A	0.4 nL (grain mount); 1.4 nL (thin section)	380 to 540 (grain mount); 50 to 340 (thin section)	None	None	N/A	3	Linkam MDBCS196 cryostage	Treated Volkesfeld sanidine feldspar FS08-VS grain mounts[396] Pakistan perthitic alkali feldspar FS06 thin section[396, 397] Austrian sanidine K-feldspar FS07 (adularia) thin section[397]

Kiselev 2021;[396] PipeJet droplet generator	Printed droplet array (based on Peckhaus 2016)[384]	Capillary tube	Piezoelectric actuaction	N/A	21.6 nL	70	None	None	N/A	3	Linkam MDBCS196 cryostage	Volkesfeld sanidine K-feldspar FS08-VS[396] Pakistan perthitic alkali feldspar FS06[397] Austrian sanidine K-feldspar FS07 (adularia)[397]
Microcavity-based arrays												
Häusler 2018;[321] "Freezing on a Chip"	Microcavity droplet array	Silicon or gold wafer	Microcavities	40 ± 4 nominal (20 to 80 range)	34 ± 11 nominal (4 to 300 range)	25	Paraffin oil	None	±0.4	2	TEC (water-ice cooled)	Purified water[321] K-feldspar microcline[321] Snomax®[321] *B. pendula* (silver birch) pollen washing water[321] *J. communis* (common juniper) pollen washing water[321]
Lee 2023;[379] "Nanoliter osmometer"	Microinjected droplet array (based on nanoliter osmometer)[398]	Droplets injected into silver sample grid	Microinjector	~280 to 350	~10 nL to ~20 nL	12	Unknown oil	None	N/A	2 nominal (0.5 and 1 also used)	TEC (water cooled)	Bacterial ice-nucleating proteins (from *P. syringae* and *P. borealis*)[376, 379] Snomax®[379] *E. coli* (ArcticExpress strain)[379] Phosphate buffered saline (PBS) [379] Miller's LB broth medium[379]
Tubing-based arrays												
Atig 2018[385]	Millifluidic spiral tubing-based array	PFA capillary (1 mm ∅)	Capillary-based T-junction or capillary-based flow focusing	~800 to ~1,200	~300 nL to ~900 nL	~70	3M™ Fluorinert™ FC-770 fluorocarbon or *n*-hexane, or cyclopentane as a hydrate-former	None	N/A	0.5	TEC (cooled via a cold bath)	Purified water[385] Dissolved CO_2 in water[385] Montmorillonite clay[385] Titanium dioxide[385] Silver iodide[385]
Isenrich 2022;[386] "MINCZ"	Microfluidic serpentine tubing-based array	PDMS on glass with PFA capillary (75 µm ∅)	Flow focusing	75 ± 5 or 100 ± 5	221 ± 44 or 524 ± 79	750	3M™ Novec™ 7500 (HFE-7500) fluorocarbon	1 % v/v 008-FluoroSurfactant (RAN Biotechnologies)	±0.2	1	Ethanol bath cooled by a TEC (aq. ethylene glycol cooled TEC)	Purified water[386] Homogeneous freezing of water[399] Italian K-feldspar microcline[386] Sucrose[400]
Continuous flow												

Sgro 2007[349]	Continuous flow	PDMS on glass	T-junction	30	14	N/A	Silicone oil (AS 4) or mineral oil (M5310)	0.01 or 0.05 % w/v Span 80	N/A	~20,000	TEC (air cooled)	*Biological cell freezing (mouse B lymphocytes)*[349]
Stan 2009[207]	Continuous flow	Glass on PDMS on glass	Flow focusing nozzle	80 ± 1	268 ± 10	>10,000	PFMD fluorocarbon	2 % v/v THPFO	±0.4	120 to 6,000	Series of TECs (ethanol cooled)	Purified water[207] Homogeneous freezing of water[207] Silver iodide[207] External electric fields[406] *Temperature-controlled droplet size/velocity*[407] *Hydrodynamic droplet positioning*[408] *Droplet lift forces*[409]
Tarn 2020;[203] "LOC-NIPI"	Continuous flow	PDMS on glass	Flow focusing nozzle	86 ± 8	331 ± 89	1,000s	3M™ Novec™ 7500 (HFE-7500) fluorocarbon	0.2 or 2 % w/w Pico-Surf™ 1 (Sphere Fluidics)	±0.4 to ±0.7 (temperature dependent)	200 to 2,400	TEC (aq. PPG cooled)	Purified water[203] Homogeneous freezing of water[322] Snomax®[203] *B. pendula* (silver birch) pollen washing water[203] Eastern Mediterranean aerosol[203] Canadian river water[410] *Continuous water/ice sorting*[411]
Roy 2021[206]	Continuous flow	PDMS on silicon	Flow focusing	70 to 85	221 to 322	1,000s	Light mineral oil (CAS: 8042-47-5)	None	±0.03	140 to 720	Series of TECs (LN_2 cooled)	Snomax®[206] Aged Snomax®[206] Heat treated Snomax®[206]

* K-feldspar microcline BCS-376 is also known as "FS02" in some publications.

Abbreviations: aq. = aqueous; LN_2 = liquid nitrogen; PDMS = poly(dimethyl siloxane); PFA = perfluoroalkoxy-alkane; PFMD = perfluoromethyldecalin; PFPE = perfluoropolyether; PPG = polypropylene gycol; Span 80 = sorbitan monooleate; TEC = Peltier element-based thermoelectric cooler (TECs must be actively cooled to achieve low temperatures and the cooling methods are described in brackets here); THPFO = 1*H*,1*H*,2*H*,2*H* -perfluorooctanol; Tris = tris(hydroxymethyl)aminomethane.

REFERENCES

1. G. Vali, Bull. Am. Meteorol. Soc., **56** (11), 1180-1184 (1975)
2. J. E. Jiusto and R. L. Lavoie, Bull. Am. Meteorol. Soc., **56** (11), 1175-1179 (1975)
3. Z. A. Kanji, L. A. Ladino, H. Wex, Y. Boose, M. Burkert-Kohn, D. J. Cziczo and M. Krämer, Meteorological Monographs, **58**, 1.1-1.33 (2017)
4. B. J. Murray, D. O'Sullivan, J. D. Atkinson and M. E. Webb, Chem. Soc. Rev., **41** (19), 6519-6554 (2012)
5. B. J. Murray, K. S. Carslaw and P. R. Field, Atmos. Chem. Phys., **21** (2), 665-679 (2021)
6. U. Lohmann and J. Feichter, Atmos. Chem. Phys., **5** (3), 715-737 (2005)
7. H. R. Pruppacher and J. D. Klett, *Microphysics of Clouds and Precipitation*. (Kluwer Academic Publishers, Dordrecht, 1997).
8. J. Vergara-Temprado, A. K. Miltenberger, K. Furtado, D. P. Grosvenor, B. J. Shipway, A. A. Hill, J. M. Wilkinson, P. R. Field, B. J. Murray and K. S. Carslaw, Proc. Natl. Acad. Sci. U. S. A., **115** (11), 2687-2692 (2018)
9. R. E. Hawker, A. K. Miltenberger, J. S. Johnson, J. M. Wilkinson, A. A. Hill, B. J. Shipway, P. R. Field, B. J. Murray and K. S. Carslaw, Atmos. Chem. Phys., **21** (23), 17315-17343 (2021)
10. in *BACCHUS Ice Nucleation DataBase (INDB)* (https://www.bacchus-env.eu/in/join.php, 2023), Vol. 2023.
11. A. Welti, E. S. Thomson, J. Schrod, L. Ickes, R. O. David, Z. Dong and Z. A. Kanji, presented at the EGU General Assembly 2023, Vienna, Austria, EGU23-1458, 2023, 10.5194/egusphere-egu23-1458.
12. R. C. Schnell, presented at the IXth Nucleation Conference, Galway, Ireland, 353-356, 1977.
13. R. C. Schnell and G. Vali, J. Atmos. Sci., **33** (8), 1554-1564 (1976)
14. P. J. DeMott, K. Sassen, M. R. Poellot, D. Baumgardner, D. C. Rogers, S. D. Brooks, A. J. Prenni and S. M. Kreidenweis, Geophys. Res. Lett., **30** (14), 1732 (2003)
15. R. C. Schnell and G. Vali, Tellus, **27** (3), 321-323 (1975)
16. R. C. Schnell, J. Atmos. Sci., **34** (8), 1299-1305 (1977)
17. M. Chatziparaschos, N. Daskalakis, S. Myriokefalitakis, N. Kalivitis, A. Nenes, M. Gonçalves Ageitos, M. Costa-Surós, C. Pérez García-Pando, M. Zanoli, M. Vrekoussis and M. Kanakidou, Atmos. Chem. Phys., **23** (3), 1785-1801 (2023)
18. C. S. McCluskey, P. J. DeMott, P.-L. Ma and S. M. Burrows, Geophys. Res. Lett., **46** (13), 7838-7847 (2019)
19. C. S. McCluskey, J. Ovadnevaite, M. Rinaldi, J. Atkinson, F. Belosi, D. Ceburnis, S. Marullo, T. C. J. Hill, U. Lohmann, Z. A. Kanji, C. O'Dowd, S. M. Kreidenweis and P. J. DeMott, J. Geophys. Res. Atmos., **123** (11), 6196-6212 (2018)
20. J. Vergara-Temprado, B. J. Murray, T. W. Wilson, D. O'Sullivan, J. Browse, K. J. Pringle, K. Ardon-Dryer, A. K. Bertram, S. M. Burrows, D. Ceburnis, P. J. DeMott, R. H. Mason, C. D. O'Dowd, M. Rinaldi and K. S. Carslaw, Atmos. Chem. Phys., **17** (5), 3637-3658 (2017)
21. J. D. Atkinson, B. J. Murray, M. T. Woodhouse, T. F. Whale, K. J. Baustian, K. S. Carslaw, S. Dobbie, D. O'Sullivan and T. L. Malkin, Nature, **498** (7454), 355-358 (2013)
22. A. D. Harrison, K. Lever, A. Sanchez-Marroquin, M. A. Holden, T. F. Whale, M. D. Tarn, J. B. McQuaid and B. J. Murray, Atmos. Chem. Phys., **19** (17), 11343-11361 (2019)
23. Y. Boose, A. Welti, J. Atkinson, F. Ramelli, A. Danielczok, H. G. Bingemer, M. Plötze, B. Sierau, Z. A. Kanji and U. Lohmann, Atmos. Chem. Phys., **16** (23), 15075-15095 (2016)
24. C. S. McCluskey, T. C. J. Hill, C. M. Sultana, O. Laskina, J. Trueblood, M. V. Santander, C. M. Beall, J. M. Michaud, S. M. Kreidenweis, K. A. Prather, V. Grassian and P. J. DeMott, J. Atmos. Sci., **75** (7), 2405-2423 (2018)
25. E. K. Bigg and C. Leck, J. Geophys. Res. Atmos., **113** (D11), D11209 (2008)
26. V. Després, J. A. Huffman, S. M. Burrows, C. Hoose, A. Safatov, G. Buryak, J. Fröhlich-Nowoisky, W. Elbert, M. Andreae, U. Pöschl and R. Jaenicke, Tellus B Chem. Phys. Meteorol., **64** (1), 15598 (2012)
27. R. C. Schnell, Geophysical Research Letters, **2** (11), 500-502 (1975)
28. P. J. DeMott, T. C. J. Hill, C. S. McCluskey, K. A. Prather, D. B. Collins, R. C. Sullivan, M. J. Ruppel, R. H. Mason, V. E. Irish, T. Lee, C. Y. Hwang, T. S. Rhee, J. R. Snider, G. R. McMeeking, S. Dhaniyala, E. R. Lewis, J. J. B. Wentzell, J. Abbatt, C. Lee, C. M. Sultana, A. P. Ault, J. L. Axson, M. Diaz Martinez, I. Venero, G. Santos-Figueroa, M. D. Stokes, G. B. Deane, O. L. Mayol-Bracero, V. H. Grassian, T. H. Bertram, A. K. Bertram, B. F. Moffett and G. D. Franc, Proc. Natl. Acad. Sci. U. S. A., **113** (21), 5797-5803 (2016)
29. J. M. Creamean, J. N. Cross, R. Pickart, L. McRaven, P. Lin, A. Pacini, R. Hanlon, D. G. Schmale, J. Ceniceros, T. Aydell, N. Colombi, E. Bolger and P. J. DeMott, Geophys. Res. Lett., **46** (14), 8572-8581 (2019)
30. D. C. O. Thornton, S. D. Brooks, E. K. Wilbourn, J. Mirrielees, A. N. Alsante, G. Gold-Bouchot, A. Whitesell and K. McFadden, Atmos. Chem. Phys., **23** (19), 12707-12729 (2023)
31. P. A. Alpert, J. Y. Aller and D. A. Knopf, Atmos. Chem. Phys., **11** (12), 5539-5555 (2011)
32. L. Eickhoff, M. Bayer-Giraldi, N. Reicher, Y. Rudich and T. Koop, Biogeosciences, **20** (1), 1-14 (2023)
33. S. V. M. Tesson and T. Šantl-Temkiv, Front. Microbiol., **9**, 2681 (2018)
34. T. W. Wilson, L. A. Ladino, P. A. Alpert, M. N. Breckels, I. M. Brooks, J. Browse, S. M. Burrows, K. S. Carslaw, J. A. Huffman, C. Judd, W. P. Kilthau, R. H. Mason, G. McFiggans, L. A. Miller, J. J. Najera, E. Polishchuk, S. Rae, C. L. Schiller, M. Si, J. V. Temprado, T. F. Whale, J. P. S. Wong, O. Wurl, J. D. Yakobi-Hancock, J. P. D. Abbatt, J. Y. Aller, A. K. Bertram, D. A. Knopf and B. J. Murray, Nature, **525** (7568), 234 (2015)
35. R. Du, P. Du, Z. Lu, W. Ren, Z. Liang, S. Qin, Z. Li, Y. Wang and P. Fu, Sci. Rep., **7** (1), 39673 (2017)
36. R. J. Herbert, A. Sanchez-Marroquin, D. P. Grosvenor, K. J. Pringle, S. R. Arnold, B. J. Murray and K. S. Carslaw, EGUsphere, **2024**, 1-47 (2024)
37. D. O'Sullivan, M. P. Adams, M. D. Tarn, A. D. Harrison, J. Vergara-Temprado, G. C. E. Porter, M. A. Holden, A. Sanchez-Marroquin, F. Carotenuto, T. F. Whale, J. B. McQuaid, R. Walshaw, D. H. P. Hedges, I. T. Burke, Z. Cui and B. J. Murray, Sci. Rep., **8** (1), 13821 (2018)
38. G. Pereira Freitas, K. Adachi, F. Conen, D. Heslin-Rees, R. Krejci, Y. Tobo, K. E. Yttri and P. Zieger, Nat. Commun., **14** (1), 5997 (2023)

39. M. D. Tarn, B. V. Wyld, N. Reicher, M. Alayof, D. Gat, A. Sanchez-Marroquin, S. N. F. Sikora, A. D. Harrison, Y. Rudich and B. J. Murray, Aerosol Res., **2** (1), 161-182 (2024)
40. C. M. Beall, T. C. J. Hill, P. J. DeMott, T. Köneman, M. Pikridas, F. Drewnick, H. Harder, C. Pöhlker, J. Lelieveld, B. Weber, M. Iakovides, R. Prokeš, J. Sciare, M. O. Andreae, M. D. Stokes and K. A. Prather, Atmos. Chem. Phys., **22** (18), 12607-12627 (2022)
41. G. C. Cornwell, C. S. McCluskey, T. C. J. Hill, E. T. Levin, N. E. Rothfuss, S.-L. Tai, M. D. Petters, P. J. DeMott, S. Kreidenweis, K. A. Prather and S. M. Burrows, Sci. Adv., **9** (37), eadg3715 (2023)
42. E. Garcia, T. C. J. Hill, A. J. Prenni, P. J. DeMott, G. D. Franc and S. M. Kreidenweis, J. Geophys. Res. Atmos., **117** (D18), D18209 (2012)
43. G. Vali, M. Christensen, R. W. Fresh, E. L. Galyan, L. R. Maki and R. C. Schnell, J. Atmos. Sci., **33** (8), 1565-1570 (1976)
44. M. Joly, P. Amato, L. Deguillaume, M. Monier, C. Hoose and A. M. Delort, Atmos. Chem. Phys., **14** (15), 8185-8195 (2014)
45. Z. Brasseur, D. Castarède, E. S. Thomson, M. P. Adams, S. Drossaart van Dusseldorp, P. Heikkilä, K. Korhonen, J. Lampilahti, M. Paramonov, J. Schneider, F. Vogel, Y. Wu, J. P. D. Abbat, N. S. Atanasova, D. H. Bamford, B. Bertozzi, M. Boyer, D. Brus, M. I. Daily, R. Fösig, E. Gute, A. D. Harrison, P. Hietala, K. Höhler, Z. A. Kanji, J. Keskinen, L. Lacher, M. Lampimäki, J. Levula, A. Manninen, J. Nadolny, M. Peltola, G. C. E. Porter, P. Poutanen, U. Proske, T. Schorr, N. Silas Umo, J. Stenszky, A. Virtanen, D. Moisseev, M. Kulmala, B. J. Murray, T. Petäjä, O. Möhler and J. Duplissy, Atmos. Chem. Phys. Discuss., **2021**, 1-46 (2021)
46. S. M. Burrows, C. Hoose, U. Pöschl and M. G. Lawrence, Atmos. Chem. Phys., **13** (1), 245-267 (2013)
47. J. M. Creamean, R. M. Kirpes, K. A. Pratt, N. J. Spada, M. Maahn, G. de Boer, R. C. Schnell and S. China, Atmos. Chem. Phys., **18** (24), 18023-18042 (2018)
48. R. C. Schnell and G. Vali, Nature, **236** (5343), 163-165 (1972)
49. R. C. Schnell and G. Vali, Nature, **246** (5430), 212-213 (1973)
50. F. Vogel, M. P. Adams, L. Lacher, P. B. Foster, G. C. E. Porter, B. Bertozzi, K. Höhler, J. Schneider, T. Schorr, N. S. Umo, J. Nadolny, Z. Brasseur, P. Heikkilä, E. S. Thomson, N. Büttner, M. I. Daily, R. Fösig, A. D. Harrison, J. Keskinen, U. Proske, J. Duplissy, M. Kulmala, T. Petäjä, O. Möhler and B. J. Murray, Atmos. Chem. Phys., **24** (20), 11737-11757 (2024)
51. M. Zhang, A. Khaled, P. Amato, A. M. Delort and B. Ervens, Atmos. Chem. Phys., **21** (5), 3699-3724 (2021)
52. F. Conen, C. E. Morris, J. Leifeld, M. V. Yakutin and C. Alewell, Atmos. Chem. Phys., **11** (18), 9643-9648 (2011)
53. D. O'Sullivan, B. J. Murray, T. L. Malkin, T. F. Whale, N. S. Umo, J. D. Atkinson, H. C. Price, K. J. Baustian, J. Browse and M. E. Webb, Atmos. Chem. Phys., **14** (4), 1853-1867 (2014)
54. X. Gong, H. Wex, T. Müller, A. Wiedensohler, K. Höhler, K. Kandler, N. Ma, B. Dietel, T. Schiebel, O. Möhler and F. Stratmann, Atmos. Chem. Phys., **19** (16), 10883-10900 (2019)
55. C. E. Morris, F. Conen, J. Alex Huffman, V. Phillips, U. Pöschl and D. C. Sands, Global Change Biol., **20** (2), 341-351 (2014)
56. J. A. Huffman, A. J. Prenni, P. J. DeMott, C. Pöhlker, R. H. Mason, N. H. Robinson, J. Fröhlich-Nowoisky, Y. Tobo, V. R. Després, E. Garcia, D. J. Gochis, E. Harris, I. Müller-Germann, C. Ruzene, B. Schmer, B. Sinha, D. A. Day, M. O. Andreae, J. L. Jimenez, M. Gallagher, S. M. Kreidenweis, A. K. Bertram and U. Pöschl, Atmos. Chem. Phys., **13** (13), 6151-6164 (2013)
57. O. Möhler, P. J. DeMott, G. Vali and Z. Levin, Biogeosciences, **4** (6), 1059-1071 (2007)
58. C. E. Morris, C. L. Monteil and O. Berge, Annu. Rev. Phytopathol., **51**, 85-104 (2013)
59. B. C. Christner, R. Cai, C. E. Morris, K. S. McCarter, C. M. Foreman, M. L. Skidmore, S. N. Montross and D. C. Sands, Proc. Natl. Acad. Sci. U.S.A., **105** (48), 18854-18859 (2008)
60. M. D. Petters and T. P. Wright, Geophys. Res. Lett., **42** (20), 8758-8766 (2015)
61. C. M. Beall, J. M. Michaud, M. A. Fish, J. Dinasquet, G. C. Cornwell, M. D. Stokes, M. D. Burkart, T. C. Hill, P. J. DeMott and K. A. Prather, Atmos. Chem. Phys., **21** (11), 9031-9045 (2021)
62. B. C. Christner, C. E. Morris, C. M. Foreman, R. Cai and D. C. Sands, Science, **319** (5867), 1214-1214 (2008)
63. T. C. J. Hill, B. F. Moffett, P. J. DeMott, D. G. Georgakopoulos, W. L. Stump and G. D. Franc, Appl. Environ. Microbiol., **80** (4), 1256-1267 (2014)
64. T. Šantl-Temkiv, M. Sahyoun, K. Finster, S. Hartmann, S. Augustin-Bauditz, F. Stratmann, H. Wex, T. Clauss, N. W. Nielsen, J. H. Sørensen, U. S. Korsholm, L. Y. Wick and U. G. Karlson, Atmos. Environ., **109**, 105-117 (2015)
65. A. B. Michaud, J. E. Dore, D. Leslie, W. B. Lyons, D. C. Sands and J. C. Priscu, J. Geophys. Res. Atmos., **119** (21), 12,186-112,197 (2014)
66. M. Joly, E. Attard, M. Sancelme, L. Deguillaume, C. Guilbaud, C. E. Morris, P. Amato and A.-M. Delort, Atmos. Environ., **70**, 392-400 (2013)
67. C. Hoose, J. E. Kristjánsson, J.-P. Chen and A. Hazra, J. Atmos. Sci., **67** (8), 2483-2503 (2010)
68. K. A. Pratt, P. J. DeMott, J. R. French, Z. Wang, D. L. Westphal, A. J. Heymsfield, C. H. Twohy, A. J. Prenni and K. A. Prather, Nat. Geosci., **2** (6), 398-401 (2009)
69. A. J. Prenni, M. D. Petters, S. M. Kreidenweis, C. L. Heald, S. T. Martin, P. Artaxo, R. M. Garland, A. G. Wollny and U. Poschl, Nat. Geosci., **2** (6), 402-405 (2009)
70. W. Elbert, P. E. Taylor, M. O. Andreae and U. Pöschl, Atmos. Chem. Phys., **7** (17), 4569-4588 (2007)
71. S. Ana, L. Ulrike and S. Trude, Environ. Res. Lett., **8** (1), 014029 (2013)
72. J. A. Huffman, B. Sinha, R. M. Garland, A. Snee-Pollmann, S. S. Gunthe, P. Artaxo, S. T. Martin, M. O. Andreae and U. Pöschl, Atmos. Chem. Phys., **12** (24), 11997-12019 (2012)
73. A. Sesartic and T. N. Dallafior, Biogeosciences, **8** (5), 1181-1192 (2011)
74. P. Duan, W. Hu, Z. Wu, K. Bi, J. Zhu and P. Fu, Atmos. Res., **285**, 106659 (2023)
75. A. L. Steiner, S. D. Brooks, C. Deng, D. C. O. Thornton, M. W. Pendleton and V. Bryant, Geophys. Res. Lett., **42** (9), 3596-3602 (2015)
76. J. Sun and P. A. Ariya, Atmos. Environ., **40** (5), 795-820 (2006)
77. D. C. Gross, E. L. Proebsting, Jr. and H. Maccrindle-Zimmerman, Plant Physiol., **88** (3), 915-922 (1988)
78. T. M. Seifried, F. Reyzek, P. Bieber and H. Grothe, Atmosphere, **14** (2), 266 (2023)
79. L. Felgitsch, P. Baloh, J. Burkart, M. Mayr, M. E. Momken, T. M. Seifried, P. Winkler, D. G. Schmale Iii and H. Grothe, Atmos. Chem. Phys., **18** (21), 16063-16079 (2018)

80. R. A. Brush, M. Griffith and A. Mlynarz, Plant Physiol., **104** (2), 725-735 (1994)
81. J. O. Krog, K. E. Zachariassen, B. Larsen and O. Smidsrød, Nature, **282** (5736), 300-301 (1979)
82. R. C. Schnell and G. Vali, Bull. Am. Met. Soc. (2024)
83. G. Vali and R. C. Schnell, Bull. Am. Met. Soc., **105** (4), E778-E788 (2024)
84. Y. Vasebi, M. E. Mechan Llontop, R. Hanlon, D. G. Schmale Iii, R. Schnell and B. A. Vinatzer, Biogeosciences, **16** (8), 1675-1683 (2019)
85. I. Steinke, R. Funk, J. Busse, A. Iturri, S. Kirchen, M. Leue, O. Möhler, T. Schwartz, M. Schnaiter, B. Sierau, E. Toprak, R. Ullrich, A. Ulrich, C. Hoose and T. Leisner, J. Geophys. Res. Atmos., **121** (22), 13,559-513,576 (2016)
86. K. J. Suski, T. C. J. Hill, E. J. T. Levin, A. Miller, P. J. DeMott and S. M. Kreidenweis, Atmos. Chem. Phys., **18** (18), 13755-13771 (2018)
87. Y. Tobo, P. J. DeMott, T. C. J. Hill, A. J. Prenni, N. G. Swoboda-Colberg, G. D. Franc and S. M. Kreidenweis, Atmos. Chem. Phys., **14** (16), 8521-8531 (2014)
88. S. Pouleur, C. Richard, J.-G. Martin and H. Antoun, Appl. Environ. Microbiol., **58** (9), 2960-2964 (1992)
89. L. Felgitsch, M. Bichler, J. Burkart, B. Fiala, T. Häusler, R. Hitzenberger and H. Grothe, Atmosphere, **10** (1), 37 (2019)
90. J. M. Young, Ann. Appl. Biol., **111** (3), 697-704 (1987)
91. C. E. Morris, A.-M. Wen, X.-H. Xu and Y.-B. Di, Ecol. Epidemiol., **82** (7), 739-746 (1992)
92. C. F. Weber, Aerobiologia, **32** (2), 353-361 (2016)
93. B. F. Moffett, Lindbergia, **38** (1), 14-16 (2015)
94. U. Proske, M. P. Adams, G. C. E. Porter, M. Holden, J. Bäck and B. J. Murray, EGUsphere, **2024**, 1-22 (2024)
95. T. L. Kieft, Appl. Environ. Microbiol., **54** (7), 1678-1681 (1988)
96. B. F. Moffett, G. Getti, S. K. Henderson-Begg and T. C. J. Hill, Lindbergia, **38** (1), 39-43 (2015)
97. R. J. Eufemio, I. de Almeida Ribeiro, T. L. Sformo, G. A. Laursen, V. Molinero, J. Fröhlich-Nowoisky, M. Bonn and K. Meister, Biogeosciences, **20** (13), 2805-2812 (2023)
98. D. O'Sullivan, B. J. Murray, J. F. Ross, T. F. Whale, H. C. Price, J. D. Atkinson, N. S. Umo and M. E. Webb, Sci. Rep., **5**, 8082 (2015)
99. B. G. Pummer, H. Bauer, J. Bernardi, S. Bleicher and H. Grothe, Atmos. Chem. Phys., **12** (5), 2541-2550 (2012)
100. B. G. Pummer, C. Budke, S. Augustin-Bauditz, D. Niedermeier, L. Felgitsch, C. J. Kampf, R. G. Huber, K. R. Liedl, T. Loerting, T. Moschen, M. Schauperl, M. Tollinger, C. E. Morris, H. Wex, H. Grothe, U. Pöschl, T. Koop and J. Fröhlich-Nowoisky, Atmos. Chem. Phys., **15** (8), 4077-4091 (2015)
101. R. L. Green and G. J. Warren, Nature, **317** (6038), 645-648 (1985)
102. M. Lukas, R. Schwidetzky, R. J. Eufemio, M. Bonn and K. Meister, J. Phys. Chem. B, **126** (9), 1861-1867 (2022)
103. A. T. Kunert, M. L. Pöhlker, K. Tang, C. S. Krevert, C. Wieder, K. R. Speth, L. E. Hanson, C. E. Morris, D. G. Schmale Iii, U. Pöschl and J. Fröhlich-Nowoisky, Biogeosciences, **16** (23), 4647-4659 (2019)
104. P. Wolber and G. Warren, Trends Biochem. Sci., **14** (5), 179-182 (1989)
105. P. Bieber and N. Borduas-Dedekind, Sci. Adv., **10** (27), eadn6606 (2024)
106. K. Dreischmeier, C. Budke, L. Wiehemeier, T. Kottke and T. Koop, Sci. Rep., **7** (1), 41890 (2017)
107. N. L. H. Kinney, C. A. Hepburn, M. I. Gibson, D. Ballesteros and T. F. Whale, Biogeosciences, **21** (13), 3201-3214 (2024)
108. D. O'Sullivan, B. J. Murray, J. F. Ross and M. E. Webb, Atmos. Chem. Phys., **16** (12), 7879-7887 (2016)
109. T. C. J. Hill, P. J. DeMott, Y. Tobo, J. Fröhlich-Nowoisky, B. F. Moffett, G. D. Franc and S. M. Kreidenweis, Atmos. Chem. Phys., **16** (11), 7195-7211 (2016)
110. M. P. Adams, N. S. Atanasova, S. Sofieva, J. Ravantti, A. Heikkinen, Z. Brasseur, J. Duplissy, D. H. Bamford and B. J. Murray, Biogeosciences, **18** (14), 4431-4444 (2021)
111. M. Cascajo-Castresana, R. O. David, M. A. Iriarte-Alonso, A. M. Bittner and C. Marcolli, Atmos. Chem. Phys., **20** (6), 3291-3315 (2020)
112. J. M. Creamean, J. E. Ceniceros, L. Newman, A. D. Pace, T. C. J. Hill, P. J. DeMott and M. E. Rhodes, Biogeosciences, **18** (12), 3751-3762 (2021)
113. P. Westh, J. Kristiansen and A. Hvidt, Comp. Biochem. Physiol. A Physiol., **99** (3), 401-404 (1991)
114. R. A. F. Reaumur, *Mémoires pour servir à l'histoire des insectes*. (A Paris : De l'imprimerie royale, Paris, 1734).
115. W. Block, J. G. Baust, F. Franks, I. A. Johnston and J. Bale, Philos. Trans. R. Soc. Lond. B Biol. Sci., **326** (1237), 613-633 (1990)
116. L. Shen, S. Zhang and G. Chen, Environ. Sci. Pollut. Res., **28** (48), 68006-68024 (2021)
117. K. E. Zachariassen and H. T. Hammel, Nature, **262** (5566), 285-287 (1976)
118. H. Tsumuki, H. Konno, T. Maeda and Y. Okamoto, J. Insect Physiol., **38** (2), 119-125 (1992)
119. H. Tsumuki and H. Konno, Biosci. Biotechnol. Biochem., **58** (3), 578-579 (1994)
120. S. N. Bagwell and J. V. Ricker, Bios, **90** (3), 158-170 (2019)
121. A. Hudait, N. Odendahl, Y. Qiu, F. Paesani and V. Molinero, J. Am. Chem. Soc., **140** (14), 4905-4912 (2018)
122. M. Bar Dolev, I. Braslavsky and P. L. Davies, Annu. Rev. Biochem., **85**, 515-542 (2016)
123. A. L. DeVries and D. E. Wohlschlag, Science, **163** (3871), 1073-1075 (1969)
124. A. L. Devries, Science, **172** (3988), 1152-1155 (1971)
125. S. Huang, W. Hu, J. Chen, Z. Wu, D. Zhang and P. Fu, Environ. Int., **146**, 106197 (2021)
126. G. J. Warren, Biotechnol. Genet. Eng. Rev., **5** (1), 107-136 (1987)
127. L. R. Maki, E. L. Galyan, M.-M. Chang-Chien and D. R. Caldwell, Appl. Microbiol., **28** (3), 456-459 (1974)
128. Y. Hasegawa, Y. Ishihara and T. Tokuyama, Biosci. Biotechnol. Biochem., **58** (12), 2273-2274 (1994)
129. O. Berge, C. L. Monteil, C. Bartoli, C. Chandeysson, C. Guilbaud, D. C. Sands and C. E. Morris, PLOS ONE, **9** (9), e105547 (2014)
130. S. E. Lindow, Ann. Rev. Phytopathol., **21** (Volume 21, 1983), 363-384 (1983)
131. I. Coluzza, J. Creamean, M. J. Rossi, H. Wex, P. A. Alpert, V. Bianco, Y. Boose, C. Dellago, L. Felgitsch, J. Fröhlich-Nowoisky, H. Herrmann, S. Jungblut, Z. A. Kanji, G. Menzl, B. Moffett, C. Moritz, A. Mutzel, U. Pöschl, M. Schauperl, J. Scheel, E. Stopelli, F. Stratmann, H. Grothe and D. G. Schmale, Atmosphere, **8** (8), 138 (2017)

132. M. Tang, J. Chen and Z. Wu, Atmos. Environ., **192**, 206-208 (2018)
133. T. Šantl-Temkiv, B. Sikoparija, T. Maki, F. Carotenuto, P. Amato, M. Yao, C. E. Morris, R. Schnell, R. Jaenicke, C. Pöhlker, P. J. DeMott, T. C. J. Hill and J. A. Huffman, Aerosol Sci. Technol., **54** (5), 520-546 (2020)
134. M. I. Daily, M. D. Tarn, T. F. Whale and B. J. Murray, Atmos. Meas. Tech., **15** (8), 2635-2665 (2022)
135. V. R. Després, J. F. Nowoisky, M. Klose, R. Conrad, M. O. Andreae and U. Pöschl, Biogeosciences, **4** (6), 1127-1141 (2007)
136. J. Fröhlich-Nowoisky, T. C. J. Hill, B. G. Pummer, P. Yordanova, G. D. Franc and U. Pöschl, Biogeosciences, **12** (4), 1057-1071 (2015)
137. A. Sanchez-Marroquin, D. H. P. Hedges, M. Hiscock, S. T. Parker, P. D. Rosenberg, J. Trembath, R. Walshaw, I. T. Burke, J. B. McQuaid and B. J. Murray, Atmos. Meas. Tech., **12** (11), 5741-5763 (2019)
138. R. Krejci, J. Ström, M. de Reus and W. Sahle, Atmos. Chem. Phys., **5** (12), 3331-3344 (2005)
139. R. Schwidetzky, I. de Almeida Ribeiro, N. Bothen, A. T. Backes, A. L. DeVries, M. Bonn, J. Fröhlich-Nowoisky, V. Molinero and K. Meister, Proc. Natl. Acad. Sci. U. S. A., **120** (46), e2303243120 (2023)
140. K. C. Failor, D. G. Schmale, B. A. Vinatzer and C. L. Monteil, ISME J., **11** (12), 2740-2753 (2017)
141. K. C. Failor, H. Liu, M. E. M. Llontop, S. LeBlanc, N. Eckshtain-Levi, P. Sharma, A. Reed, S. Yang, L. Tian, C. T. Lefevre, N. Menguy, L. Du, C. L. Monteil and B. A. Vinatzer, ISME J., **16** (3), 890-897 (2022)
142. G. J. Warren, in *Biological ice nucleation and its applications*, edited by R. E. Lee, G. J. Warren and L. V. Gusta (APS Press, St. Paul, MN, 1995), pp. 85-99.
143. A. R. Edwards, R. A. Van den Bussche, H. A. Wichman and C. S. Orser, Mol. Biol. Evol., **11** (6), 911-920 (1994)
144. S. E. Lindow, E. Lahue, A. G. Govindarajan, N. J. Panopoulos and D. Gies, Mol. Plant. Microbe Interact., **2** (5), 262-272 (1989)
145. H. C. Jung, J. M. Lebeault and J. G. Pan, Nat. Biotechnol., **16** (6), 576-580 (1998)
146. D. Schmid, D. Pridmore, G. Capitani, R. Battistutta, J. R. Neeser and A. Jann, FEBS Lett., **414** (3), 590-594 (1997)
147. Q. Li, Q. Yan, J. Chen, Y. He, J. Wang, H. Zhang, Z. Yu and L. Li, Int. J. Biol. Sci., **8** (8), 1097-1108 (2012)
148. K. Abe, S. Watabe, Y. Emori, M. Watanabe and S. Arai, FEBS Lett., **258** (2), 297-300 (1989)
149. A. M. Miller, J. E. Figueiredo, G. A. Linde, N. B. Colauto and L. D. Paccola-Meirelles, Genet. Mol. Res., **15** (1), 15017863 (2016)
150. G. Warren, L. Corotto and P. Wolber, Nucleic Acids Res., **14** (20), 8047-8060 (1986)
151. Y. Michigami, S. Watabe, K. Abe, H. Obata and S. Arai, Biosci. Biotechnol. Biochem., **58** (4), 762-764 (1994)
152. J.-I. Zhao and C. S. Orser, Mol. Gen. Genet., **223** (1), 163-166 (1990)
153. Z. Wu, L. Qin and V. K. Walker, Microbiology, **155** (4), 1164-1169 (2009)
154. G. Warren and L. Corotto, Gene, **85** (1), 239-242 (1989)
155. N. Convery and N. Gadegaard, Micro. Nano. Eng., **2**, 76-91 (2019)
156. A. Manz, N. Graber and H. M. Widmer, Sens. Actuators B: Chem., **1** (1-6), 244-248 (1990)
157. D. R. Reyes, D. Iossifidis, P. A. Auroux and A. Manz, Anal. Chem., **74** (12), 2623-2636 (2002)
158. M. D. Tarn and N. Pamme, in *Elsevier Reference Module in Chemistry, Molecular Sciences and Chemical Engineering*, edited by J. Reedijk (Elsevier, Waltham, MA, 2014).
159. D. E. W. Patabadige, S. Jia, J. Sibbitts, J. Sadeghi, K. Sellens and C. T. Culbertson, Anal. Chem., **88** (1), 320-338 (2016)
160. S.-M. Yang, S. Lv, W. Zhang and Y. Cui, Sensors, **22** (4), 1620 (2022)
161. X. Wang, X.-Z. Hong, Y.-W. Li, Y. Li, J. Wang, P. Chen and B.-F. Liu, Mil. Med. Res., **9** (1), 11 (2022)
162. B. H. Lapizco-Encinas and Y. V. Zhang, Electrophoresis, **44** (1-2), 217-245 (2023)
163. V. Iyer, Z. Yang, J. Ko, R. Weissleder and D. Issadore, Lab Chip, **22** (17), 3110-3121 (2022)
164. J. C. Jokerst, J. M. Emory and C. S. Henry, Analyst, **137** (1), 24-34 (2012)
165. X. Zhu, K. Wang, H. Yan, C. Liu, X. Zhu and B. Chen, Environ. Sci. Technol., **56** (2), 711-731 (2022)
166. P. Aryal, C. Hefner, B. Martinez and C. S. Henry, Lab Chip, **24** (5), 1175-1206 (2024)
167. A. M. Nightingale, A. D. Beaton and M. C. Mowlem, Sens. Actuators B: Chem., **221**, 1398-1405 (2015)
168. C. D. M. Campos and J. A. F. da Silva, RSC Adv., **3** (40), 18216-18227 (2013)
169. J. Saez, R. Catalan-Carrio, R. M. Owens, L. Basabe-Desmonts and F. Benito-Lopez, Anal. Chim. Acta, **1186**, 338392 (2021)
170. P. Mesquita, L. Gong and Y. Lin, Front. Lab. Chip. Technol., **1**, 1074009 (2022)
171. R. Pol, F. Céspedes, D. Gabriel and M. Baeza, TrAC Trends Anal. Chem., **95**, 62-68 (2017)
172. V. M. C. Rérolle, C. F. A. Floquet, A. J. K. Harris, M. C. Mowlem, R. R. G. J. Bellerby and E. P. Achterberg, Anal. Chim. Acta, **786**, 124-131 (2013)
173. A. D. Beaton, C. L. Cardwell, R. S. Thomas, V. J. Sieben, F.-E. Legiret, E. M. Waugh, P. J. Statham, M. C. Mowlem and H. Morgan, Environ. Sci. Technol., **46** (17), 9548-9556 (2012)
174. C. Slater, J. Cleary, K.-T. Lau, D. Snakenborg, B. Corcoran, J. P. Kutter and D. Diamond, Water Sci. Technol., **61** (7), 1811-1818 (2010)
175. M. M. Grand, G. S. Clinton-Bailey, A. D. Beaton, A. M. Schaap, T. H. Johengen, M. N. Tamburri, D. P. Connelly, M. C. Mowlem and E. P. Achterberg, Front. Mar. Sci., **4**, 255 (2017)
176. S. Morgan, E. Luy, A. Furlong and V. Sieben, Anal. Methods, **14** (1), 22-33 (2022)
177. D. Zhang, H. Bi, B. Liu and L. Qiao, Anal. Chem., **90** (9), 5512-5520 (2018)
178. L. Wang, W. Qi, Y. Liu, D. Essien, Q. Zhang and J. Lin, Anal. Chem., **93** (26), 9013-9022 (2021)
179. I. Lee, E. Jeon and J. Lee, TrAC Trends in Analytical Chemistry, **158**, 116880 (2023)
180. M. Li, L. Wang, W. Qi, Y. Liu and J. Lin, Micromachines, **12** (7), 798 (2021)
181. J. A. Huffman, A. E. Perring, N. J. Savage, B. Clot, B. Crouzy, F. Tummon, O. Shoshanim, B. Damit, J. Schneider, V. Sivaprakasam, M. A. Zawadowicz, I. Crawford, M. Gallagher, D. Topping, D. C. Doughty, S. C. Hill and Y. Pan, Aerosol Sci. Tech., **54** (5), 465-495 (2020)
182. S. Ezrre, M. A. Reyna, C. Anguiano, R. L. Avitia and H. Márquez, Biosensors, **12** (4), 191 (2022)
183. A. Priye, S. Wong, Y. Bi, M. Carpio, J. Chang, M. Coen, D. Cope, J. Harris, J. Johnson, A. Keller, R. Lim, S. Lu, A. Millard, A. Pangelinan, N. Patel, L. Smith, K. Chan and V. M. Ugaz, Anal. Chem., **88** (9), 4651-4660 (2016)
184. Y. Jia, W. Wu, J. Zheng, Z. Ni and H. Sun, Biomicrofluidics, **13** (5), 054103 (2019)

185. O. Kemppinen, J. C. Laning, R. D. Mersmann, G. Videen and M. J. Berg, Sci. Rep., **10** (1), 16085 (2020)
186. E. Marinou, M. Tesche, A. Nenes, A. Ansmann, J. Schrod, D. Mamali, A. Tsekeri, M. Pikridas, H. Baars, R. Engelmann, K. A. Voudouri, S. Solomos, J. Sciare, S. Groß, F. Ewald and V. Amiridis, Atmos. Chem. Phys., **19** (17), 11315-11342 (2019)
187. A. J. Miller, F. Ramelli, C. Fuchs, N. Omanovic, R. Spirig, H. Zhang, U. Lohmann, Z. A. Kanji and J. Henneberger, Atmos. Meas. Tech., **17** (2), 601-625 (2024)
188. P. Bieber, T. M. Seifried, J. Burkart, J. Gratzl, A. Kasper-Giebl, D. G. Schmale and H. Grothe, Remote Sens., **12** (3), 552 (2020)
189. J. Schrod, D. Weber, J. Drücke, C. Keleshis, M. Pikridas, M. Ebert, B. Cvetković, S. Nickovic, E. Marinou, H. Baars, A. Ansmann, M. Vrekoussis, N. Mihalopoulos, J. Sciare, J. Curtius and H. G. Bingemer, Atmos. Chem. Phys., **17** (7), 4817-4835 (2017)
190. C. Jimenez-Sanchez, R. Hanlon, K. A. Aho, C. Powers, C. E. Morris and D. G. Schmale, Front. Microbiol., **9**, 1667 (2018)
191. G. C. E. Porter, S. N. F. Sikora, M. P. Adams, U. Proske, A. D. Harrison, M. D. Tarn, I. M. Brooks and B. J. Murray, Atmos. Meas. Tech., **13** (6), 2905-2921 (2020)
192. J. M. Creamean, K. M. Primm, M. A. Tolbert, E. G. Hall, J. Wendell, A. Jordan, P. J. Sheridan, J. Smith and R. C. Schnell, Atmos. Meas. Tech., **11** (7), 3969-3985 (2018)
193. M. Pan, J. A. Lednicky and C. Y. Wu, J. Appl. Microbiol., **127** (6), 1596-1611 (2019)
194. J. S. West and R. B. E. Kimber, Ann. Appl. Biol., **166** (1), 4-17 (2015)
195. A. R. Metcalf, S. Narayan and C. S. Dutcher, Aerosol Sci. Technol., **52** (3), 310-329 (2018)
196. S. Krokhine, H. Torabi, A. Doostmohammadi and P. Rezai, Colloids Surf. B Biointerfaces, **206**, 111962 (2021)
197. J. Hanlon, K. S. Galea and S. Verpaele, Int. J. Environ. Res. Public Health, **18** (13) (2021)
198. R. J. Sherwood and M. Lippmann, J. Occup. Environ. Hyg., **12** (4), 229-234 (1997)
199. E. K. Bigg, G. T. Miles and K. J. Heffernan, J. Atmos. Sci., **18** (6), 804-806 (1961)
200. E. K. Bigg, S. C. Mossop, R. T. Meade and N. S. C. Thorndike, J. Appl. Meteorol. Climatol., **2** (2), 266-269 (1963)
201. M. D. Tarn, S. N. F. Sikora, G. C. E. Porter, D. O'Sullivan, M. Adams, T. F. Whale, A. D. Harrison, J. Vergara-Temprado, T. W. Wilson, J.-u. Shim and B. J. Murray, Microfluid. Nanofluid., **22** (5), 52 (2018)
202. M. P. Adams, M. D. Tarn, A. Sanchez-Marroquin, G. C. E. Porter, D. O'Sullivan, A. D. Harrison, Z. Cui, J. Vergara-Temprado, F. Carotenuto, M. A. Holden, M. I. Daily, T. F. Whale, S. N. F. Sikora, I. T. Burke, J. U. Shim, J. B. McQuaid and B. J. Murray, J. Geophys. Res. Atmos., **125** (22), e2020JD032938 (2020)
203. M. D. Tarn, S. N. F. Sikora, G. C. E. Porter, B. V. Wyld, M. Alayof, N. Reicher, A. D. Harrison, Y. Rudich, J.-u. Shim and B. J. Murray, Lab Chip, **20** (16), 2889-2910 (2020)
204. T. Brubaker, M. Polen, P. Cheng, V. Ekambaram, J. Somers, S. L. Anna and R. C. Sullivan, Aerosol Sci. Tech., **54** (1), 79-93 (2020)
205. L. G. Jahl, T. A. Brubaker, M. J. Polen, L. G. Jahn, K. P. Cain, B. B. Bowers, W. D. Fahy, S. Graves and R. C. Sullivan, Sci. Adv., **7** (9), eabd3440 (2021)
206. P. Roy, M. L. House and C. S. Dutcher, Micromachines, **12** (3), 296 (2021)
207. C. A. Stan, G. F. Schneider, S. S. Shevkoplyas, M. Hashimoto, M. Ibanescu, B. J. Wiley and G. M. Whitesides, Lab Chip, **9** (16), 2293-2305 (2009)
208. A. Desai, L. Sang-Wook and T. Yu-Chong, presented at the Proceedings IEEE Thirteenth Annual International Conference on Micro Electro Mechanical Systems (Cat. No.00CH36308), 733-738, 2000, 10.1109/MEMSYS.2000.838609.
209. A. Desai, S. W. Lee and Y. C. Tai, presented at the Proceedings MEMS 98. IEEE. Eleventh Annual International Workshop on Micro Electro Mechanical Systems. An Investigation of Micro Structures, Sensors, Actuators, Machines and Systems (Cat. No.98CH36176, 121-126, 1998, 10.1109/MEMSYS.1998.659740.
210. Y. Zhao and S. K. Cho, presented at the The 13th International Conference on Solid-State Sensors, Actuators and Microsystems, 2005. Digest of Technical Papers. TRANSDUCERS '05., 129-134 Vol. 121, 2005, 10.1109/SENSOR.2005.1496376.
211. Y. Zhao, S. K. Chung, U.-C. Yi and S. K. Cho, J. Micromech. Microeng., **18** (2), 025030 (2008)
212. Y. Zhao and S. K. Cho, Lab Chip, **6** (1), 137-144 (2006)
213. W. C. Nelson and C.-J. C. Kim, J. Adhes. Sci. Technol., **26** (12-17), 1747-1771 (2012)
214. J. Li and C.-J. C. Kim, Lab Chip, **20** (10), 1705-1712 (2020)
215. M. Jönsson-Niedziółka, F. Lapierre, Y. Coffinier, S. J. Parry, F. Zoueshtiagh, T. Foat, V. Thomy and R. Boukherroub, Lab Chip, **11** (3), 490-496 (2011)
216. Q. Liu, X. Zhang, Y. Yao, W. Jing, S. Liu and G. Sui, Sens. Actuators B: Chem., **258**, 1138-1145 (2018)
217. A. Hazra, M. Saha, U. K. De, J. Mukherjee and K. Goswami, J. Aerosol Sci., **35** (11), 1405-1414 (2004)
218. G. J. Newton, O. G. Raabe and B. V. Mokler, J. Aerosol Sci., **8** (5), 339-347 (1977)
219. K. R. May, J. Sci. Instrum., **22** (10), 187-195 (1945)
220. N. Reicher, L. Segev and Y. Rudich, Atmos. Meas. Tech., **11** (1), 233-248 (2018)
221. N. Reicher, C. Budke, L. Eickhoff, S. Raveh-Rubin, I. Kaplan-Ashiri, T. Koop and Y. Rudich, Atmos. Chem. Phys., **19**, 11143–11158 (2019)
222. G. C. E. Porter, M. P. Adams, I. M. Brooks, L. Ickes, L. Karlsson, C. Leck, M. E. Salter, J. Schmale, K. Siegel, S. N. F. Sikora, M. D. Tarn, J. Vüllers, H. Wernli, P. Zieger, J. Zinke and B. J. Murray, J. Geophys. Res. Atmos., **127** (6), e2021JD036059 (2022)
223. N. A. Berezinski, G. V. Stepanov and V. G. Khorguani, presented at the Atmospheric Aerosols and Nucleation, Berlin, Heidelberg, 709-712, 1988.
224. A. Welti, F. Lüönd, O. Stetzer and U. Lohmann, Atmos. Chem. Phys., **9** (18), 6705-6715 (2009)
225. P. A. Alpert, W. P. Kilthau, R. E. O'Brien, R. C. Moffet, M. K. Gilles, B. Wang, A. Laskin, J. Y. Aller and D. A. Knopf, Sci. Adv., **8** (44), eabq6842 (2022)
226. R. H. Mason, C. Chou, C. S. McCluskey, E. J. T. Levin, C. L. Schiller, T. C. J. Hill, J. A. Huffman, P. J. DeMott and A. K. Bertram, Atmos. Meas. Tech., **8** (6), 2449-2462 (2015)

227. R. H. Mason, M. Si, C. Chou, V. E. Irish, R. Dickie, P. Elizondo, R. Wong, M. Brintnell, M. Elsasser, W. M. Lassar, K. M. Pierce, W. R. Leaitch, A. M. MacDonald, A. Platt, D. Toom-Sauntry, R. Sarda-Estève, C. L. Schiller, K. J. Suski, T. C. J. Hill, J. P. D. Abbatt, J. A. Huffman, P. J. DeMott and A. K. Bertram, Atmos. Chem. Phys., **16** (3), 1637-1651 (2016)
228. J. Chen, Z. Wu, J. Chen, N. Reicher, X. Fang, Y. Rudich and M. Hu, Atmos. Chem. Phys., **21** (5), 3491-3506 (2021)
229. S. L. Barr, B. Wyld, J. B. McQuaid, R. R. Neely III and B. J. Murray, Sci. Adv., **9** (33), eadg3708 (2023)
230. T. A. Cahill, P. J. Feeney and R. A. Eldred, Nucl. Instrum. Methods Phys. Res., B, **22** (1), 344-348 (1987)
231. V. A. Marple, K. L. Rubow and S. M. Behm, Aerosol Sci. Technol., **14** (4), 434-446 (1991)
232. M. K. Tan, J. R. Friend and L. Y. Yeo, Lab Chip, **7** (5), 618-625 (2007)
233. Y.-H. Kim, J.-Y. Maeng, D. Park, I.-H. Jung, J. Hwang and Y.-J. Kim, Appl. Phys. Lett., **91** (4), 043512 (2007)
234. B. Damit, Aerosol Sci. Tech., **51** (4), 488-500 (2017)
235. J. Choi, S. C. Hong, W. Kim and J. H. Jung, ACS Sens., **2** (4), 513-521 (2017)
236. I. Mirzaee, M. Song, M. Charmchi and H. Sun, Lab Chip, **16** (12), 2254-2264 (2016)
237. S. D. Noblitt, G. S. Lewis, Y. Liu, S. V. Hering, J. L. Collett and C. S. Henry, Anal. Chem., **81** (24), 10029-10037 (2009)
238. H.-B. Kwon, S.-J. Yoo, U.-S. Hong, K. Kim, J. Han, M.-K. Kim, D.-H. Kang, J. Hwang and Y.-J. Kim, Lab Chip, **19** (8), 1471-1483 (2019)
239. T. G. Foat, W. J. Sellors, M. D. Walker, P. A. Rachwal, J. W. Jones, D. D. Despeyroux, L. Coudron, I. Munro, D. K. McCluskey, C. K. L. Tan and M. C. Tracey, J. Aerosol Sci., **95**, 43-53 (2016)
240. Z. Ma, Y. Zheng, Y. Cheng, S. Xie, X. Ye and M. Yao, J. Aerosol Sci., **95** (Supplement C), 84-94 (2016)
241. J.-W. Park, H. R. Kim and J. Hwang, Anal. Chim. Acta, **941**, 101-107 (2016)
242. W. Jing, W. Zhao, S. Liu, L. Li, C.-T. Tsai, X. Fan, W. Wu, J. Li, X. Yang and G. Sui, Anal. Chem., **85** (10), 5255-5262 (2013)
243. M. Maldonado-Garcia, V. Kumar, S. Pourkamali and J. C. Wilson, presented at the 2015 IEEE SENSORS, 1-4, 2015, 10.1109/ICSENS.2015.7370667.
244. J. S. Kang, K. S. Lee, K. H. Lee, H. J. Sung and S. S. Kim, Aerosol Sci. Technol., **46** (9), 966-972 (2012)
245. H.-B. Kwon, H.-L. Kim, U.-S. Hong, S.-J. Yoo, K. Kim, J. Han, M.-K. Kim, J. Hwang and Y.-J. Kim, Lab Chip, **18** (17), 2642-2652 (2018)
246. V. A. Marple, Aerosol Sci. Technol., **38** (3), 247-292 (2004)
247. E. Limpert, F. Godet and K. Müller, Agric. For. Meteorol., **97** (4), 293-308 (1999)
248. M. Jwa-Young, D. Park, K. Yong-Ho, H. Jungho and K. Yong-Jun, presented at the 2007 IEEE 20th International Conference on Micro Electro Mechanical Systems (MEMS), 619-622, 2007, 10.1109/MEMSYS.2007.4433121.
249. D. Park, Y.-H. Kim, C. Woo Park, J. Hwang and Y.-J. Kim, J. Aerosol Sci., **40** (5), 415-422 (2009)
250. Y.-H. Kim, D. Park, J. Hwang and Y.-J. Kim, Lab Chip, **9** (18), 2722-2728 (2009)
251. M.-g. Kim, Y.-H. Kim, H.-L. Kim, C. W. Park, Y.-H. Joe, J. Hwang and Y.-J. Kim, J. Micromech. Microeng., **20** (3), 035034 (2010)
252. Y.-H. Kim, D. Park, J. Hwang and Y.-J. Kim, Lab Chip, **8** (11), 1950-1956 (2008)
253. J. Zhao, M. Liu, L. Liang, W. Wang and J. Xie, Sens. Actuators A: Phys., **238**, 379-388 (2016)
254. Y. Wang, Y. Wang, D. Chen, X. Liu, C. Wu and J. Xie, IEEE Sens. J., **18** (15), 6130-6137 (2018)
255. Y. Wang, X. Mei, Z. Xu and J. Qian, ACS Omega, **9** (5), 5751-5760 (2024)
256. Y. Wang, Y. Wang, W. Liu, D. Chen, C. Wu and J. Xie, Sens. Actuators A: Phys., **288**, 67-74 (2019)
257. Y. H. Kim, D. Park, J. Hwang and Y. J. Kim, presented at the 2008 IEEE 21st International Conference on Micro Electro Mechanical Systems, 547-550, 2008, 10.1109/MEMSYS.2008.4443714.
258. Y. Li, Y. Xu, J. Jiang, X. Zhu, R. Guo and J. Sun, Micromachines, **13** (2), 252 (2022)
259. R. Wang, H. Zhao, X. Wang and J. Li, Micromachines, **14** (1), 183 (2023)
260. T. Chen, J. Sun, T. Ma, T. Li, C. Liu, X. Zhu and N. Xue, Micromachines, **10** (8), 497 (2019)
261. R. Wang, H. Zhao, J. Li and X. Wang, in *Micromachines* (2022), Vol. 13.
262. P. Wang, S. Yuan, N. Yang and A. Wang, Aerosol Air Qual. Res., **21** (4), 200269 (2021)
263. P. Wang, S. Yuan, P. K. Oppong and N. Yang, J. Aerosol Sci., **164**, 105999 (2022)
264. J. Sun, K. Yang, Z. Liu and Y. Lu, presented at the 2015 12th IEEE International Conference on Electronic Measurement & Instruments (ICEMI), 1183-1187, 2015, 10.1109/ICEMI.2015.7494466.
265. J. Liu, W. Hao, M. Liu, Y. Liang and S. He, in *Appl. Sci.* (2018), Vol. 8, pp. 82.
266. M. A. Rahman and M. Z. Saghir, Int. J. Heat Mass Transf., **73**, 693-705 (2014)
267. T. Šantl-Temkiv, P. Amato, U. Gosewinkel, R. Thyrhaug, A. Charton, B. Chicot, K. Finster, G. Bratbak and J. Löndahl, Environ. Sci. Technol., **51** (19), 11224-11234 (2017)
268. A. J. Miller, K. P. Brennan, C. Mignani, J. Wieder, R. O. David and N. Borduas-Dedekind, Atmos. Meas. Tech., **14** (4), 3131-3151 (2021)
269. N. Els, C. Larose, K. Baumann-Stanzer, R. Tignat-Perrier, C. Keuschnig, T. M. Vogel and B. Sattler, Aerobiologia, **35** (4), 671-701 (2019)
270. E. Carvalho, C. Sindt, A. Verdier, C. Galan, L. O'Donoghue, S. Parks and M. Thibaudon, Aerobiologia, **24** (4), 191-201 (2008)
271. C. H. Lee, H. Seok, W. Jang, J. T. Kim, G. Park, H.-U. Kim, J. Rho, T. Kim and T. D. Chung, Biosens. Bioelectron., **192**, 113499 (2021)
272. I. V. Novosselov and P. C. Ariessohn, Aerosol Sci. Technol., **48** (2), 163-172 (2014)
273. J. Zhang, S. Yan, D. Yuan, G. Alici, N.-T. Nguyen, M. Ebrahimi Warkiani and W. Li, Lab Chip, **16** (1), 10-34 (2016)
274. D. Di Carlo, Lab Chip, **9** (21), 3038-3046 (2009)
275. G. SegrÉ and A. Silberberg, Nature, **189** (4760), 209-210 (1961)
276. S. C. Hur, S.-E. Choi, S. Kwon and D. D. Carlo, Appl. Phys. Lett., **99** (4) (2011)
277. I. D. Johnston, M. B. McDonnell, C. K. L. Tan, D. K. McCluskey, M. J. Davies and M. C. Tracey, Microfluid. Nanofluid., **17** (3), 509-518 (2014)
278. J. Choi, J. Lee and J. H. Jung, Biosens. Bioelectron., **169**, 112611 (2020)
279. M. E. Lacey and J. S. West, *The Air Spora*. (Springer, Dordrecht, The Netherlands, 2006).

280. S. N. Vicentini, N. J. Hawkins, K. M. King, S. I. Moreira, A. A. de Paiva Custódio, R. P. Leite Júnior, D. Portalanza, F. R. Garcés-Fiallos, L. D. Krug, J. S. West, B. A. Fraaije, W. C. De Jesus Júnior and P. C. Ceresini, Agronomy, **13** (5), 1238 (2023)
281. H. Klein, W. Haunold, U. Bundke, B. Nillius, T. Wetter, S. Schallenberg and H. Bingemer, Atmos. Res., **96** (2), 218-224 (2010)
282. N. Sandstrom, T. Frisk, G. Stemme and W. v. d. Wijngaart, presented at the 2008 IEEE 21st International Conference on Micro Electro Mechanical Systems, 595-598, 2008, 10.1109/MEMSYS.2008.4443726.
283. G. Pardon, L. Ladhani, N. Sandström, M. Ettori, G. Lobov and W. van der Wijngaart, Sens. Actuators B: Chem., **212**, 344-352 (2015)
284. F. Shen, M. Tan, Z. Wang, M. Yao, Z. Xu, Y. Wu, J. Wang, X. Guo and T. Zhu, Environ. Sci. Technol., **45** (17), 7473-7480 (2011)
285. H. R. Kim, S. An and J. Hwang, ACS Sens., **5** (9), 2763-2771 (2020)
286. A. D. Stroock, S. K. W. Dertinger, A. Ajdari, I. Mezić, H. A. Stone and G. M. Whitesides, Science, **295** (5555), 647-651 (2002)
287. W. Jing, X. Jiang, W. Zhao, S. Liu, X. Cheng and G. Sui, Anal. Chem., **86** (12), 5815-5821 (2014)
288. Q. Liu, X. Zhang, X. Li, S. Liu and G. Sui, J. Aerosol Sci., **115**, 173-180 (2018)
289. Q. Liu, Y. Zhang, W. Jing, S. Liu, D. Zhang and G. Sui, Analyst, **141** (5), 1637-1640 (2016)
290. X. Bian, Y. Lan, B. Wang, Y. S. Zhang, B. Liu, P. Yang, W. Zhang and L. Qiao, Anal. Chem., **88** (23), 11504-11512 (2016)
291. N. Pamme, Lab Chip, **7**, 1644-1659 (2007)
292. A. Lenshof and T. Laurell, Chem. Soc. Rev., **39** (3), 1203-1217 (2010)
293. Y. Song, D. Li and X. Xuan, Electrophoresis, **44** (11-12), 910-937 (2023)
294. S.-w. Choe, B. Kim and M. Kim, Biosensors, **11** (11), 464 (2021)
295. H.-D. Xi, H. Zheng, W. Guo, A. M. Gañán-Calvo, Y. Ai, C.-W. Tsao, J. Zhou, W. Li, Y. Huang, N.-T. Nguyen and S. H. Tan, Lab Chip, **17** (5), 751-771 (2017)
296. M. Bayareh, Chem. Eng. Process.: Process Intensif., **153**, 107984 (2020)
297. A. Farahinia, W. Zhang and I. Badea, Sensors, **23** (11), 5300 (2023)
298. X. Xu, X. Huang, J. Sun, R. Wang, J. Yao, W. Han, M. Wei, J. Chen, J. Guo, L. Sun and M. Yin, Analyst, **146** (23), 7070-7086 (2021)
299. J. McGrath, M. Jimenez and H. Bridle, Lab Chip, **14** (21), 4139-4158 (2014)
300. M. Hejazian, W. Li and N.-T. Nguyen, Lab Chip, **15** (4), 959-970 (2015)
301. M. Wu, A. Ozcelik, J. Rufo, Z. Wang, R. Fang and T. Jun Huang, Microsyst. Nanoeng., **5** (1), 32 (2019)
302. A. Jonas and P. Zemanek, Electrophoresis, **29** (24), 4813-4851 (2008)
303. Y. Li, Y. Wang, K. Wan, M. Wu, L. Guo, X. Liu and G. Wei, Nanoscale, **13** (8), 4330-4358 (2021)
304. D. P. Poenar, Micromachines, **10** (7), 483 (2019)
305. A. M. Schaap, W. C. Chu and B. Stoeber, IEEE Sens. J., **11** (11), 2790-2797 (2011)
306. A. Schaap, W. C. Chu and B. Stoeber, Phys. Fluids, **24** (8) (2012)
307. S. C. Hong, J. S. Kang, J. E. Lee, S. S. Kim and J. H. Jung, Lab Chip, **15** (8), 1889-1897 (2015)
308. S. Qian, M. Jiang and Z. Liu, Particuology, **55**, 23-34 (2021)
309. I. S. Akhatov, J. M. Hoey, O. F. Swenson and D. L. Schulz, Microfluid. Nanofluid., **5** (2), 215-224 (2008)
310. I. S. Akhatov, J. M. Hoey, O. F. Swenson and D. L. Schulz, J. Aerosol Sci., **39** (8), 691-709 (2008)
311. F. Tavakoli, S. K. Mitra and J. S. Olfert, J. Aerosol Sci., **42** (5), 321-328 (2011)
312. L. R. Huang, E. C. Cox, R. H. Austin and J. C. Sturm, Science, **304** (5673), 987-990 (2004)
313. A. Hochstetter, R. Vernekar, R. H. Austin, H. Becker, J. P. Beech, D. A. Fedosov, G. Gompper, S.-C. Kim, J. T. Smith, G. Stolovitzky, J. O. Tegenfeldt, B. H. Wunsch, K. K. Zeming, T. Krüger and D. W. Inglis, ACS Nano, **14** (9), 10784-10795 (2020)
314. H. Yin, H. Wan and A. J. Mason, presented at the Proceedings of the 2017 IEEE International Symposium on Circuits and Systems (ISCAS), Baltimore, MD, USA, 28–31 May 2017.
315. S.-m. Kwon, Y.-H. Kim, I.-H. Jung, D. Park, J. Hwang and Y.-J. Kim, Curr. Appl. Phys., **9** (4, Supplement), e308-e310 (2009)
316. R. T. Turgeon and M. T. Bowser, Anal. Bioanal. Chem., **394** (1), 187-198 (2009)
317. P. J. DeMott, O. Möhler, D. J. Cziczo, N. Hiranuma, M. D. Petters, S. S. Petters, F. Belosi, H. G. Bingemer, S. D. Brooks, C. Budke, M. Burkert-Kohn, K. N. Collier, A. Danielczok, O. Eppers, L. Felgitsch, S. Garimella, H. Grothe, P. Herenz, T. C. J. Hill, K. Höhler, Z. A. Kanji, A. Kiselev, T. Koop, T. B. Kristensen, K. Krüger, G. Kulkarni, E. J. T. Levin, B. J. Murray, A. Nicosia, D. O'Sullivan, A. Peckhaus, M. J. Polen, H. C. Price, N. Reicher, D. A. Rothenberg, Y. Rudich, G. Santachiara, T. Schiebel, J. Schrod, T. M. Seifried, F. Stratmann, R. C. Sullivan, K. J. Suski, M. Szakáll, H. P. Taylor, R. Ullrich, J. Vergara-Temprado, R. Wagner, T. F. Whale, D. Weber, A. Welti, T. W. Wilson, M. J. Wolf and J. Zenker, Atmos. Meas. Tech., **11** (11), 6231-6257 (2018)
318. P. J. DeMott, T. C. J. Hill, M. D. Petters, A. K. Bertram, Y. Tobo, R. H. Mason, K. J. Suski, C. S. McCluskey, E. J. T. Levin, G. P. Schill, Y. Boose, A. M. Rauker, A. J. Miller, J. Zaragoza, K. Rocci, N. E. Rothfuss, H. P. Taylor, J. D. Hader, C. Chou, J. A. Huffman, U. Pöschl, A. J. Prenni and S. M. Kreidenweis, Atmos. Chem. Phys., **17** (18), 11227-11245 (2017)
319. N. Hiranuma, S. Augustin-Bauditz, H. Bingemer, C. Budke, J. Curtius, A. Danielczok, K. Diehl, K. Dreischmeier, M. Ebert, F. Frank, N. Hoffmann, K. Kandler, A. Kiselev, T. Koop, T. Leisner, O. Möhler, B. Nillius, A. Peckhaus, D. Rose, S. Weinbruch, H. Wex, Y. Boose, P. J. DeMott, J. D. Hader, T. C. J. Hill, Z. A. Kanji, G. Kulkarni, E. J. T. Levin, C. S. McCluskey, M. Murakami, B. J. Murray, D. Niedermeier, M. D. Petters, D. O'Sullivan, A. Saito, G. P. Schill, T. Tajiri, M. A. Tolbert, A. Welti, T. F. Whale, T. P. Wright and K. Yamashita, Atmos. Chem. Phys., **15** (5), 2489-2518 (2015)
320. G. Vali, J. Atmos. Sci., **28** (3), 402-409 (1971)
321. T. Häusler, L. Witek, L. Felgitsch, R. Hitzenberger and H. Grothe, Atmosphere, **9** (4), 140 (2018)
322. M. D. Tarn, S. N. F. Sikora, G. C. E. Porter, J.-u. Shim and B. J. Murray, Micromachines, **12** (2), 223 (2021)
323. N. Hiranuma, K. Adachi, D. M. Bell, F. Belosi, H. Beydoun, B. Bhaduri, H. Bingemer, C. Budke, H. C. Clemen, F. Conen, K. M. Cory, J. Curtius, P. J. DeMott, O. Eppers, S. Grawe, S. Hartmann, N. Hoffmann, K. Höhler, E. Jantsch, A. Kiselev, T. Koop, G. Kulkarni, A. Mayer, M. Murakami, B. J. Murray, A. Nicosia, M. D. Petters, M. Piazza, M. Polen, N. Reicher, Y. Rudich, A. Saito, G. Santachiara, T. Schiebel, G. P. Schill, J. Schneider, L. Segev, E. Stopelli, R. C. Sullivan, K. Suski, M. Szakáll, T. Tajiri, H. Taylor, Y. Tobo, R. Ullrich, D. Weber, H. Wex, T. F. Whale, C. L. Whiteside, K. Yamashita, A. Zelenyuk and O. Möhler, Atmos. Chem. Phys., **19** (7), 4823-4849 (2019)

324. L. Ickes, A. Welti, C. Hoose and U. Lohmann, Phys. Chem. Chem. Phys., **17** (8), 5514-5537 (2015)
325. T. Koop and B. J. Murray, J. Chem. Phys., **145** (21), 211915 (2016)
326. T. F. Whale, B. J. Murray, D. O'Sullivan, T. W. Wilson, N. S. Umo, K. J. Baustian, J. D. Atkinson, D. A. Workneh and G. J. Morris, Atmos. Meas. Tech., **8** (6), 2437-2447 (2015)
327. J. D. Hader, T. P. Wright and M. D. Petters, Atmos. Chem. Phys., **14** (11), 5433-5449 (2014)
328. M. Polen, T. Brubaker, J. Somers and R. C. Sullivan, Atmos. Meas. Tech., **11** (9), 5315-5334 (2018)
329. K. R. Barry, T. C. J. Hill, C. Jentzsch, B. F. Moffett, F. Stratmann and P. J. DeMott, Atmos. Res., **250**, 105419 (2021)
330. D. A. Knopf and M. D. Lopez, Phys. Chem. Chem. Phys., **11** (36), 8056-8068 (2009)
331. T. Koop, H. P. Ng, L. T. Molina and M. J. Molina, J. Phys. Chem. A, **102** (45), 8924-8931 (1998)
332. B. J. Murray, S. L. Broadley, T. W. Wilson, J. D. Atkinson and R. H. Wills, Atmos. Chem. Phys., **11** (9), 4191-4207 (2011)
333. T. P. Wright, M. D. Petters, J. D. Hader, T. Morton and A. L. Holder, J. Geophys. Res. Atmos., **118** (18), 10,535-510,543 (2013)
334. L. Nan, H. Zhang, D. A. Weitz and H. C. Shum, Lab Chip, **24** (5), 1135-1153 (2024)
335. L. Shang, Y. Cheng and Y. Zhao, Chem Rev, **117** (12), 7964-8040 (2017)
336. Y. Ding, P. D. Howes and A. J. deMello, Anal. Chem., **92** (1), 132-149 (2020)
337. T. Thorsen, R. W. Roberts, F. H. Arnold and S. R. Quake, Phys. Rev. Lett., **86** (18), 4163-4166 (2001)
338. S. L. Anna, N. Bontoux and H. A. Stone, Appl. Phys. Lett., **82** (3), 364-366 (2003)
339. J. U. Shim, R. T. Ranasinghe, C. A. Smith, S. M. Ibrahim, F. Hollfelder, W. T. S. Huck, D. Klenerman and C. Abell, ACS Nano, **7** (7), 5955-5964 (2013)
340. Y. Doucet and E. Brun, in *Technical Translation, National Research Council of Canada. Division of Mechanical Engineering; 81* (National Research Council of Canada, Division of Mechanical Engineering, 1948).
341. D. G. Fahrenheit, Philos. Trans. R. Soc., **33** (381-391), 78-84 (1724)
342. A. Mousson, Bibl. Univ. de Genève, **3**, 296 (1858)
343. A. Mousson, *Sur la Fusion et la Solidification de L'eau*. (Ramboz et Schuchardt, Genève, Zentralbibliothek Zürich, NP 2930.14, 1858).
344. G. Van der Mensbrugge, Philos. Mag. Ser. 5, **4** (22), 40-48 (1877)
345. H. C. Sorby, Philos. Mag. Ser. 4, **18** (118), 105-108 (1859)
346. M. L. Dufour, Philos. Mag. Ser. 4, **21** (143), 543-544 (1861)
347. L. Dufour, Annalen der Physik, **190** (12), 530-554 (1862)
348. M. L. Dufour, Bibl. Univ., **10**, 346 (1861)
349. A. E. Sgro, P. B. Allen and D. T. Chiu, Anal. Chem., **79** (13), 4845-4851 (2007)
350. G. Vali, Atmos. Meas. Tech., **12** (2), 1219-1231 (2019)
351. W. D. Fahy, C. R. Shalizi and R. C. Sullivan, Atmos. Meas. Tech., **15** (22), 6819-6836 (2022)
352. P. Roy, S. Liu and C. S. Dutcher, Annu. Rev. Phys. Chem., **72**, 73-97 (2021)
353. A. Hauptmann, K. F. Handle, P. Baloh, H. Grothe and T. Loerting, J. Chem. Phys., **145** (21), 211923 (2016)
354. A. A. Dos-Reis-Delgado, A. Carmona-Dominguez, G. Sosa-Avalos, I. H. Jimenez-Saaib, K. E. Villegas-Cantu, R. C. Gallo-Villanueva and V. H. Perez-Gonzalez, Electrophoresis, **44** (1-2), 268-297 (2023)
355. V. Miralles, A. Huerre, F. Malloggi and M.-C. Jullien, Diagnostics, **3** (1), 33 (2013)
356. M. B. Kulkarni and S. Goel, Sens. Actuators A: Phys., **341**, 113590 (2022)
357. F. Yang, N. Yang, X. Huo and S. Xu, Biomicrofluidics, **12** (4) (2018)
358. J. Puigmartí-Luis, Chem. Soc. Rev., **43** (7), 2253-2271 (2014)
359. H.-h. Shi, Y. Xiao, S. Ferguson, X. Huang, N. Wang and H.-x. Hao, Lab Chip, **17** (13), 2167-2185 (2017)
360. R. Chauhan, N. Minocha, P. Coliaie, P. G. Singh, A. Korde, M. S. Kelkar, M. Langston, C. Liu, N. Nazemifard, D. Patience, D. Skliar, N. K. Nere and M. R. Singh, Chem. Eng. Res. Des., **197**, 908-930 (2023)
361. C. Devos, T. Van Gerven and S. Kuhn, Cryst. Growth Des., **21** (4), 2541-2565 (2021)
362. J. Jang, W.-S. Kim, T. S. Seo and B. J. Park, Chem. Eng. J. , **495**, 153657 (2024)
363. S. Sui and S. L. Perry, Struct. Dyn., **4** (3), 032202 (2017)
364. J. U. Shim, G. Cristobal, D. R. Link, T. Thorsen and S. Fraden, Cryst. Growth Des., **7** (11), 2192-2194 (2007)
365. E. C. dos Santos, G. M. Maggioni and M. Mazzotti, Cryst. Growth Des., **19** (11), 6159-6174 (2019)
366. Y.-Y. Kim, C. L. Freeman, X. Gong, M. A. Levenstein, Y. Wang, A. Kulak, C. Anduix-Canto, P. A. Lee, S. Li, L. Chen, H. K. Christenson and F. C. Meldrum, Angew. Chem. Int. Ed., **56** (39), 11885-11890 (2017)
367. B. Riechers, F. Wittbracht, A. Huetten and T. Koop, Phys. Chem. Chem. Phys., **15** (16), 5873-5887 (2013)
368. S. Lignel, A. Drelich, D. Sunagatullina, D. Clausse, E. Leclerc and I. Pezron, Can. J. Chem. Eng., **92** (2), 337-343 (2014)
369. L. Weng, S. N. Tessier, K. Smith, J. F. Edd, S. L. Stott and M. Toner, Langmuir, **32** (36), 9229-9236 (2016)
370. J. D. Atkinson, B. J. Murray and D. O'Sullivan, J. Phys. Chem. A, **120** (33), 6513-6520 (2016)
371. B. J. Murray, S. L. Broadley, T. W. Wilson, S. J. Bull, R. H. Wills, H. K. Christenson and E. J. Murray, Phys. Chem. Chem. Phys., **12** (35), 10380-10387 (2010)
372. G. C. E. Porter, M. D. Tarn, S. N. F. Sikora, M. E. Salter, T. W. Wilson, T. F. Whale, J.-u. Shim and B. J. Murray, presented at the The 21st International Conference on Miniaturized Systems for Chemistry and Life Sciences (MicroTAS 2017), Savannah, GA, USA, 1429-1430, 2017.
373. J. F. Edd, K. J. Humphry, D. Irimia, D. A. Weitz and M. Toner, Lab Chip, **9** (13), 1859-1865 (2009)
374. C. H. J. Schmitz, A. C. Rowat, S. Koster and D. A. Weitz, Lab Chip, **9** (1), 44-49 (2009)
375. J. Forbes, A. Bissoyi, L. Eickhoff, N. Reicher, T. Hansen, C. G. Bon, V. K. Walker, T. Koop, Y. Rudich, I. Braslavsky and P. L. Davies, Nat. Commun., **13** (1), 5019 (2022)
376. T. Hansen, J. C. Lee, N. Reicher, G. Ovadia, S. Guo, W. Guo, J. Liu, I. Braslavsky, Y. Rudich and P. L. Davies, eLife, **12**, RP91976 (2023)

377. S. Hartmann, M. Ling, L. S. A. Dreyer, A. Zipori, K. Finster, S. Grawe, L. Z. Jensen, S. Borck, N. Reicher, T. Drace, D. Niedermeier, N. C. Jones, S. V. Hoffmann, H. Wex, Y. Rudich, T. Boesen and T. Šantl-Temkiv, Front. Microbiol., **13**, 872306 (2022)
378. A. Bissoyi, N. Reicher, M. Chasnitsky, S. Arad, T. Koop, Y. Rudich and I. Braslavsky, Biomolecules, **9** (10), 532 (2019)
379. J. C. Lee, T. Hansen and P. L. Davies, Cryobiology, **113**, 104584 (2023)
380. L. Eickhoff, M. Keßler, C. Stubbs, J. Derksen, M. Viefhues, D. Anselmetti, M. I. Gibson, B. Hoge and T. Koop, J. Chem. Phys., **158** (15), 154504 (2023)
381. A. E. Sgro and D. T. Chiu, Lab Chip, **10** (14), 1873-1877 (2010)
382. L. Weng, A. Swei and M. Toner, Cryobiology, **84**, 91-94 (2018)
383. M. D. Tarn, K. H. Bastin, S. N. F. Sikora, F. C. Meldrum, H. K. Christensen, B. J. Murray and M. A. Holden, presented at the The 25th International Conference on Miniaturized Systems for Chemistry and Life Sciences (MicroTAS 2021), Palm Springs, CA, USA & Online, 1049-1050, 2021.
384. A. Peckhaus, A. Kiselev, T. Hiron, M. Ebert and T. Leisner, Atmos. Chem. Phys., **16** (18), 11477-11496 (2016)
385. D. Atig, A. Touil, M. Ildefonso, L. Marlin, P. Bouriat and D. Broseta, Chem. Eng. Sci., **192**, 1189-1197 (2018)
386. F. N. Isenrich, N. Shardt, M. Rösch, J. Nette, S. Stavrakis, C. Marcolli, Z. A. Kanji, A. J. deMello and U. Lohmann, Atmos. Meas. Tech., **15** (18), 5367-5381 (2022)
387. H. Boukellal, Š. Selimović, Y. Jia, G. Cristobal and S. Fraden, Lab Chip, **9** (2), 331-338 (2009)
388. P. Roy, L. E. Mael, T. C. J. Hill, L. Mehndiratta, G. Peiker, M. L. House, P. J. DeMott, V. H. Grassian and C. S. Dutcher, ACS Earth Space Chem., **5** (8), 1916-1928 (2021)
389. M. L. House and C. S. Dutcher, Aerosol Sci. Technol., **58** (4), 427-439 (2024)
390. M. L. House and C. S. Dutcher, Aerosol Sci. Technol., **58** (10), 1168-1181 (2024)
391. L. Nandy, S. Liu, C. Gunsbury, X. Wang, M. A. Pendergraft, K. A. Prather and C. S. Dutcher, ACS Earth Space Chem., **3** (7), 1260-1267 (2019)
392. P. Roy, L. E. Mael, I. Makhnenko, R. Martz, V. H. Grassian and C. S. Dutcher, ACS Earth Space Chem., **4** (9), 1527-1539 (2020)
393. L. Nandy and C. S. Dutcher, J. Phys. Chem. B, **122** (13), 3480-3490 (2018)
394. M. A. Holden, T. F. Whale, M. D. Tarn, D. O'Sullivan, R. D. Walshaw, B. J. Murray, F. C. Meldrum and H. K. Christenson, Sci. Adv., **5** (2), eaav4316 (2019)
395. A. Abdelmonem, E. H. G. Backus, N. Hoffmann, M. A. Sánchez, J. D. Cyran, A. Kiselev and M. Bonn, Atmos. Chem. Phys., **17** (12), 7827-7837 (2017)
396. A. A. Kiselev, A. Keinert, T. Gaedeke, T. Leisner, C. Sutter, E. Petrishcheva and R. Abart, Atmos. Chem. Phys., **21** (15), 11801-11814 (2021)
397. A. Keinert, K. Deck, T. Gaedeke, T. Leisner and A. A. Kiselev, Faraday Discuss., **235** (0), 148-161 (2022)
398. I. Braslavsky and R. Drori, J. Vis. Exp., **72**, e4189 (2013)
399. N. Shardt, F. N. Isenrich, B. Waser, C. Marcolli, Z. A. Kanji, A. J. deMello and U. Lohmann, Phys. Chem. Chem. Phys., **24** (46), 28213-28221 (2022)
400. L.-T. Deck, N. Shardt, I. El-Bakouri, F. N. Isenrich, C. Marcolli, A. J. deMello and M. Mazzotti, Langmuir, **40** (12), 6304-6316 (2024)
401. L. Hajba and A. Guttman, J. Flow Chem., **6** (1), 8-12 (2016)
402. M. D. Tarn, M. J. Lopez-Martinez and N. Pamme, Anal. Bioanal. Chem. (2013)
403. M. Antfolk and T. Laurell, Anal. Chim. Acta, **965**, 9-35 (2017)
404. Y. Zhang and H.-R. Jiang, Anal. Chim. Acta, **914**, 7-16 (2016)
405. S. Wildeman, S. Sterl, C. Sun and D. Lohse, Phys. Rev. Lett., **118** (8), 084101 (2017)
406. C. A. Stan, S. K. Y. Tang, K. J. M. Bishop and G. M. Whitesides, J. Phys. Chem. B, **115** (5), 1089-1097 (2011)
407. C. A. Stan, S. K. Y. Tang and G. M. Whitesides, Anal. Chem., **81** (6), 2399-2402 (2009)
408. C. A. Stan, L. Guglielmini, A. K. Ellerbee, D. Caviezel, H. A. Stone and G. M. Whitesides, Phys. Rev. E, **84** (3) (2011)
409. C. A. Stan, A. K. Ellerbee, L. Guglielmini, H. A. Stone and G. M. Whitesides, Lab Chip, **13** (3), 365-376 (2013)
410. M. D. Tarn, K. H. Bastin, R. E. Sipler and B. J. Murray, presented at the The 27th International Conference on Miniaturized Systems for Chemistry and Life Sciences (MicroTAS 2023), Katowice, Poland, 2023.
411. G. C. E. Porter, S. N. F. Sikora, J.-u. Shim, B. J. Murray and M. D. Tarn, Lab Chip, **20** (21), 3876-3887 (2020)
412. A. Krizhevsky, I. Sutskever and G. E. Hinton, Commun. ACM, **60** (6), 84–90 (2017)
413. G. M. Fahy, J. Saur and R. J. Williams, Cryobiology, **27** (5), 492-510 (1990)
414. G. M. Fahy, in *Biological Ice Nucleation and Its Applications*, edited by R. E. Lee Jr., G. J. Warren and L. V. Gusta (APS Press, St. Paul, MN, 1995), pp. 331.
415. Y. Kamijo and R. Derda, Langmuir, **35** (2), 359-364 (2019)
416. Y. Kamijo and R. Derda, ChemRxiv, doi: 10.26434/chemrxiv-22021-26419l26462. This content is a preprint and has not been peer-reviewed. (2021)
417. Y. Chang, X. Chen, Y. Zhou and J. Wan, Ind. Eng. Chem. Res., **59** (9), 3916-3921 (2020)
418. Y. Chen, K. Guo, L. Jiang, S. Zhu, Z. Ni and N. Xiang, Talanta, **251**, 123815 (2023)
419. H. Chen, J. Guo, F. Bian and Y. Zhao, Smart Med., **1** (1), e20220001 (2022)
420. A. Lenshof, C. Magnusson and T. Laurell, Lab Chip, **12** (7), 1210-1223 (2012)
421. A. R. Abate, T. Hung, P. Mary, J. J. Agresti and D. A. Weitz, Proc. Natl. Acad. Sci. U. S. A., **107** (45), 19163-19166 (2010)
422. M. Rhee, Y. K. Light, S. Yilmaz, P. D. Adams, D. Saxena, R. J. Meagher and A. K. Singh, Lab on a Chip, **14** (23), 4533-4539 (2014)
423. D. J. Eastburn, A. Sciambi and A. R. Abate, PLOS ONE, **8** (4), e62961 (2013)
424. J. Breukers, H. Op de Beeck, I. Rutten, M. López Fernández, S. Eyckerman and J. Lammertyn, Lab on a Chip, **22** (18), 3475-3488 (2022)
425. H. Ahmed and B. T. Stokke, Lab Chip, **21** (11), 2232-2243 (2021)

426. H. Ahmed, E. A. Khan and B. T. Stokke, Soft Matter, **19** (1), 69-79 (2023)
427. Y. Yang, S. Liu, C. Jia, H. Mao, Q. Jin, J. Zhao and H. Zhou, AIP Adv., **6** (12), 125039 (2016)
428. J. Q. Cui, B. Cui, F. X. Liu, Y. Lin and S. Yao, Sens. Actuators B: Chem., **371**, 132573 (2022)
429. M. J. Siedlik and D. Issadore, Microsyst. Nanoeng., **8** (1), 46 (2022)
430. H. Zhang, A. R. Guzman, J. A. Wippold, Y. Li, J. Dai, C. Huang and A. Han, Lab Chip, **20** (21), 3948-3959 (2020)
431. L. Nan, T. Mao and H. C. Shum, Microsyst. Nanoeng., **9** (1), 24 (2023)
432. N. Shi and C. J. Easley, Micromachines, **11** (6), 620 (2020)
433. B. O'Donovan, D. J. Eastburn and A. R. Abate, Lab Chip, **12** (20), 4029-4032 (2012)
434. H. Yuan, Y. Pan, J. Tian, Y. Chao, J. Li and H. Cheung Shum, Sens. Actuators B: Chem., **298**, 126766 (2019)
435. S. Li, M. Zeng, T. Gaule, M. J. McPherson and F. C. Meldrum, Small, **13** (41), 1702154 (2017)
436. X. Niu, S. Gulati, J. B. Edel and A. J. deMello, Lab Chip, **8** (11), 1837-1841 (2008)
437. S. F. Berlanda, M. Breitfeld, C. L. Dietsche and P. S. Dittrich, Anal. Chem., **93** (1), 311-331 (2021)
438. K. J. Shaw, C. Birch, E. M. Hughes, A. D. Jakes, J. Greenman and S. J. Haswell, Eng. Life Sci., **11** (2), 121-132 (2011)
439. C. H. Chon and D. Li, in *Encyclopedia of Microfluidics and Nanofluidics*, edited by D. Li (Springer US, Boston, MA, 2008), pp. 1976-1980.
440. Y.-J. Wei, Y.-N. Zhao, X. Zhang, X. Wei, M.-L. Chen and X.-W. Chen, TrAC Trends Anal. Chem., **158**, 116865 (2023)
441. J. R. Mejía-Salazar, K. Rodrigues Cruz, E. M. Materón Vásques and O. Novais de Oliveira Jr, Sensors, **20** (7), 1951 (2020)
442. G. Zhao and J. Fu, Biotechnol. Adv., **35** (2), 323-336 (2017)
443. J. C. Bischof and X. He, Ann. N. Y. Acad. Sci., **1066** (1), 12-33 (2006)
444. A. Pribylka, A. V. Almeida, M. O. Altmeyer, J. Petr, J. Sevcik, A. Manz and P. Neuzil, Lab Chip (2013)
445. Z. Fohlerova, H. Zhu, J. Hubalek, S. Ni, L. Yobas, P. Podesva, A. Otahal and P. Neuzil, Sci. Rep., **10** (1), 6925 (2020)
446. M. O. Altmeyer, A. Manz and P. Neužil, Anal. Chem., **87** (12), 5997-6003 (2015)
447. Y. Wang, W. Zhang and Z. Ouyang, Chem. Sci., **11** (38), 10506-10516 (2020)
448. K. M. King, G. G. M. Canning and J. S. West, Pathogens, **13** (4), 330 (2024)
449. W. G. Weisburg, S. M. Barns, D. A. Pelletier and D. J. Lane, J. Bacteriol., **173** (2), 697-703 (1991)
450. T. J. White, T. D. Bruns, S. B. Lee and J. W. Taylor, in *PCR Protocols*, edited by M. A. Innis, D. H. Gelfand, J. J. Sninsky and T. J. White (Academic Press, San Diego, 1990), pp. 315-322.
451. J. Fröhlich-Nowoisky, D. A. Pickersgill, V. R. Després and U. Pöschl, Proc. Natl. Acad. Sci. U. S. A., **106** (31), 12814-12819 (2009)
452. Y. Wang, Y. Zhao, A. Bollas, Y. Wang and K. F. Au, Nat. Biotechnol., **39** (11), 1348-1365 (2021)
453. in *Oxford Nanopore Technologies, Environmental research and conservation: https://nanoporetech.com/applications/research-areas/environmental-research-and-conservation, accessed 25th June 2024*.
454. N. Forin, S. Nigris, S. Voyron, M. Girlanda, A. Vizzini, G. Casadoro and B. Baldan, Front. Ecol. Evol., **6** (2018)
455. J. S. West, S. D. Atkins, J. Emberlin and B. D. Fitt, Trends Microbiol., **16** (8), 380-387 (2008)
456. M. Madadelahi and M. J. Madou, Micromachines, **14** (8), 1533 (2023)
457. M. U. Kopp, A. J. d. Mello and A. Manz, Science, **280** (5366), 1046-1048 (1998)
458. D. Das, C.-W. Lin and H.-S. Chuang, Biosensors, **12** (12), 1068 (2022)
459. Z. Li, Y. Bai, M. You, J. Hu, C. Yao, L. Cao and F. Xu, Biosens. Bioelectron., **177**, 112952 (2021)
460. Y. Schaerli, R. C. Wootton, T. Robinson, V. Stein, C. Dunsby, M. A. A. Neil, P. M. W. French, A. J. deMello, C. Abell and F. Hollfelder, Anal. Chem., **81** (1), 302-306 (2009)
461. D. Xu, W. Zhang, H. Li, N. Li and J.-M. Lin, Lab Chip, **23** (5), 1258-1278 (2023)
462. W. Fang, X. Liu, M. Maiga, W. Cao, Y. Mu, Q. Yan and Q. Zhu, Biosensors, **14** (2), 64 (2024)
463. L. Wang and P. C. H. Li, Anal. Chim. Acta, **687** (1), 12-27 (2011)
464. J. Song, C. Liu, M. G. Mauk, J. Peng, T. Schoenfeld and H. H. Bau, Anal. Chem., **90** (2), 1209-1216 (2018)
465. K. Tsougeni, A. Kanioura, A. S. Kastania, K. Ellinas, A. Stellas, V. Constantoudis, G. Moschonas, N. D. Andritsos, M. Velonakis, P. S. Petrou, S. E. Kakabakos, E. Gogolides and A. Tserepi, Biosensors, **14** (5), 228 (2024)
466. M. L. Coluccio, G. Perozziello, N. Malara, E. Parrotta, P. Zhang, F. Gentile, T. Limongi, P. M. Raj, G. Cuda, P. Candeloro and E. Di Fabrizio, Microelectron. Eng., **208**, 14-28 (2019)
467. G. S. Ugolini, M. Wang, E. Secchi, R. Pioli, M. Ackermann and R. Stocker, Lab Chip, **24** (5), 1394-1418 (2024)
468. D. E. Ingber, Nat. Rev. Genet., **23** (8), 467-491 (2022)
469. M. Pousti, M. P. Zarabadi, M. Abbaszadeh Amirdehi, F. Paquet-Mercier and J. Greener, Analyst, **144** (1), 68-86 (2019)
470. J. Cao, X. Chen, S. Huang, W. Shi, Q. Fan, Y. Gong, Y. Peng, L. Wu and C. Yang, TrAC Trends Anal. Chem., **158**, 116868 (2023)
471. W.-m. Zhou, Y.-y. Yan, Q.-r. Guo, H. Ji, H. Wang, T.-t. Xu, B. Makabel, C. Pilarsky, G. He, X.-y. Yu and J.-y. Zhang, J. Nanobiotechnology, **19** (1), 312 (2021)
472. Z. Jiang, H. Shi, X. Tang and J. Qin, TrAC Trends Anal. Chem., **159**, 116932 (2023)
473. D. G. Wild, *The Immunoassay Handbook*, 3rd ed. (Elsevier, Kidlington, UK, 2005).
474. M. D. Tarn and N. Pamme, Expert Rev. Mol. Diagn., **11** (7), 711-720 (2011)
475. K. Wu, X. He, J. Wang, T. Pan, R. He, F. Kong, Z. Cao, F. Ju, Z. Huang and L. Nie, Front. Bioeng. Biotechnol., **10**, 1112327 (2022)
476. Y. Shi, P. Ye, K. Yang, J. Meng, J. Guo, Z. Pan, Q. Bayin and W. Zhao, J. Healthc. Eng., **2021** (1), 2959843 (2021)
477. Y. Shi, P. Ye, K. Yang, J. Meng, J. Guo, Z. Pan, W. Zhao and J. Guo, Analyst, **146** (19), 5800-5821 (2021)
478. N. Pamme, Curr. Opin. Chem. Biol., **16** (3–4), 436-443 (2012)
479. L. Coudron, M. B. McDonnell, I. Munro, D. K. McCluskey, I. D. Johnston, C. K. L. Tan and M. C. Tracey, Biosens. Bioelectron., **128**, 52-60 (2019)
480. P. Yang, L. Zhao, Y. G. Gao and Y. Xia, Plants, **12** (9), 1765 (2023)
481. A. Iwata and A. Matsuki, Atmos. Chem. Phys., **18** (3), 1785-1804 (2018)

482. A. Iwata, M. Imura, M. Hama, T. Maki, N. Tsuchiya, R. Kunihisa and A. Matsuki, Atmosphere, **10** (10), 605 (2019)
483. K. J. Baustian, D. J. Cziczo, M. E. Wise, K. A. Pratt, G. Kulkarni, A. G. Hallar and M. A. Tolbert, J. Geophys. Res. Atmos., **117** (D6) (2012)
484. L. E. Mael, H. Busse and V. H. Grassian, Anal. Chem., **91**, 11138-11145 (2019)
485. A. F. Chrimes, K. Khoshmanesh, P. R. Stoddart, A. Mitchell and K. Kalantar-zadeh, Chem. Soc. Rev., **42** (13), 5880-5906 (2013)
486. R. Panneerselvam, H. Sadat, E.-M. Höhn, A. Das, H. Noothalapati and D. Belder, Lab Chip, **22** (4), 665-682 (2022)
487. J. Poonoosamy, A. Kaspor, S. Rudin, G. L. Murphy, D. Bosbach and G. Deissmann, Minerals, **13** (5), 636 (2023)
488. C. Dallari, C. Credi, E. Lenci, A. Trabocchi, R. Cicchi and F. S. Pavone, J. Phys. Photonics, **2** (2), 024008 (2020)
489. M. D. Tarn, M. M. Esfahani, L. Patinglag, Y. C. Chan, J. X. Buch, C. C. Onyije, P. J. Gawne, D. J. Gambin, N. J. Brown, S. J. Archibald and N. Pamme, presented at the Proceedings of the 21st International Conference on Miniaturized Systems for Chemistry and Life Sciences, Savannah, GA, USA, 22-26, 2017.
490. Y. Park, U. J. Kim, S. Lee, H. Kim, J. Kim, H. Ma, H. Son, Y. Z. Yoon, J.-s. Lee, M. Park, H. Choo, Q. H. Park and Y.-G. Roh, Sens. Actuators B: Chem., **381**, 133442 (2023)
491. E. Toprak and M. Schnaiter, Atmos. Chem. Phys., **13** (1), 225-243 (2013)
492. J. Schneider, K. Höhler, P. Heikkilä, J. Keskinen, B. Bertozzi, P. Bogert, T. Schorr, N. S. Umo, F. Vogel, Z. Brasseur, Y. Wu, S. Hakala, J. Duplissy, D. Moisseev, M. Kulmala, M. P. Adams, B. J. Murray, K. Korhonen, L. Hao, E. S. Thomson, D. Castarède, T. Leisner, T. Petäjä and O. Möhler, Atmos. Chem. Phys., **21** (5), 3899-3918 (2021)
493. Y. Boose, B. Sierau, M. I. García, S. Rodríguez, A. Alastuey, C. Linke, M. Schnaiter, P. Kupiszewski, Z. A. Kanji and U. Lohmann, Atmos. Chem. Phys., **16** (14), 9067-9087 (2016)
494. D. Măriuţa, S. Colin, C. Barrot-Lattes, S. Le Calvé, J. G. Korvink, L. Baldas and J. J. Brandner, Microfluid. Nanofluid., **24** (9), 65 (2020)
495. J. S. Kang, K. S. Lee, S. S. Kim, G.-N. Bae and J. H. Jung, Lab Chip, **14** (1), 244-251 (2014)
496. J. Choi, M. Kang and J. H. Jung, Sci. Rep., **5**, 15983 (2015)
497. T. Li, J. A. Díaz-Real and T. Holm, Adv. Mater. Technol., **6** (12), 2100569 (2021)
498. J. Leva-Bueno, S. A. Peyman and P. A. Millner, Med. Microbiol. Immunol., **209** (3), 343-362 (2020)
499. Y. Qasim Almajidi, S. M. Algahtani, O. Sajjad Alsawad, H. Setia Budi, S. Mansouri, I. R. Ali, M. Mazin Al-Hamdani and R. Mireya Romero-Parra, Microchem. J., **190**, 108733 (2023)
500. P. P. Behera, N. Kumar, M. Kumari, S. Kumar, P. K. Mondal and R. K. Arun, Sens. Diagn., **2** (6), 1437-1459 (2023)
501. F. Cook, R. Lord, G. Sitbon, A. Stephens, A. Rust and W. Schwarzacher, Atmos. Meas. Tech., **13** (5), 2785-2795 (2020)
502. S. A. Pullano, S. K. Islam and A. S. Fiorillo, IEEE Sens. J., **14** (8), 2725-2730 (2014)
503. S. A. Pullano, A. S. Fiorillo and S. K. Islam, presented at the 2014 40th Annual Northeast Bioengineering Conference (NEBEC), 1-2, 2014, 10.1109/NEBEC.2014.6972911.
504. S. A. Pullano, I. Mahbub, S. K. Islam and A. S. Fiorillo, Sensors, **17** (4), 850 (2017)
505. D. J. Guckenberger, T. E. de Groot, A. M. D. Wan, D. J. Beebe and E. W. K. Young, Lab Chip, **15** (11), 2364-2378 (2015)
506. U. M. Attia, S. Marson and J. R. Alcock, Microfluid. Nanofluid., **7** (1), 1-28 (2009)
507. H. Becker and C. Gärtner, Anal. Bioanal. Chem., **390** (1), 89-111 (2008)
508. H. Becker and L. E. Locascio, Talanta, **56** (2), 267-287 (2002)
509. J. Giboz, T. Copponnex and P. Mélé, J. Micromech. Microeng., **17** (6), R96-R109 (2007)
510. Y.-J. Juang and Y.-J. Chiu, Polymers, **14** (10) (2022)
511. D. Zaragotas, N. T. Liolios and E. Anastassopoulos, Cryobiology, **72** (3), 239-243 (2016)
512. A. D. Harrison, T. F. Whale, R. Rutledge, S. Lamb, M. D. Tarn, G. C. E. Porter, M. P. Adams, J. B. McQuaid, G. J. Morris and B. J. Murray, Atmos. Meas. Tech., **11** (10), 5629-5641 (2018)
513. M. I. Daily, T. F. Whale, R. Partanen, A. D. Harrison, P. Kilbride, S. Lamb, G. J. Morris, H. M. Picton and B. J. Murray, Cryobiology, **93**, 62-69 (2020)
514. M. I. Daily, T. F. Whale, P. Kilbride, S. Lamb, G. John Morris, H. M. Picton and B. J. Murray, J. R. Soc. Interface, **20** (199), 20220682 (2023)
515. A. T. Kunert, M. Lamneck, F. Helleis, U. Pöschl, M. L. Pöhlker and J. Fröhlich-Nowoisky, Atmos. Meas. Tech., **11** (11), 6327-6337 (2018)
516. C. Wieber, M. Rosenhøj Jeppesen, K. Finster, C. Melvad and T. Šantl-Temkiv, Atmos. Meas. Tech., **17** (9), 2707-2719 (2024)
517. P. Yi, A. A. Kayani, A. F. Chrimes, K. Ghorbani, S. Nahavandi, K. Kalantar-zadeh and K. Khoshmanesh, Lab Chip, **12** (14), 2520-2525 (2012)
518. A. Khater, M. Mohammadi, A. Mohamad and A. S. Nezhad, Sci. Rep., **9** (1), 3832 (2019)
519. J.-H. Wang, L.-J. Chien, T.-M. Hsieh, C.-H. Luo, W.-P. Chou, P.-H. Chen, P.-J. Chen, D.-S. Lee and G.-B. Lee, Sens. Actuators B: Chem., **141** (1), 329-337 (2009)
520. B. Selva, P. Mary and M.-C. Jullien, Microfluid. Nanofluid., **8** (6), 755-765 (2010)
521. J. Wu, W. Cao, W. Wen, D. C. Chang and P. Sheng, Biomicrofluidics, **3** (1) (2009)
522. A. Parody-Morreale, G. Bishop, R. Fall and S. J. Gill, Anal. Biochem., **154** (2), 682-690 (1986)
523. A. Kumar, C. Marcolli, B. Luo and T. Peter, Atmos. Chem. Phys., **18**, 7057-7079 (2018)
524. L. Kaufmann, C. Marcolli, B. Luo and T. Peter, Atmos. Chem. Phys., **17** (5), 3525-3552 (2017)
525. Y. Yao, P. Ruckdeschel, R. Graf, H.-J. Butt, M. Retsch and G. Floudas, J. Phys. Chem. B, **121** (1), 306-313 (2017)
526. P. Gill, T. T. Moghadam and B. Ranjbar, J. Biomol. Tech., **21** (4), 167-193 (2010)
527. S. Yu, Y. Wu, S. Wang, M. Siedler, P. M. Ihnat, D. I. Filoti, M. Lu and L. Zuo, Biosensors, **12** (6), 422 (2022)
528. Y. Jia, B. Wang, J. Zhu and Q. Lin, presented at the 2014 IEEE 27th International Conference on Micro Electro Mechanical Systems (MEMS), 306-309, 2014, 10.1109/MEMSYS.2014.6765637.
529. B. Wang and Q. Lin, Sens. Actuators B: Chem., **180**, 60-65 (2013)

530. S. Yu, S. Wang, M. Lu and L. Zuo, Front. Mech. Eng., **12** (4), 526-538 (2017)
531. S. I. R. Lane, J. Butement, J. Harrington, T. Underwood, J. Shrimpton and J. West, Lab Chip, **19** (22), 3771-3775 (2019)
532. B. Horstkotte, R. Suárez, P. Solich and V. Cerdà, Anal. Chim. Acta, **788**, 52-60 (2013)
533. N. Pamme, R. Koyama and A. Manz, Lab Chip, **3** (3), 187-192 (2003)
534. G. Goodwin, S. Metzger and C. Alexander-White, *Evidence report: PFAS in UK waters - presence, detection, and remediation*. (Royal Society of Chemistry, London, UK, 2023).
535. I. T. Cousins, G. Goldenman, D. Herzke, R. Lohmann, M. Miller, C. A. Ng, S. Patton, M. Scheringer, X. Trier, L. Vierke, Z. Wang and J. C. DeWitt, Environ. Sci.: Process. Impacts, **21** (11), 1803-1815 (2019)
536. C. F. Kwiatkowski, D. Q. Andrews, L. S. Birnbaum, T. A. Bruton, J. C. DeWitt, D. R. U. Knappe, M. V. Maffini, M. F. Miller, K. E. Pelch, A. Reade, A. Soehl, X. Trier, M. Venier, C. C. Wagner, Z. Wang and A. Blum, Environ. Sci. Technol. Lett., **7** (8), 532-543 (2020)
537. K. S. Elvira, F. Gielen, S. S. H. Tsai and A. M. Nightingale, Lab Chip, **22** (5), 859-875 (2022)
538. J.-C. Baret, Lab Chip, **12** (3), 422-433 (2012)
539. C. Holtze, A. C. Rowat, J. J. Agresti, J. B. Hutchison, F. E. Angile, C. H. J. Schmitz, S. Koster, H. Duan, K. J. Humphry, R. A. Scanga, J. S. Johnson, D. Pisignano and D. A. Weitz, Lab Chip, **8** (10), 1632-1639 (2008)
540. P. Gruner, B. Riechers, L. A. Chacòn Orellana, Q. Brosseau, F. Maes, T. Beneyton, D. Pekin and J.-C. Baret, Curr. Opin. Colloid Interface Sci., **20** (3), 183-191 (2015)
541. M. Rasekh, S. Harrison, S. Schobesberger, P. Ertl and W. Balachandran, Biomed Microdevices, **26** (3), 28 (2024)
542. A. Melchum, F. Córdoba, E. Salinas, L. Martínez, G. Campos, I. Rosas, E. Garcia-Mendoza, A. Olivos-Ortiz, G. B. Raga, B. Pizano, M. M. Silva and L. A. Ladino, Atmos. Res., **293**, 106893 (2023)
543. M. Watanabe and S. Arai, Agric. Biol. Chem., **51** (2), 557-563 (1987)
544. J. R. Wallin, D. V. Loonan and C. A. C. Gardner, Plant Dis. Rep., **63**, 751-752 (1979)
545. M. A. Ponder, S. J. Gilmour, P. W. Bergholz, C. A. Mindock, R. Hollingsworth, M. F. Thomashow and J. M. Tiedje, FEMS Microbiol. Ecol., **53** (1), 103-115 (2005)
546. S. E. Lindow, D. C. D. C. Arny and C. D. Upper, Phytopathology, **68**, 523-527 (1978)
547. C. A. Deininger, G. M. Mueller and P. K. Wolber, J. Bacteriol., **170** (2), 669-675 (1988)
548. P. Phelps, T. H. Giddings, M. Prochoda and R. Fall, J. Bacteriol., **167** (2), 496-502 (1986)
549. H. Obata, K. Takinami, J.-i. Tanishita, Y. Hasegawa, S. Kawate, T. Tokuyama and T. Ueno, Agric. Biol. Chem., **54** (3), 725-730 (1990)
550. M. R. Worland and A. Lukešová, Polar Biol., **23** (11), 766-774 (2000)
551. M. J. Wolf, A. Coe, L. A. Dove, M. A. Zawadowicz, K. Dooley, S. J. Biller, Y. Zhang, S. W. Chisholm and D. J. Cziczo, Environ. Sci. Technol., **53** (3), 1139-1149 (2019)
552. C. M. Foreman, R. M. Cory, C. E. Morris, M. D. SanClements, H. J. Smith, J. T. Lisle, P. L. Miller, Y.-P. Chin and D. M. McKnight, Environ. Res. Lett., **8** (3), 035022 (2013)
553. H. Obata, N. Muryoi, H. Kawahara, K. Yamade and J. Nishikawa, Cryobiology, **38** (2), 131-139 (1999)
554. N. Muryoi, H. Kawahara and H. Obata, Biosci. Biotechnol. Biochem., **67** (9), 1950-1958 (2003)
555. T. L. Vanderveer, J. Choi, D. Miao and V. K. Walker, Cryobiology, **69** (1), 110-118 (2014)
556. H. K. Kim, C. Orser, S. E. Lindow and D. C. Sands, Plant Dis., **71** (11), 994-997 (1987)
557. L. R. Maki and K. J. Willoughby, J. Appl. Meteorol. Climatol., **17** (7), 1049-1053 (1978)
558. H. Xu, M. Griffith, C. L. Patten and B. R. Glick, Can. J. Microbiol., **44** (1), 64-73 (1998)
559. S. A. Yankofsky, Z. Levin, T. Bertold and N. Sandlerman, J. Appl. Meteorol., **20** (9), 1013-1019 (1981)
560. P. Amato, M. Parazols, M. Sancelme, P. Laj, G. Mailhot and A.-M. Delort, FEMS Microbiol. Ecol., **59** (2), 242-254 (2007)
561. H. Wex, S. Augustin-Bauditz, Y. Boose, C. Budke, J. Curtius, K. Diehl, A. Dreyer, F. Frank, S. Hartmann, N. Hiranuma, E. Jantsch, Z. A. Kanji, A. Kiselev, T. Koop, O. Möhler, D. Niedermeier, B. Nillius, M. Rösch, D. Rose, C. Schmidt, I. Steinke and F. Stratmann, Atmos. Chem. Phys., **15** (3), 1463-1485 (2015)
562. S. E. Lindow, C. A. Deane and C. D. Upper, Plant Physiol., **70** (4), 1084-1089 (1982)
563. in *www.snomax.com*, Vol. accessed October 2024.
564. S. E. Wood, M. B. Baker and B. D. Swanson, Review of Scientific Instruments, **73** (11), 3988-3996 (2002)
565. C. Budke and T. Koop, Atmos. Meas. Tech., **8** (2), 689-703 (2015)
566. M. Polen, E. Lawlis and R. C. Sullivan, J. Geophys. Res. Atmos., **121** (19), 11,666-611,678 (2016)
567. Y. Tobo, Sci. Rep., **6**, 32930 (2016)
568. J. A. Anderson and E. N. Ashworth, Plant Physiol, **80** (4), 956-960 (1986)
569. H. Obata, T. Nakai, J. Tanishita and T. Tokuyama, J. Ferment. Bioeng., **67** (3), 143-147 (1989)
570. J.-P. Paulin and J. Luisetti, presented at the Proceedings of the 4th International Conference on Plant Pathological Bacteria, Beaucouzé, France, 725-731, 1978.
571. M. Vaïtilingom, E. Attard, N. Gaiani, M. Sancelme, L. Deguillaume, A. I. Flossmann, P. Amato and A.-M. Delort, Atmos. Environ., **56**, 88-100 (2012)
572. L. A. Ladino, J. D. Yakobi-Hancock, W. P. Kilthau, R. H. Mason, M. Si, J. Li, L. A. Miller, C. L. Schiller, J. A. Huffman, J. Y. Aller, D. A. Knopf, A. K. Bertram and J. P. D. Abbatt, Atmos. Environ., **132**, 1-10 (2016)
573. T. Šantl-Temkiv, R. Lange, D. Beddows, U. Rauter, S. Pilgaard, M. Dall'Osto, N. Gunde-Cimerman, A. Massling and H. Wex, Environ. Sci. Technol., **53** (18), 10580-10590 (2019)
574. R. Iannone, D. I. Chernoff, A. Pringle, S. T. Martin and A. K. Bertram, Atmos. Chem. Phys., **11** (3), 1191-1201 (2011)
575. T. Seifi, S. Ketabchi, H. Aminian, H. R. Etebarian and M. Kamali, Int. J. Farm & Alli. Sci., **3** (5), 518-528 (2014)
576. T. L. Humphreys, L. A. Castrillo and M. R. Lee, Curr. Microbiol., **42** (5), 330-338 (2001)
577. C. Richard, Phytoprotection, **77** (2), 83-92 (1996)

578. C. E. Morris, D. C. Sands, C. Glaux, J. Samsatly, S. Asaad, A. R. Moukahel, F. L. T. Gonçalves and E. K. Bigg, Atmos. Chem. Phys., **13** (8), 4223-4233 (2013)
579. E. Gute and J. P. D. Abbatt, Atmos. Environ., **231**, 117488 (2020)
580. N. von Blohn, S. K. Mitra, K. Diehl and S. Borrmann, Atmos. Res., **78** (3–4), 182-189 (2005)
581. B. H. Matthews, A. N. Alsante and S. D. Brooks, ACS Earth Space Chem., **7** (6), 1207-1218 (2023)
582. K. Diehl, S. Matthias-Maser, R. Jaenicke and S. K. Mitra, Atmos. Res., **61** (2), 125-133 (2002)
583. K. Diehl, C. Quick, S. Matthias-Maser, S. K. Mitra and R. Jaenicke, Atmos. Res., **58** (2), 75-87 (2001)
584. H. J. Tong, B. Ouyang, N. Nikolovski, D. M. Lienhard, F. D. Pope and M. Kalberer, Atmos. Meas. Tech., **8** (3), 1183-1195 (2015)
585. S. Augustin, H. Wex, D. Niedermeier, B. Pummer, H. Grothe, S. Hartmann, L. Tomsche, T. Clauss, J. Voigtländer, K. Ignatius and F. Stratmann, Atmos. Chem. Phys., **13** (21), 10989-11003 (2013)
586. K. A. Murray, N. L. H. Kinney, C. A. Griffiths, M. Hasan, M. I. Gibson and T. F. Whale, Sci. Rep., **12** (1), 12295 (2022)
587. M. Burkert-Kohn, H. Wex, A. Welti, S. Hartmann, S. Grawe, L. Hellner, P. Herenz, J. D. Atkinson, F. Stratmann and Z. A. Kanji, Atmos. Chem. Phys., **17** (18), 11683-11705 (2017)
588. R. Lundheim, J. Phycol., **33** (5), 739-742 (1997)
589. J. Kvíderová, J. Hájek and R. M. Worland, CryoLetters, **34** (2), 137-148 (2013)
590. P. A. Alpert, J. Y. Aller and D. A. Knopf, Phys. Chem. Chem. Phys., **13** (44), 19882-19894 (2011)
591. in *Sektion Phykologie der Deutschen Botanischen Gesellschaft (DBG), Alga of the Year winners: https://www.dbg-phykologie.de/en/alga-of-the-year, last accessed June 2024*.
592. R. Fall and R. C. Schnell, J. Mar. Res., **43**, 257-265 (1985)
593. L. Ickes, G. C. E. Porter, R. Wagner, M. P. Adams, S. Bierbauer, A. K. Bertram, M. Bilde, S. Christiansen, A. M. L. Ekman, E. Gorokhova, K. Höhler, A. A. Kiselev, C. Leck, O. Möhler, B. J. Murray, T. Schiebel, R. Ullrich and M. E. Salter, Atmos. Chem. Phys., **20** (18), 11089-11117 (2020)
594. D. A. Knopf, P. A. Alpert, B. Wang and J. Y. Aller, Nat. Geosci., **4** (2), 88-90 (2011)
595. E. N. Ashworth and T. L. Kieft, Cryobiology, **29** (3), 400-406 (1992)
596. T. L. Kieft and T. Ruscetti, J. Bacteriol., **172** (6), 3519-3523 (1990)
597. S. Hengherr, A. Reuner, F. Brümmer and R. O. Schill, Comp. Biochem. Physiol. A Physiol., **156** (1), 151-155 (2010)
598. D. A. Knopf, P. A. Alpert, A. Zipori, N. Reicher and Y. Rudich, NPJ Clim. Atmos. Sci., **3** (1), 2 (2020)
599. L. Eickhoff, K. Dreischmeier, A. Zipori, V. Sirotinskaya, C. Adar, N. Reicher, I. Braslavsky, Y. Rudich and T. Koop, J. Phys. Chem. Lett., **10** (5), 966-972 (2019)
600. A. Zipori, N. Reicher, Y. Erel, D. Rosenfeld, A. Sandler, D. A. Knopf and Y. Rudich, J. Geophys. Res. Atmos., **123** (22), 12,762-712,777 (2018)